

ResearchOnline@JCU

This file is part of the following reference:

Susilo, Adi (2004) *Groundwater flow in arid tropical tidal wetlands and estuaries*. PhD thesis, James Cook University.

Access to this file is available from:

<http://researchonline.jcu.edu.au/8677/>

If you believe that this work constitutes a copyright infringement, please contact ResearchOnline@jcu.edu.au and quote <http://researchonline.jcu.edu.au/8677/>

**GROUNDWATER FLOW
IN ARID TROPICAL TIDAL WETLANDS AND
ESTUARIES**

Thesis submitted by

Adi Susilo MS, UGM

For the Degree of Doctor of Philosophy
in the School of Mathematical and Physical Sciences

James Cook University, Australia

2004

STATEMENT OF ACCESS

I, the undersigned author of this work, understand that James Cook University will make this thesis available for use within the University Library and, via the Australian Digital Theses network, for use elsewhere.

I understand that, as an unpublished work, a thesis has significant protection under the Copyright Act and;

I do not wish to place any further restriction on access to this work

Signature

30/2/2005
Date

ELECTRONIC COPY

I, the undersigned, the author of this work, declare that the electronic copy of this thesis provided to the James Cook University Library, is an accurate copy of the print thesis submitted, within the limits of the technology available.

Signature

30/2/2005

Date

STATEMENT ON SOURCES

Declaration

I declare that this thesis is my own work and has not been submitted in any form for another degree or diploma at any university or other institution of tertiary education. Information derived from the published or unpublished work of others has been acknowledged in the text and a list of references is given.

.....
(Signature)

30/1/2005
.....
(Date)

Abstract

The flow of groundwater in mangrove forests is very important to the mangrove trees and organisms that live within the soil. Groundwater flow is responsible for preventing salinity of the water around the mangrove roots from reaching lethal levels. Further the flow of nutrients between the swamp and creeks is important to the nutrient budget of the swamps.

Groundwater flow in mangrove swamps is complicated by the presence of abundant animal burrows. These have the effect of greatly increasing the hydraulic conductivity of the soil. However, using conventional methods, it is difficult to determine the bulk hydraulic conductivity of the soil when the effect of the burrows is taken into account. In this work, a simple method is described for determining the hydraulic conductivity of mangrove sediment, including the effect of macropores such as crab burrows. The method uses the existing animal burrows as piezometers. Experiments to measure the hydraulic conductivity of the sediment were carried out in a variety of mangrove forests. It was found that hydraulic conductivity varied from around 1 m/day to 10 m/day, which is at least 10 times greater than would be expected if there were no burrows.

In order to check the validity of the method, conventional piezometers were used to determine the free water table level in an area of mangroves fringing a creek. From these measurements, hydraulic conductivity was determined independently and found to be consistent with the new methodology.

Tidal groundwater in a mangrove swamp can return to the mangrove creek by one of two mechanisms: (a) it can either flow through the swamp soil due to the water table difference between the creek and the groundwater in the swamp; or (b) it can flow via tidal flushing of animal burrows. The second section of this thesis compares the magnitude of these two mechanisms for different regions of a mangrove swamp. Direct groundwater flow rates resulting from water stored in the sediment as a consequence of infiltration, especially during and after tidal inundation, were calculated for every square meter in the surface of a mangrove forest from piezometer

data. Flow rates of water due to burrow flushing were determined based on published surveys, by estimating the burrow volume and the percentage of the burrow water that is flushed at each tidal inundation. Although direct groundwater flux was found to decrease further away from the creek compared to close to the creek, it was also found to have a similar range as burrow flushing flow. Specifically, direct groundwater flow ranged from 0.004 to 0.04 $\text{m}^3/(\text{m}^2 \text{ day})$, whilst burrow flushing flux ranged from 0.01 to 0.04 $\text{m}^3/(\text{m}^2 \text{ day})$. Considering the errors involved in the experiments and calculations, these ranges can be considered as being the same and none of the two processes can be considered as negligible compared to the other.

The final section of the thesis is the development of a simple analytical model that was used to calculate the groundwater flow to the creek. Data from piezometers were used in the model calculation. It was found that the model results agreed well with experimentally determined calculations of groundwater fluxes. Fluxes ranged from 0.007 to 0.026 $\frac{\text{m}^3}{\text{m}^2 \text{ day}}$ with the lowest fluxes being recorded at the end of the neap tide period. This model is easily adaptable to most mangrove geometries.

Acknowledgements

I would firstly like to thank my supervisor, Dr Peter Ridd and Dr Wayne Read, for the huge time spent and guidance throughout my candidature. I am particularly thankful for your any time that I needed you. Your door was always opened for me.

Thanks to my colleagues in the School of Math. and Phys. and Earth Sciences at JCU, especially Alessandra Mantovanelli, Eduardo Da Silva, Mr. Jeffrey Cavanagh, Mr. Paul Givney and Jonathan Bathgate, who helped me to do my fieldwork.

Thanks to all my Indonesian friends who helped me in my fieldwork; Fayakun Satria, Ifan Muttaqien, Didik Restanto, Moh. Jadmiko, Arief Setyanto, Johan Arief and Eko Suyono. Your help was very useful.

Thank to my institution, Physics Department, Brawijaya University, Malang, Indonesia allowing me to take my PhD study at James Cook University

Thanks to my late Father and Brother (Kasenun, Warno), who passed away when I was in Townsville, and for whose burial I was unable to return. Thanks to my Mother and Parents in law.

I cannot say how thankful I am for, and grateful I am to, my wife, Fikriyati H. Suwardani, my children Rizka Khairani, Ahmad A. Susilo and Salsabila Y. Susilo who always supported me in any situation. All of you are my diversion, whenever I got problem in my study. More specifically, thank to my wife, who also helped me with my fieldwork on many occasions.

Finally, I give my thank and praise to my Lord, Allah swt. You have been every part of this. I praise You for the continuing blessings in my whole life. "Verily, along with every hardship is relief. So when you have finished (your occupation), devote yourself for Allah's worship. And to your Lord turn intentions and hopes" Q94:6-8

Adi Susilo

Contents

Statement of Access to Thesis.....	ii
Declaration.....	iii
Abstract.....	iv
Acknowledgements.....	vi
Contents.....	vii
List of Tables	xi
List of Figures	xii
Chapter 1. Introduction1	
1.1. Definitions of wetlands, mangroves and salt-flats.....	1
1.1.1. Wetlands.....	1
1.1.2. Mangroves.....	2
1.1.3. Salt flats.....	2
1.2. Underground processes in wetlands.....	4
1.2.1. Evapotranspiration and build up of salt at mangroves roots.....	4
1.2.2. Animal burrows, salt diffusion and flushing.....	5
1.2.3. Infiltration processes.....	7
1.3. Significance of hydrology in wetlands.....	8
1.3.1. Contribution to nutrient and salt cycling.....	8
1.3.2. Influence of groundwater in mangrove swamps.....	10
1.3.3. Factors influencing groundwater flow and hydraulic conductivity	11
1.4. Groundwater modeling.....	12
1.4.1. Various groundwater flow models.....	12
1.4.2. Series solution models.....	13
1.5 Conclusion.....	13
1.5.1 Focus of the Thesis.....	13
1.5.2. Publication outcome of thesis.....	15
Chapter 2: Description of the study areas.....	17
2.1 General description of the study area	17
2.1.1. Physical setting.....	17
2.1.2. Climate and Tides	18
2.1.3 Sea level variability.....	20

2.2 Field study locations.....	21
2.2.1 Cocoa Creek.....	22
2.2.2 Gordon Creek.....	26
2.2.3 Three Mile Creek.....	30
Chapter 3: Investigations of physical characteristics of sediment and groundwater in mangrove and salt flats.....	33
3.1 Introduction.....	33
3.2 Physical characteristics of the sediment.....	34
3.2.1 Method.....	34
3.2.1.1 Analysis of sediment cores.....	37
3.2.1.2 Particle size analysis.....	38
3.2.1.3 Bulk electrical conductivity measurement.....	39
3.2.2 Results.....	42
3.2.2.1 Core analysis.....	42
3.2.2.2 Particle size distribution.....	43
3.2.2.3 Bulk sediment electrical conductivity.....	46
3.2.3 Discussion.....	47
3.3 Salinity and density of the groundwater.....	49
3.3.1 Method.....	49
3.3.1.1 Salinity of the groundwater.....	49
3.3.1.2 Density of the groundwater.....	49
3.3.2 Results.....	50
3.3.2.1. Groundwater salinity.....	50
3.3.2.2. Groundwater density.....	51
3.3.3 Discussion.....	52
3.4 Hydraulic conductivity of salt flat sediment: laboratory measurements....	52
3.4.1 Method.....	52
3.4.2 Result.....	56
Chapter 4. The bulk hydraulic conductivity of mangrove soil perforated with animal burrows.....	57
4.1 Introduction.....	57
4.2 Methods.....	58
4.2.1 Measurement of the bulk hydraulic conductivity of mangrove soils using crab burrows.....	58

4.2.2 Measurement of Bulk Hydraulic Conductivity using a Piezometer Array.....	62
4.2.2.1 Determining degree of saturation F_s	66
4.2.2.2 Determining the fraction occupied by burrows, F_b	67
4.2.2.3 Determining porosity p	67
4.2.3 Description of field sites.....	68
4.3 Results.....	70
4.3.1 Sediment Physical Properties in the field area.....	70
4.3.2. Measurement of hydraulic conductivity of sediment using animal burrows.....	71
4.3.3. Calculation of hydraulic conductivity using the piezometer array.....	72
4.4 Discussion.....	75
Chapter 5. Comparison between tidally-driven groundwater flow and flushing of animal burrows in tropical mangrove swamps.....	77
5.1 Introduction.....	77
5.2 Methods.....	79
5.2.1 Study sites.....	79
5.2.2 Piezometer arrays.....	80
5.2.3 Piezometer description.....	82
5.2.4 Model description.....	84
5.3 Results.....	87
5.3.1 Fluctuations of groundwater levels at Cocoa Creek.....	87
5.3.2 Fluctuations of groundwater levels at Gordon Creek.....	90
5.3.3 Direct groundwater flow.....	92
5.3.4 Calculation of burrow flushing during tidal inundation.....	93
5.4 Discussion.....	94
Chapter 6: Groundwater flow model in the mangrove forest.....	96
6.1 Introduction.....	96
6.2 Methods.....	97
6.2.1 Laplace equation.....	97
6.2.2 Boundary conditions.....	98
6.2.3 Solution for the hydraulic potential, $\Phi(x, y)$,	

of the groundwater.....	99
6.2.4 The stream function, $\Psi(x, y)$, of the groundwater.....	100
6.2.5 Solving for $\Psi(x, y)$	102
6.2.5.1 Calculation of α_n coefficient.....	102
6.2.5.2 Error analysis.....	104
6.2.6 Calculation of the flux (q).....	105
6.2.7 Programming.....	106
6.2.7.1 Determination of the sediment surface, water table and free surface water.....	106
6.2.7.2 Steps in the program.....	106
6.3 Results.....	107
6.4 Discussion.....	116
Chapter 7. Conclusions and Recommendations.....	117
7.1 Introduction.....	117
7.2 Practical and Academic significance of the study.....	117
7.3 Recommendations for future research work.....	118
7.4 Conclusions.....	119
References.....	121
Appendix 1 Visual Analysis and Colour Photographing of the Cores.....	129
Appendix 2 Grain Size Analysis of the Cores.....	140
Appendix 3 Calculation of Stream Values of the Groundwater Flow Modelling.....	150
Appendix 4 Calculation of the porosity, equation 4.10 on Chapter 4.....	156

List of Tables

Table 3.1: Depth of core into sediment (column 2) and actual core length (column 3), showing compaction at the drilling sites of Cocoa Creek. The compaction factor (column 4) was not constant.....	36
Table 3.2 Hydraulic conductivity of salt flat sediment.....	56
Table 4.1: Hydraulic conductivity at different field sites measured by removing water from the animal burrows.....	72
Table 4.2: Average and standard deviation (in brackets) of hydraulic conductivity calculation of mangrove sediment using Evapotranspiration 1 mm/day and 2 mm/day and porosity, p, of 0.46 ± 0.05	74
Table 5.1: Position and name of piezometers used for recording groundwater level.....	80
Table 5.1: Average and standard deviation of speed of infiltration obtained from each piezometer in two areas (Cocoa and Gordon Creeks, column 2), and volume of infiltrated water at each site (column 3).....	92
Table 6.1: The comparison between the result of the flux calculated from the model (stream function) and from the field measurement.....	115

List of Figures

Figure 1.1: Cross section of a salt flat/mangrove swamp and possible water flows (after Ridd *et. al.*, 1997). “Flood 35 kg/m³” indicates the salt concentration of creek water entering the salt flat as surface water during tidal inundation. “Ebb 36 kg/m³” indicates the salt concentration of surface water during ebb tide. “Creek 35 kg/m³” indicates the creek water salt concentration. “Groundwater 100 – 200 kg/m³” indicates the groundwater salt concentration.....3

Figure 1.2: View of a salt flat and mangrove forest in the upper reaches of Cocoa Creek, Townsville, North Queensland, Australia at flooding tide. The brown land is salt flat sediment, which is higher than the mangrove sediment. When the tide rises higher than shown on this photo, the salt flat sediment may be totally covered by tidal waters..... 4

Figure 1.3: Resin cast of a *Sesarma messa. alpheus cf. macklay* burrow excavated from *Rhizophora stylosa* forest at Gordon Creek mangrove forest area (photo courtesy of T. Stieglitz, 2000).....6

Figure 1.4: Hydrological processes in a tidal wetland (after Mitsch and Gosselink, 1993).....10

Figure 2.1: Physiography of the Townsville plains.....17

Figure 2.2: Sea-level curve of Larcombe *et al.* (1995a) taken for the central GBR shelf region.....20

Figure 2.3: Study sites: Cocoa Creek (salt flat and mangrove forest), Gordon Creek mangrove forest) and Three Mile Creek estuary (mangrove forest).....22

Figure 2.4: Cocoa Creek, one of the field sites, is one of the important creeks that flow into Cleveland Bay.....23

Figure 2.5: Cocoa Creek topography and vegetation. B is the area where electromagnetic induction and resistivity methods were used to measure groundwater salt concentration and groundwater salinity by Sam & Ridd (1998), Ridd & Sam (1996b) and Sam (1996). A is the field area of this study.....25

Figure 2.6: Gordon Creek area, *ca.* 5 km south of Townsville. Mangrove forests grow along the creek and salt flats lie beyond the mangrove forest.....27

Figure 2.7: Gordon Creek is a tributary of Ross River, flowing into Cleveland Bay. The experimental site was located in the mangrove forest within the middle section of the creek.....	29
Figure 2.8: Aerial photograph of Three Mile Creek, located <i>ca.</i> 15 km Northwest of Townsville.....	31
Figure 2.9: Three Mile Creek flows along the mangrove area, salt flat and finally enters Rowes Bay. The study area was in the mangrove sediment, on the East side of the road.....	32
Figure 3.1: Drilling locations in the upper reaches of Cocoa Creek. Two cores were collected at locations A, D and E at two different depths (2m & 4 m, 2 m & 3.35 m, and 2 m & 2.91 m respectively), and one core was collected at 2 m depth at all other locations.....	34
Figure 3.2: Vibrocoring conducted on a salt flat in the upper reaches of Cocoa Creek, on October 18 th and 19 th 2000.....	35
Figure 3.3: Schematic diagram of the resistivity probe used for measuring conductivity of the sediment (after Ridd and Sam, 1996b).....	40
Figure 3.4: Comparison between colour photographing and visual analysis for core from site A4. The length of the core is 3.04 m, but original length in the filed is 4 m. The core is stretched to become 4 m length (depth).....	43
Figure 3.5: Particle size analysis for site A4. A4Top means the sample is taken from the top of the core, and A65 means the sample is taken from 0.65 cm depth in the core, etc.....	44
Figure 3.6: Reconstruction of <i>in-situ</i> sediment stratigraphy based on visual analysis, colour photographing and particle size analysis for mangrove area, dead mangrove area and salt flat areas at upper reaches of Cocoa Creek.....	45
Figure 3.7: Depth contour plots of sediment bulk conductivity along the transect that crossed mangrove, dead mangrove and salt flat sediments.....	46
Figure 3.8: The horizontal variation of groundwater salinity in Cocoa Creek study area. The data at the 0 m position was taken from water in the creek	50
Figure 3.9: The horizontal variation of groundwater density in Cocoa Creek study area. The data at the 0 m position was taken from water in the creek	51
Figure 3.10: Sketch of a falling-head permeameter as used in this study, after modification of a design by De Marsily (1986).....	53

Figure 4.1: Schematic diagram of crab burrows that are intermingled with, but separate from each other. (a) shows the case when a quantity of water is pumped from burrow B. (b) shows the normal relative water levels in the burrows, i.e. where the closer the burrow to the creek, the lower the water level in the burrow. Note the burrows size is greatly exaggerated compared to the size of the creek. (c) shows the plan view of three burrows systems that intermingle with each other.....60

Figure 4.2: Model of groundwater flow in the mangrove swamp during neap tides...64

Figure 4.3: The location of experiments at Cocoa Creek, Gordon Creek and Three mile Creek. Piezometer experiments were carried out at Cocoa Creek only, while burrow experiment were at all three locations.....68

Figure 4.4: Array of piezometers in the upper reaches of Cocoa Creek.....69

Figure 4.5: Sediment particle size distribution at the study sites. The samples were taken at the mangrove forest of *Rhizophora stylosa* at Cocoa and Three mile Creeks and *Ceriops spp.* at Gordon Creek.....71

Figure 4.1: Fluctuation of groundwater and creek water level at site A, B and C at Cocoa creek recorded using pressure sensors. Of particular note is the water level at the site closer to the creek (A), shows a very pronounced tidal signature. At site C there is no tidal signature at the diurnal and semidiurnal frequency but the spring-neap oscillation is evident the tidal signature is so small.....73

Figure 5.1: Groundwater flow paths through a mangrove swamp during tidal inundation, via direct flow caused by infiltration and via burrow flushing.....78

Figure 5.2: Piezometers transects as installed: (a) in the upper reaches of Cocoa Creek, with three instruments amongst live mangroves, and one in a mixed zone of dead and live trees; and, (b) at Gordon Creek.....81

Figure 5.3: Schematic view of the PVC tube used to install piezometers in the field at Cocoa Creek. The same setup was used at Gordon Creek, except that no bentonite barrier was used above the sand screen.....83

Figure 5.4: Position of the underground water table during ebb tide. During a few hours (days), when ebb or small high tides occur, the water table in the sediment body will drop in relation with the porosity of the sediment.....85

Figure 5.2: Fluctuations of groundwater level and tides at Cocoa Creek sites with respect to the sediment surface level. Swamp sediment surface level at each site and tidal levels taken from tide tables at Townsville are also shown.....89

Figure 5.3: Fluctuations of groundwater level (from piezometer records) and tides (from tide table) at the Gordon Creek sites	91
Figure 5.7: Comparison of direct groundwater flow and burrow flushing flow rates.....	93
Figure 6. 1: Model of the groundwater seepage to the creek. In this model, h_2 is 0 m ..	98
Figure 6. 4: The condition of the sediment, free water table and stream line, when sediment is water saturated or dry zero	108
Figure 6.3: The condition of the sediment and free water table and stream line, when one day after inundation.....	109
Figure 6.4: The condition of the sediment and free water table and stream line, on two days after inundation	110
Figure 6.5: The condition of the sediment and free water table and stream line, on three days after inundation	111
Figure 6.6: The condition of the sediment and free water table and stream line, on four days after inundation	112
Figure 6.7: The condition of the sediment and free water table and stream line, on five days after inundation	113
Figure 6.8: Stream value for each distance from the end of the sediment to the creek bank at the sediment is water saturated (as a condition on Figure 2).....	114
Figure 6.9: Visualisation of Table 6.1	115

Chapter 1. Introduction

1.1. Definitions of wetlands, mangroves and salt-flats

1.1.1. Wetlands

A wetland is an area that has transitional communities between land and water, and can be seasonally or continually covered by water. One definition of wetlands is given as *“areas of marsh, fen, peatland or water, whether natural or artificial, permanent or temporary, with water that is static or flowing, fresh, brackish or salty, including areas of marine waters, the depth of which at low tide does not exceed six meters (and) riparian and coastal zones adjacent to the wetlands or islands or bodies of marine water deeper than six meters at low tide lying within”* (Matthews, 1993; Falconer and Goodwin, 1994). Another definition of wetlands is given by the Fish and Wildlife Service (United States) as: *“lands transitional between terrestrial and aquatic systems where the water table at or close to the land surface or the land is covered totally by water”* (Roggeri, 1995).

Saline wetlands are the wetlands that are filled with saline water. The volumes of saline wetlands and fresh water wetlands in the world are similar, with 124 103 km³ and 126 103 km³, respectively. These volumes represent 0.008% of all water volume on earth for saline wetland and 0.009 % for fresh water wetlands, with the largest volume found in the oceans with 97.61 % of all global water volume (Williams & Kokkinn, 1988). Economically, saline wetlands are important, as they can become a source of mineral and organic products, water, energy, etc. Marine wetlands are one form of saline wetlands, and include mangrove swamps and salt flats.

1.1.2. Mangroves

Mangroves are trees and shrubs that live in many tropical and some subtropical wetlands and typically form a tidal forest (Taal, 1994). Mangroves exist in relatively high salinity conditions, but these trees can rapidly die if the environment changes. These forests can be found along the length of an estuary, in lagoons that have entrance channels to the sea, between estuaries, creeks and salt flats etc, depending on the type of mangroves. Mangrove forests are believed to be effective in conserving nutrients for animal communities around this ecosystem (Taal, 1994).

Mangroves can live in tropical and sub-tropical regions. Their southernmost margin is at 37°S in Auckland Harbour, New Zealand, and their northernmost margin is in Bermuda and the Kyushu Island of Japan, approximately 33° N (Taal, 1994). The optimum geographical area for mangroves to grow appears to be on tropical shorelines characterized by a large intertidal field with muddy areas produced by overbank deposition, with a plentiful supply of fine-grained sediment and of freshwater. However, these trees can also live on sand, volcanic lava and carbonate sediments and be deprived of freshwater supply for months.

1.1.3. Salt flats

Tropical tidal salt flats are a type of arid tidal wetlands, which are located in the highest intertidal zone, have a high evaporation rate and occur in dry areas (Ridd *et al.*, 1997). These areas rarely experience tidal inundation and receive low rainfall. Because of these conditions, the groundwater in the salt flats contains a high salt concentration. A possible hydrological system of a salt flat and mangrove swamp is shown in Figure 1.1 and a photo of a salt flat and mangrove forest is shown in Figure 1.2.

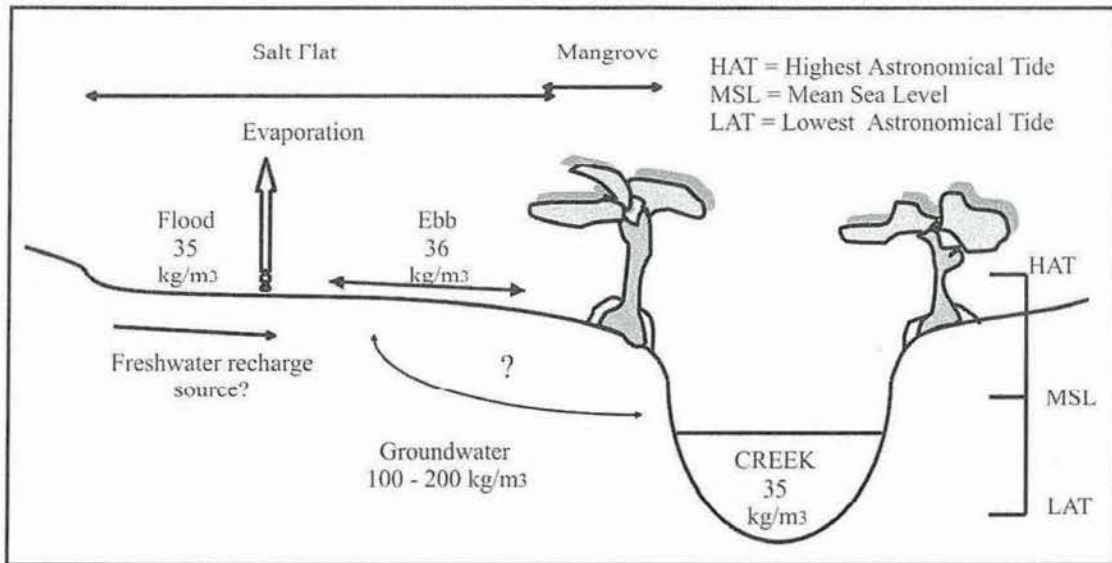


Figure 1.1: Cross section of a salt flat/mangrove swamp and possible water flows (after Ridd *et al.*, 1997). “Flood 35 kg/m³” indicates the salt concentration of creek water entering the salt flat as surface water during tidal inundation. “Ebb 36 kg/m³” indicates the salt concentration of surface water during ebb tide. “Creek 35 kg/m³” indicates the creek water salt concentration. “Groundwater 100 – 200 kg/m³” indicates the groundwater salt concentration.

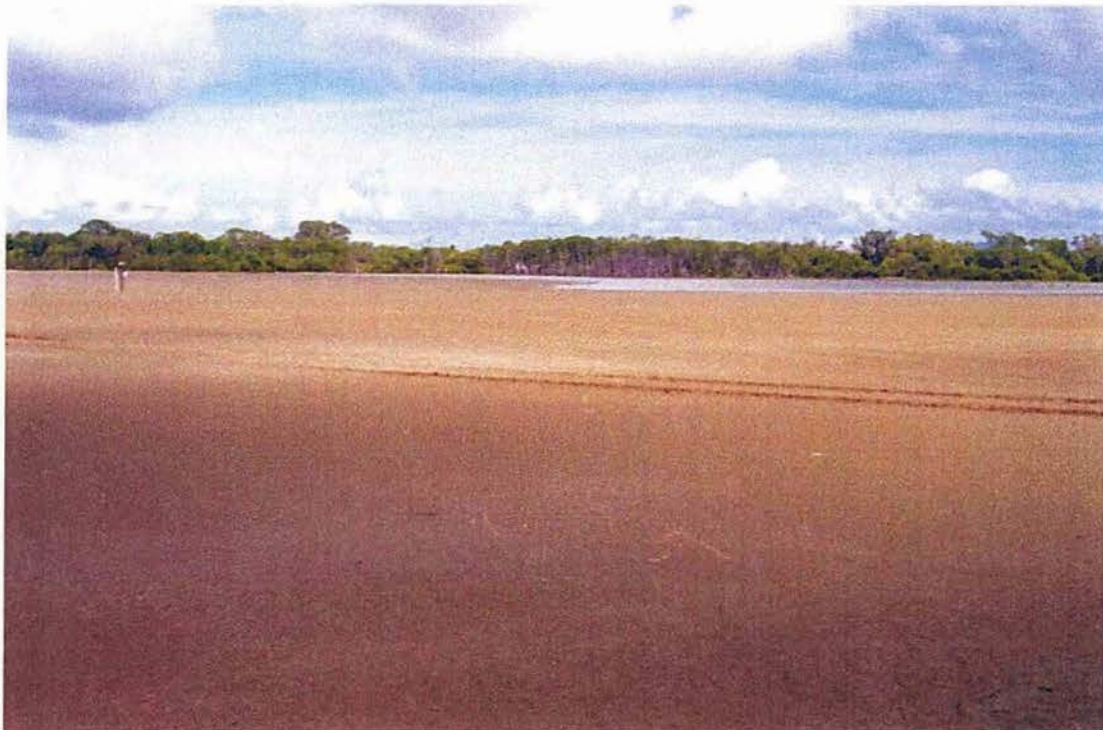


Figure 1.2: View of a salt flat and mangrove forest in the upper reaches of Cocoa Creek, Townsville, North Queensland, Australia at flooding tide. The brown land is salt flat sediment, which is higher than the mangrove sediment. When the tide rises higher than shown on this photo, the salt flat sediment may be totally covered by tidal waters.

1.2. Underground processes in wetlands

1.2.1. Evapotranspiration and build up of salt at mangroves roots

Salt concentration in salt flat and mangrove environments changes with time due to evaporation from the surface and evapotranspiration from mangrove trees. Evaporation is a process where a liquid (in this case water) is transformed entirely into a gas. Transpiration is the same transformation process of the water into vapor (gas) within a plant (Burman and Pochop, 1994). The combination of both processes, evaporation from the surrounding soil and transpiration from the leaves is called evapotranspiration. Hollins & Ridd (1997) and Wolanski & Ridd (1986) found that evaporation and evapotranspiration at salt flat and mangrove environment ranged from 1 to 5 mm/day and 2 mm/day respectively. When evaporation and evapotranspiration occur at the sediment level, salt is left at the surface. By inundation by tidal water, some salt may be entrained by the water that infiltrates into the sediment and some may flow back to the creek via surface runoff.

Mangroves tend to salinize the soil around their roots by excluding salt from the seawater that they absorb (Passioura *et al.*, 1992). Typically, roots exclude 90% or more of the salt present in the absorbed seawater, so that with time, there is the potential for significant buildup of salt around roots. The removal of the accumulated salt is a vital mechanism to the mangrove tree if the groundwater salinity is to remain below lethal levels. If groundwater salinity is greater than 90, conditions typically become fatal to mangrove trees (Semeniuk, 1983).

1.2.2. Animal burrows, salt diffusion and flushing

Mangrove forest sediments are characterised by the presence of many macropores, more specifically animal burrows. Stieglitz *et al.* (2000a) found that the volume of a crab burrow of *Sesarma messa alpheus cf. macklay* at Gordon Creek is in the order of 0.07 m^3 or about 10 % of the total volume of the surrounding sediment, its depth is *ca.* 1.2 m, and one burrow system may have up to 9 openings. They also found that burrows are discrete systems (Figure 1.3) that are partly intermingled with each other, but not interconnected. This is likely to increase the fraction of soil occupied by burrow galleries.

Burrows that are produced by crabs or other organisms, and by dead roots from mangrove trees, can modify physical characteristics of the sediment (Ridd, 1996a), such as its hydraulic conductivity. Sediment hydraulic conductivity is usually determined by the sediment particle size distribution (Wilson, 1994), and mangrove sediment, which has a high clay content, is thus potentially highly impermeable with a very low hydraulic conductivity (Stieglitz *et al.*, 2000a; Heron, 2001a). Hughes *et al.* (1998a) estimated that the surface hydraulic conductivity of intertidal zone sediment in estuarine wetlands of the Hunter Valley, Australia, based on laboratory measurements (slug test, Guelph permeameter and falling head permeameter) was approximately 0.01 m/day. However, in the presence of numerous burrow systems and smaller macropores in mangrove sediment, which are believed to intermingle with one another, the soil hydraulic conductivity was estimated to increase by one to two orders of magnitude (0.1 to 1 m/day) (Hughes *et al.*, 1998a).

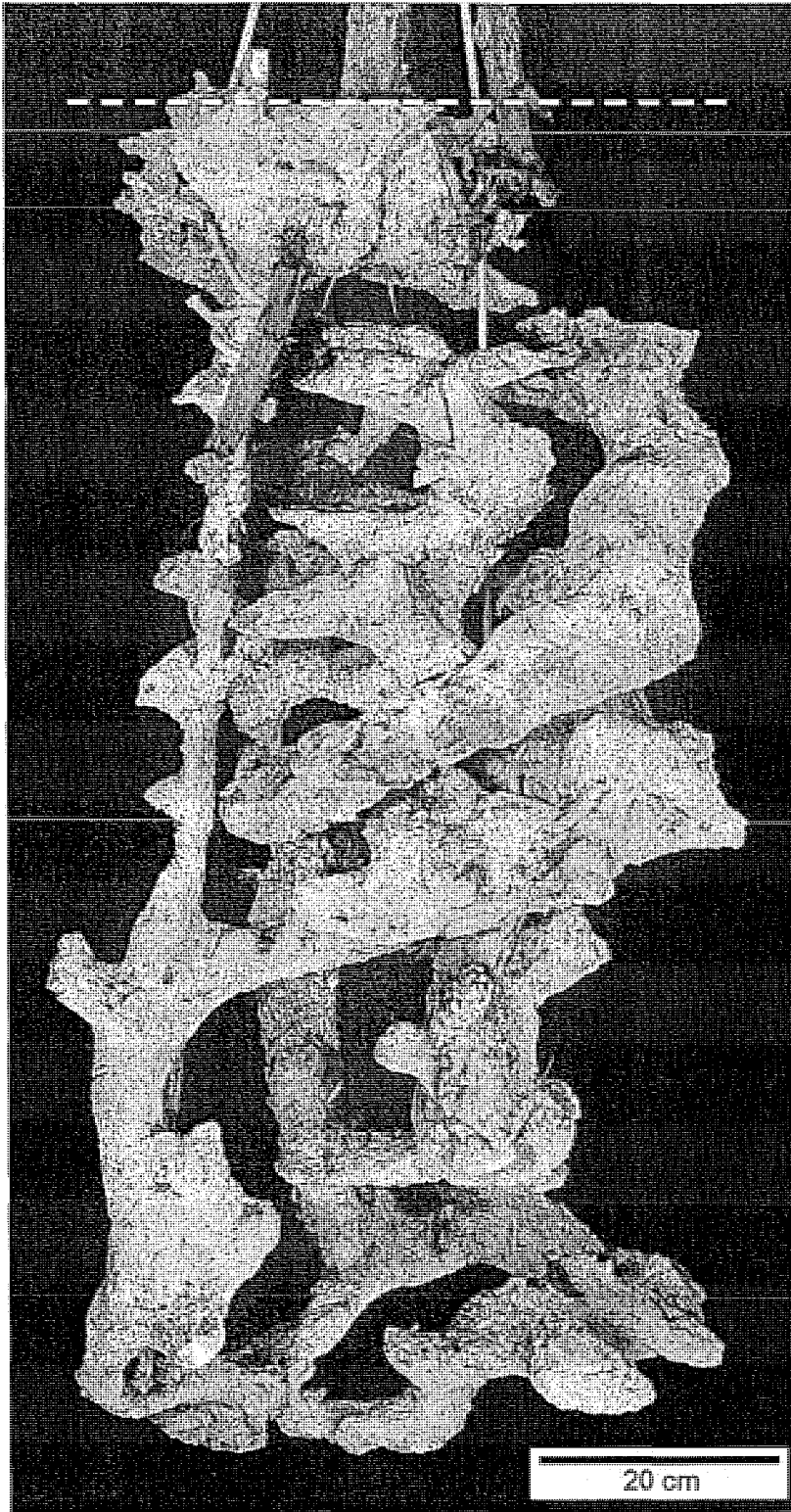


Figure 1.3: Resin cast of a *Sesarma messa. alpeus cf. macklay* burrow excavated from *Rhizophora stylosa* forest at Gordon Creek mangrove forest area (photo courtesy of T. Stieglitz, 2000).

Flushing of burrow water occurs especially during tidal inundation and is caused by a pressure difference across the numerous openings of the burrow due to the surface water slope (Aucan & Ridd, 2000). It was estimated that *ca.* 30% of burrow water is flushed per tide during that process (Hollins and Ridd, accepted), entraining salt and other material out of the burrow and into the creek. This proportion depends only on the area inundated by the tide and on the burrow volume.

This flushing mechanism is particularly important when considering the diffusion process of salt that occurs in mangrove sediment, i.e. the diffusion of salt from mangrove root areas (due to evapotranspiration) towards surrounding burrows over short distances, which is between 0.1 and 0.15 m (Heron, 2001a). If the salt accumulated around mangrove roots is not removed from the root zone, concentrations can limit growth of mangrove trees and lead to fatal hypersaline conditions (Passioura *et al.*, 1992; Tomlinson, 1986). With diffusion of salt occurring from mangrove root areas to burrows, the salinity, conductivity and density of the burrow water increases significantly, before flushing occurs during successive tidal inundations (Stieglitz *et al.*, 2000b; Hollins *et al.*, 2000; Heron and Ridd, 2001b).

1.2.3. Infiltration processes

Infiltration in the wetland environment (mangrove and salt flat) depends on the vegetation cover of the area, the duration of rainfall or inundation of the tide, the slope of the land surface, the type of soil and especially the soil surface porosity, and the depth of the zone of saturation and water table (phreatic surface). Vegetation covering the wetlands or salt flat is very important as it shelters the soil. Initial rainfall will merely wet the vegetation. If the duration of the rainfall is longer than the time needed to wet the vegetation or anything covering the wetlands/salt flat, the rainfall will penetrate the soil if the soil surface is permeable. Once the water can pass the surface soil, it percolates downwards until it reaches the saturation zone at the phreatic surface (Wilson, 1994).

The infiltration process from inundation and rainfall through the sediment surface, and especially through mangrove and salt flat sediment surfaces, depends on soil properties and conditions (Ward & Elliot, 1995). Soil properties include soil water content, texture, density, organic matter content, hydraulic conductivity and porosity, and in mangrove areas they also include the presence of crab burrows and other smaller macropores. Conditions of soil surface include compaction, topography, slope and roughness. As an example of the influence of some soil properties, in this case the presence of burrows, Hughes *et al.* (1998a) and Hughes (1998b) measured the infiltration in an estuarine wetland at Hunter River, Australia, where crab burrows were present. They found that, because of crab holes and other smaller macropores, the overall surface infiltration increased 1 to 2 order of magnitude compared to a situation where there was no hole.

1.3. Significance of hydrology in wetlands

1.3.1. Contribution to nutrient and salt cycling

Groundwater flow in mangrove creeks has attracted a large amount of scientific research in recent years (Lara and Dittmar, 1999; Cohen *et al.*, 1999; Kitheka *et al.*, 1999; Stieglitz *et al.*, 2000a; Heron, 2001a; and Hollins *et al.*, 2000). Groundwater flow is a main pathway for nutrient transport from the land or swamp area to the creek, along with surface flow due to rain runoff or due to tidal inundation (Lara and Dittmar, 1999). Mazda *et al.* (1990) and Wolanski (1992) predicted that groundwater flow through mangrove swamps is an important factor in determining the nutrient budget and water properties of the receiving mangrove creek. Kitheka *et al.* (1999) found that the contribution of groundwater seepage, including nitrite and nitrate components, was highest during the dry season in Mida Creek, Kenya. Nevertheless, groundwater flow typically decreases in absolute volume over the dry season. Lara and Dittmar (1999) and Cohen *et al.* (1999) reported that nutrient concentrations in a

mangrove creek in Brazil had a tendency to decrease towards the end of the dry season, which may be linked to a reduced groundwater flow dynamics.

This illustrates the fact that groundwater flow in mangrove swamps may be particularly important in areas where rainfall is limited or highly seasonal and where surface flow is therefore reduced or non-existent for most of the year. For instance, groundwater seepage due to the tide passing through mangrove swamps has been found to maintain mangrove trees during the dry season, although nutrient shortage and high salinity were occurring in the mangrove forest (Kitheka *et al.*, 1999). Hughes *et al.* (1998a) also found that groundwater flow in the Hunter River estuary, Australia, resulting from tidal forcing was a preferred pathway for the tidal water to return to the creek during dry periods. By such mechanisms, groundwater flow can potentially contribute to the nutrient cycle of a mangrove swamp, which is thought to be important for the ecology of mangrove ecosystems (Wolanski, 1992).

Hence, the hydrology of a wetland is arguably the most important factor in maintaining the wetland environment. The tidal average hydrological processes, including precipitation, evapotranspiration, evaporation, groundwater flow, inundation during a high tide, surface runoff, etc, (as shown in Figure 1.4), will determine the transport of energy and nutrients from and to the wetland, and a change in the hydrological cycle can change the physical and chemical properties of nutrients in the wetland (Mitsch and Gosselink, 1993).

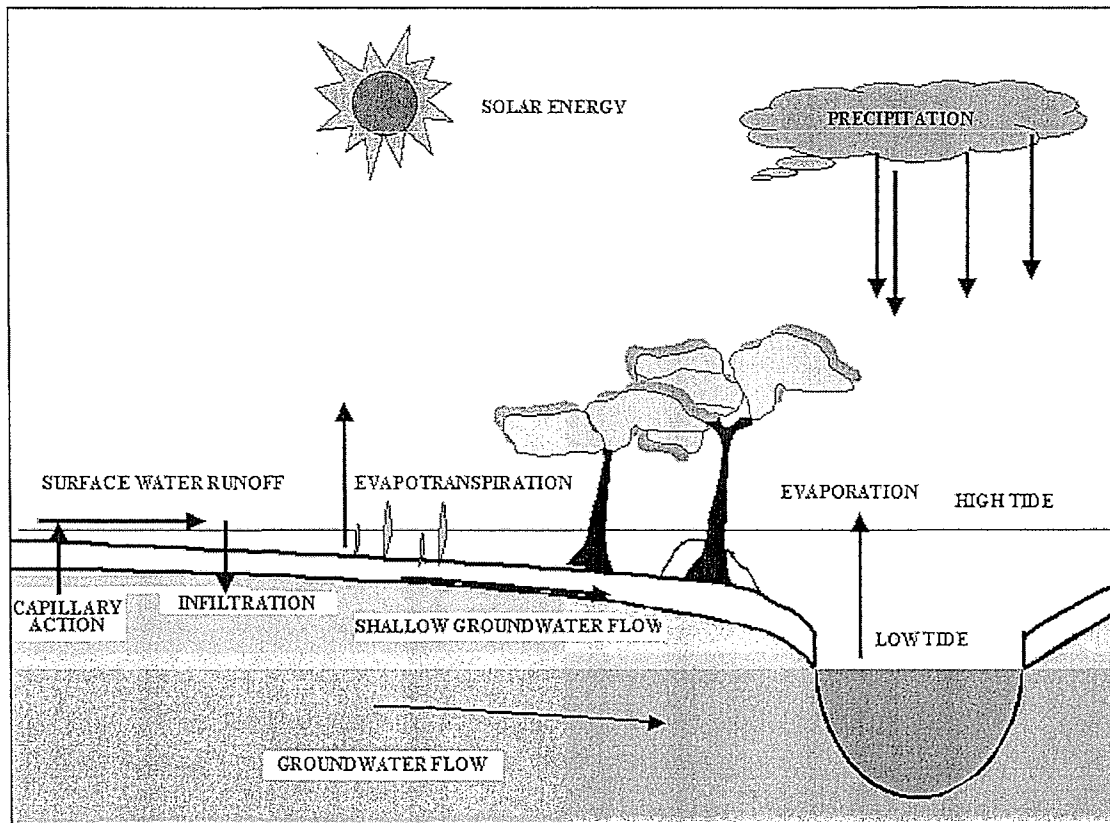


Figure 1.4: Hydrological processes in a tidal wetland (after Mitsch and Gosselink, 1993).

1.3.2. Influence of groundwater in mangrove swamps

As mentioned previously, groundwater salinity has a significant influence on the growth of mangrove trees. Mangroves growing in areas that are frequently inundated by tide, or in freshwater regions of the estuary, are likely to grow more rapidly than those living in regions where the swamp is rarely flushed, and where groundwater salinity is very high (Tomlinson, 1986). In the tropics where rainfall is often highly seasonal, river flow in the wet season contributes significant quantities of organic matter, nutrients and sediment particles to the estuaries (Mitchell and Furnas, 1996). However during the dry season, when there is often little river flow, groundwater is likely to become the main factor for nutrients cycling between creek and swamp.

Besides affecting the nutrient cycling and water properties in the mangrove swamp, groundwater flow swamps also influences the porewater salinity of the soil in these areas. Two mechanisms have been identified by which salt can be removed from the root zone. Firstly, it may be dissolved and carried to the mangrove creek by direct groundwater flow through the sediment. Secondly, it can diffuse through the soil to nearby crab burrows (Stieglitz *et al.*, 2000a; Hollins *et al.*, 2000), from where it may be flushed during tidal inundation by the burrow flushing mechanism mentioned earlier (Ridd, 1996a; Stieglitz *et al.*, 2000a; Heron, 2001a). These mechanisms are vital for mangrove trees if salt concentrations are to remain below fatal levels.

1.3.3. Factors influencing groundwater flow and hydraulic conductivity

The movement of groundwater from a wetland to a place lower than the wetland, e.g. a creek, depends on soil characteristics (hydraulic conductivity) and water level between the wetland and the creek. If the hydraulic conductivity is homogeneous and isotropic, the water table depends on the water level of the creek. The smaller the hydraulic gradient of the water table, the smaller the seepage velocity of the groundwater (Raghunath, 1987). Hydraulic conductivity of a soil/layer in a wetland is influenced by temperature and ionic composition of water. Temperature affects the viscosity of the water. The higher the temperature the smaller the viscosity, and thus the easier it is for the water to pass through the soil. As a consequence, increased temperature will increase the soil hydraulic conductivity. The ionic composition of water is related to the equilibrium of cations of water, especially if the soil is clay. A change in ion concentrations may change the condition of the clay particles from a flocculated to a dispersed condition. This, in turn, can cause a decrease or increase of the hydraulic conductivity (K). The value of K depends also on the salinity of the water flowing to the soil. If the salinity of the water increases, the K value of the soil will decrease. Changes in salt concentration of groundwater can occur when this

water flows through dense clay. The pores of these clays can be smaller than the ions in the water and these clays can behave as a filter (Bouwer, 1978).

Other factors influencing the hydraulic conductivity of a soil layer is the presence of air in the soil itself, particle size and porosity of the soil. Presence of air trapped in dry soil or aquifer physically blocks the pores and causes difficulty for the water to pass through the soil. This can cause the hydraulic conductivity to be much smaller than if the soil was entirely water saturated. Peat, sand pumice and silt, for example, which are sometime present in wetland environments, have a high permeability, while clay has a low permeability. Porosity of the soil can determine whether the hydraulic conductivity of a soil layer is high or low, even though the basic rock or material composition of the soil may be the same. If the material composing the soil has good interconnection between particles (i.e. the porosity is low), the hydraulic conductivity will be lower than that if the material composing the soil has bad interconnection (i.e. the porosity is high). Particle size of the rock or material is also an important factor in determining the value of hydraulic conductivity. Generally, the higher the particle size composing the soil, the higher the value of hydraulic conductivity (De Marsily, 1986).

1.4. Groundwater modeling

1.4.1. Various groundwater flow models

Groundwater flow models in wetlands and in particular in mangrove environments have attracted several researchers (Bradley 1996 and Thompson & Hollis 1995). Most of these models involve inputs such as evapotranspiration, rainfall, hydraulic conductivity of the sediment and inundated area. Bradley (1996) developed a three-layer groundwater model in a floodplain wetland in England using MODFLOW software. Thompson & Hollis (1995) calculated simulation of water balance model for each month in Hedejia-Nguru wetlands, Nigeria. The model involved volume of water in the flood plain, water discharge in each site of observation, weighted mean rainfall, evaporation etc.

1.4.2. Series solution models

Another usable model to calculate groundwater flow uses a series solution. Series solutions for two-dimensional potential flow problems is a method to calculate hydraulic potential and stream function of the groundwater flow (Gill and Read 1996, Read 1993, Read 1996a, Read 1996b). The Laplace equation in the plane for potential flow is the basis of this formulation, i.e. $\nabla^2\Phi(x,y)=0$. This equation is solved using some boundary conditions (bottom, top, right and left) and the separation variable method is applied for this solution (Gill & Read, 1996). Solutions are sought in the form of a series, i.e. $\Phi(x,y)=A_0+\sum_{n=1}^{\infty}(A_n u_n(x,y)+B_n v_n(x,y))$ (Read, 1996a). A_0 is a constant, A_n and B_n are series coefficients, and $u_n(x,y)$ and $v_n(x,y)$ are trigonometry functions. It is impossible to calculate the series solution with an infinite number of series coefficient. Hence the solution of this equation uses the calculation of a finite number of series coefficient (n) that are defined by minimising the error between free water table, which is recorded and hydraulic potential, which is calculated. The calculation of the error uses Root Mean Square error method (Gill and Read, 1996)

1.5 Conclusion

1.5.1 Focus of the Thesis

From the forgoing discussion it is clear that there has been very little work done on groundwater issues in mangrove swamps, particularly in Australia. One of the factors inhibiting this work is the ability to easily and cheaply measure simple hydraulic parameters such hydraulic conductivity. In this thesis the primary objective is not to

study a particular area of mangroves but to develop general methods which may have more general application in many different regions.

This project has three aims, *viz.*,

1. **to develop a new method to determine the hydraulic conductivity of the mangrove sediment;**
2. **to calculate the relative magnitude of burrow flushing or direct groundwater flow to determine which process is most important in removing groundwater, and;**
3. **to develop a simple analytical model to calculate groundwater fluxes**

The rationale for each of these is given briefly below.

The development of a new method to determine the hydraulic conductivity of the mangrove sediment;

The hydraulic conductivity of the soil is a key parameter that determines groundwater flow. Because of the presence of animal burrows, the hydraulic conductivity is greatly modified compared with a similar soil with no burrows. Measurement of hydraulic conductivity of sediments is problematic, often requiring piezometers that are expensive and difficult to install. There is thus a need to develop a simple and inexpensive method of determining the hydraulic conductivity of the mangrove soil that takes into account of the burrows. Such a method is described in Chapter 4.

Calculation of the relative magnitude of burrow flushing or direct groundwater flow to determine which process is most important in removing groundwater

Groundwater can return to the mangrove creek by two mechanisms. The first is via conventional ground water flow down a hydraulic gradient, and the second is via the

direct flushing of water from animal burrows. Flushing of burrows occurs during tidal inundation of the swamp. This poses a question; which of these processes is most important? This is the subject of Chapter 5

The development of a simple analytical model to calculate groundwater fluxes

The ability to predict groundwater flow from the geometry of the location and measurements of hydraulic conductivity is a useful goal. In chapter 6, a simple analytical model is developed to model the flow from the mangrove swamps to the creek. The results of the model are compared with the measured groundwater fluxes described in Chapter 5

Chapters 2 and 3 describe the geographic locations of the field sites, the sediment and groundwater characteristics, and the methods used to measure these parameters.

1.5.2. Publication outcome of thesis

Some of the research carried out during this project has been presented in peer-reviewed journals and seminars. The status of these manuscripts is as follows

Susilo, A, and P.V. Ridd (in press). The bulk hydraulic conductivity of mangrove soil perforated with animal burrows. *Wetlands Ecology and Management*. This manuscript is in the Chapter 4, page 57

Susilo, A, Ridd, P.V. and Thomas, S. (in press). Comparison between tidally-driven groundwater flow and flushing of animal burrows in tropical mangrove swamps. *Wetlands Ecology and Management*. This manuscript is in the Chapter 5, page 77.

Susilo, A., Read W. W. and Ridd P. V. (in prep). A simple groundwater model for flow in mangrove swamps. *Wetlands Ecology and Management*. This manuscript is in the Chapter 6, page 96.

Chapter 2: Description of the study areas

2.1 General description of the study area

2.1.1. Physical setting

The Townsville area is located in the central Great Barrier Reef (GBR) area of North Queensland, Australia, and spreads over *ca.* 3750 km² (Hornby, 2003). The regional geological setting of Townsville is complex (Trezise and Stephenson, 1990). The basement (ancient rocks) is *ca.* 600 million years old and is mostly covered by younger volcanic rock. This younger layer has been eroded in some areas and is now covered by sediment resulting from erosion processes. Townsville area comprises coastal plains from Halifax Bay to Cleveland Bay, which can be divided into 3 regions (Hopley, 1970): Muntalunga Chenier Plain (region 1); the Bohle-Ross Plain (region 2); and the coastal plain North of Townsville (region 3) (see Figure 2.1). We restrict the scope of this study to region 1 and 2, where field experiments were conducted.

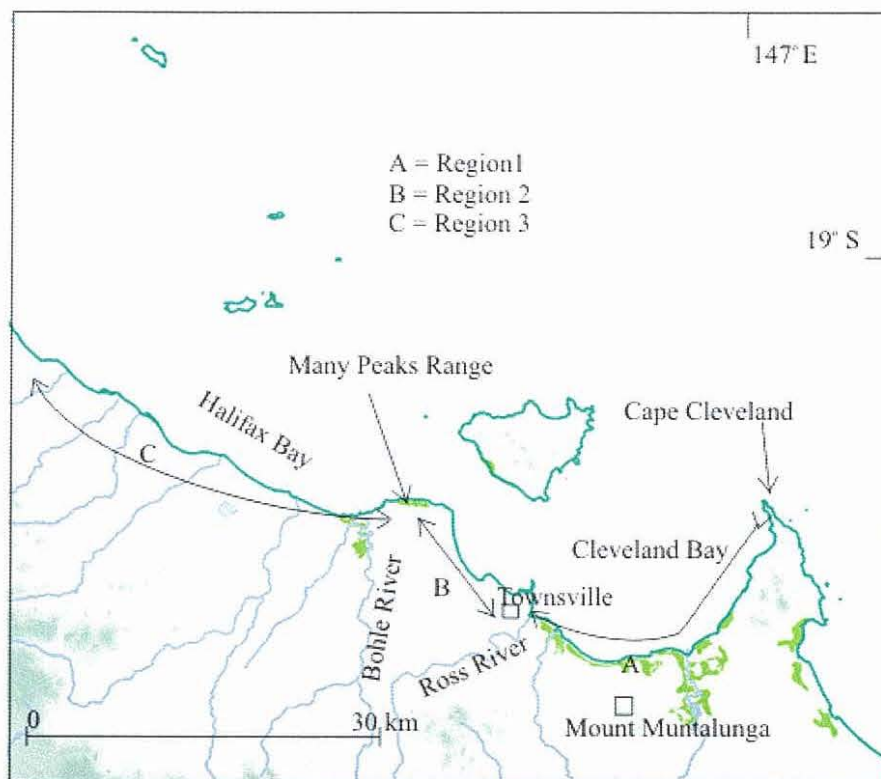


Figure 2.1: Physiography of the Townsville plains.

Muntalunga Chenier plain (region 1), named after Mount Muntalunga, which rises at 228 m asl (above sea level), lies from the mouth of Ross River in Townsville city to Cape Cleveland. Mount Muntalunga is located South-East from Townsville (see Figure 2.1). The plain is bordered by Cleveland Bay and is made of cheniers that lay over salt marshes and exhibit variations in lithology and height. This plain is typical of a low to moderate wave energy coastal environment, with mangrove forests growing along the outer edge of the coast. The lower areas, where the sediment gets most inundated by tidal waters, are colonized by *Rhizophora* and *Bruguiera*, whilst the most landward areas, which are higher areas and are less often inundated, are colonized by *Ceriops* (Hopley, 1970) before turning into a bare flat (also called salt flat) that is seldom inundated by the tide. These sediments are highly saline and therefore can only support algal mats.

The Bohle-Ross Plain (region 2) lies between the Ross River and the Bohle River. The geomorphology of the area has changed since reclamation operations occurred throughout the development of Townsville (Hopley, 1970), especially along the lower Ross River. The reclamation of the port of Townsville in particular could have changed the distribution of the sediment by blocking the dispersion of the sediment from Ross River to the north (Rowes Bay) (Aziz, 1992). Three major outcrops outline the general geomorphology of this area: Castle Hill, Mount Luisa and the Many Peaks Range. These outcrops, specifically Castle Hill and Many Peaks Range which are located hinterland of Rowes Bay, represent anchor points for the area (Trezise & Stephenson, 1990).

2.1.2. Climate and Tides

Townsville lies in the trade wind belt of the southern hemisphere. The weather in this area is largely influenced by high pressure systems crossing the continent at about 30° S. for winter and 40° S. for summer seasons (Pomery, 1987). Townsville, which has a dry tropical climate, is characterised by a bi-seasonal weather pattern, with a clear difference between dry winter and wet summer seasons. During the dry winter season

(April to November), high pressure systems cross Australia and cool southerly winds produce low winter temperature (around 20 °C). Semi permanent anti-cyclonic cells that lay in the South Pacific dominate the region. The South-Easterly air streams circulate around this anti-cyclonic cell (Hopley & Murtha, 1975) with speeds from 10 to 30 km/h (Muller, 2002). During the wet summer season (December to March), the region is influenced by the North-West monsoon. This brings the period of maximum rainfall. Hopley & Murtha (1975) stated that during 3 summer months (Jan. – Mar.), the rainfall can exceed 1100 mm, or *ca.* 65 % of the annual rainfall. Total annual rainfall ranges from 853 mm to 2571 mm, where an annual average rainfall of 1136 mm.

Under average conditions, wind speeds in Townsville are greater in the afternoon than in the morning. The annual averages of wind speed from daily reading at 3 pm and 9 am at Townsville airport are 20.4 km/h and 10.7 km/h respectively (Commonwealth Bureau Of Meteorology, 2003). Daily average temperature varies between 19.7° C and 28.8° C from winter to summer, with daily maximum and minimum of 25.0 ° C and 13.5 ° C in July (winter) and of 31.4 ° C and 24.0 ° C in December (summer). Average daily sunshine peaks in October with 9.7 hours of sunshine per day, is lowest in February with 7.2 hours of sunshine per day. The annual average is 8.4 hours per day (Hornby, 2003). Finally, Townsville lies within a cyclone area and 19 cyclones occurred in this region between 1969 and 1997 (Puotinen *et al.*, 1997). The most destructive cyclone for Townsville area over that period was “Althea”, which hit on 24th December 1971 and was associated with wind speeds up to 203.4 km/h, recorded at Townsville airport (Hopley, 1978). Evapotranspiration rates in the region are 800 mm/year (BOM, 2004).

The Townsville region has a typical spring tidal variation of 3.5 m and the tides are a mixture of diurnal and semidiurnal components.

2.1.3 Sea level variability.

The most recent sea-level curve proposed for the central Great Barrier Reef region (Figure 2.2) was based upon radiocarbon dating of 364 coastal and marine sediments samples along the central GBR (Larcombe *et al.*, 1995a; Larcombe, 1995b).

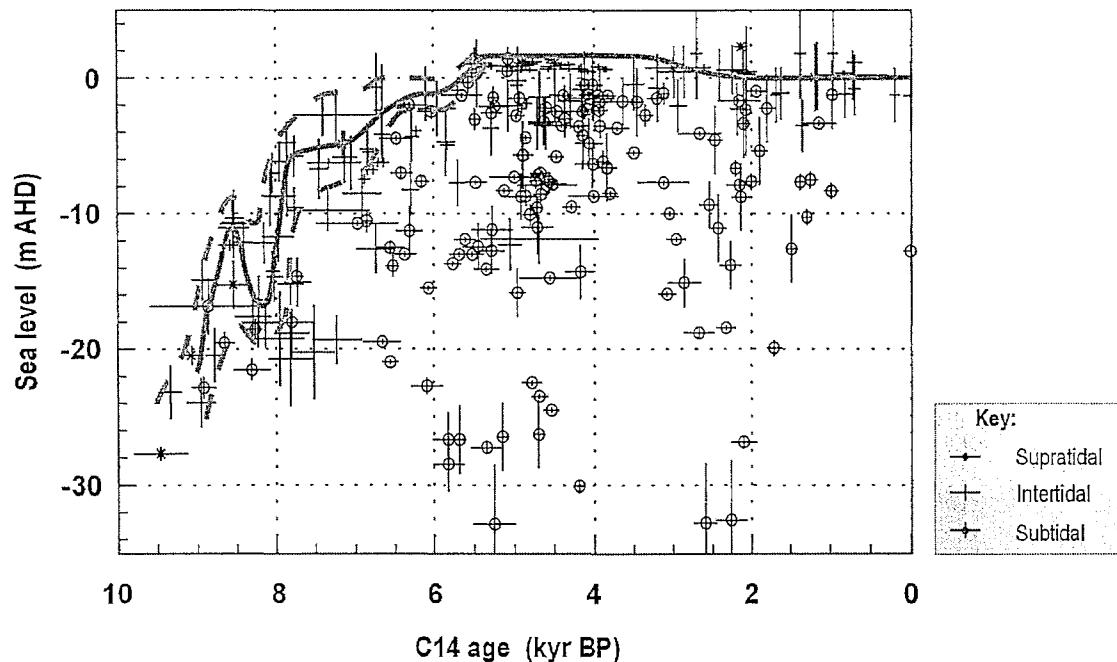


Figure 2.2: Sea-level curve of Larcombe *et al.* (1995a) taken for the central GBR shelf region.

Results indicated that sea level rise varied from 20 mm/year or 20 m/kyr for pre 8.2 kyr BP to 30 mm/year or 30 m/kyr for post 8.2 kyr BP. Evidences for periods of sea level fall from 8.5 kyr to 8.2 kyr were obtained from Cleveland Bay mangrove sediment, with younger deposits at depths of -17 m than at -12m (Larcombe *et al.*, 1995a & Larcombe, 1995b). Sea level between ca. 5.5 to 3.7 kyr BP was about +1.7 m above its present level, and the present high intertidal areas that are inundated by seawater only during spring high tides (the salt flats) were probably covered with mangrove forest during that period (remains of mangrove roots are found in the sediment, personal observation). A sea level drop by ca. 1.7 m since the sea level highstand caused the original mangrove forest to die and the areas to become salt flats. Today, these salt pans are subject to salt accumulation due to evaporation (by

ca. 2 mm/day (Hollins and Ridd, 1997)) after spring tide inundation a few times a year, and salt concentration in the groundwater exceeds 150 g/l (Sam & Ridd 1998, Sam 1996).

2.2 Field study locations

Studies were conducted at three sites of mangrove forest and salt flats in Townsville. These locations are the upper reaches of Cocoa Creek (region 1) in a mangrove forest and salt flats environment; the middle of Gordon Creek (region 1) in a mangrove forest environment; and around the estuary of Three Mile Creek (region 2) in a mangrove forest environment as well. The three study locations are shown on Figure 2.3, which are on the small black areas.

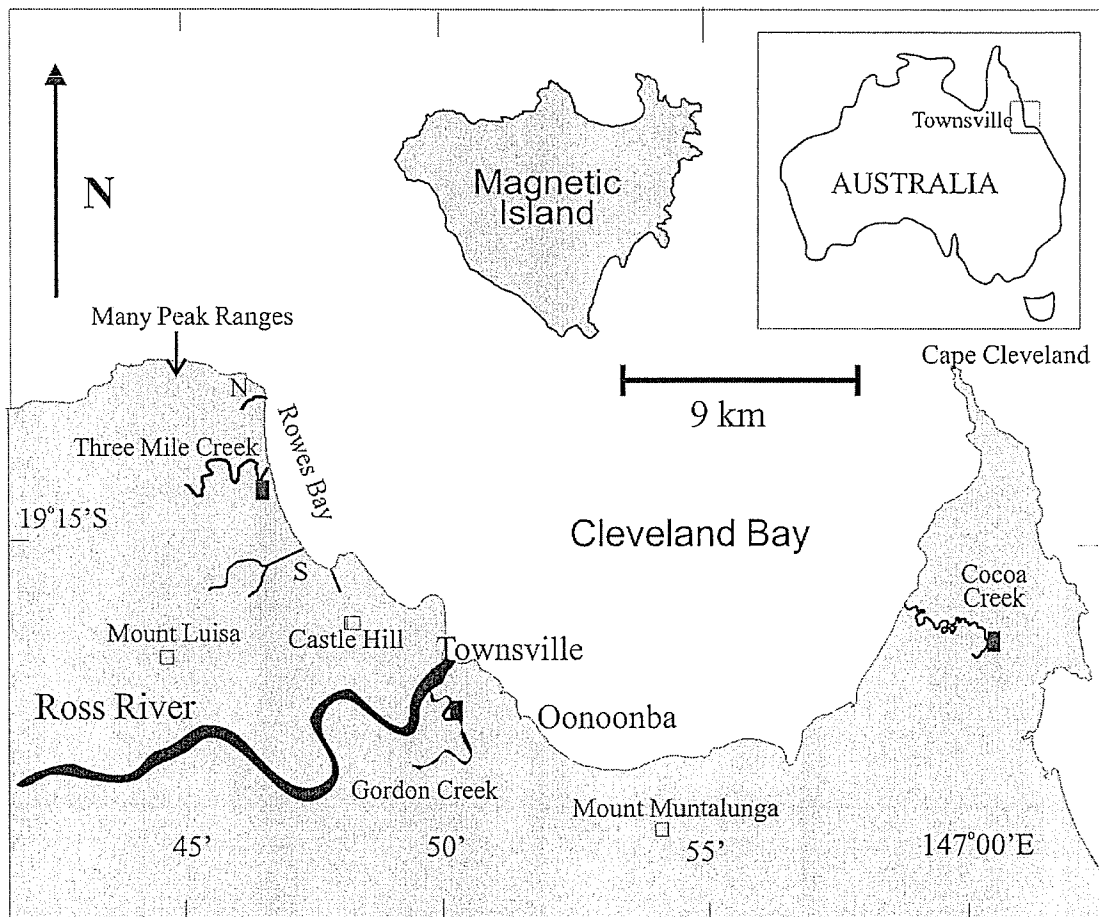


Figure 2.3: Study sites: Cocoa Creek (salt flat and mangrove forest), Gordon Creek mangrove forest) and Three Mile Creek estuary (mangrove forest).

2.2.1 Cocoa Creek

Cocoa Creek is one of three main tidal mangrove creek systems located in the southern part of Cleveland Bay, approximately 55 km south of Townsville (Figure 2.4 and Figure 2.5). Cocoa Creek is an undisturbed area within the Cape Bowling Green National Park with a total length of *ca.* 7 km and a width that ranges from approximately 50 m at the mouth of the estuary to less than 10 m at the head. Mangrove trees grow along the creek, which mainly is *Rhizophora stylosa* and the width of the mangrove fringe varies considerably along its length from a few meters to 50 m. Salt pans occupy about 8 km² of the high intertidal zone and cheniers or sand ridges occur above the intertidal zone. Grasses and some trees usually grow on the chenier ridges, but only algal mats grow on the salt pan.

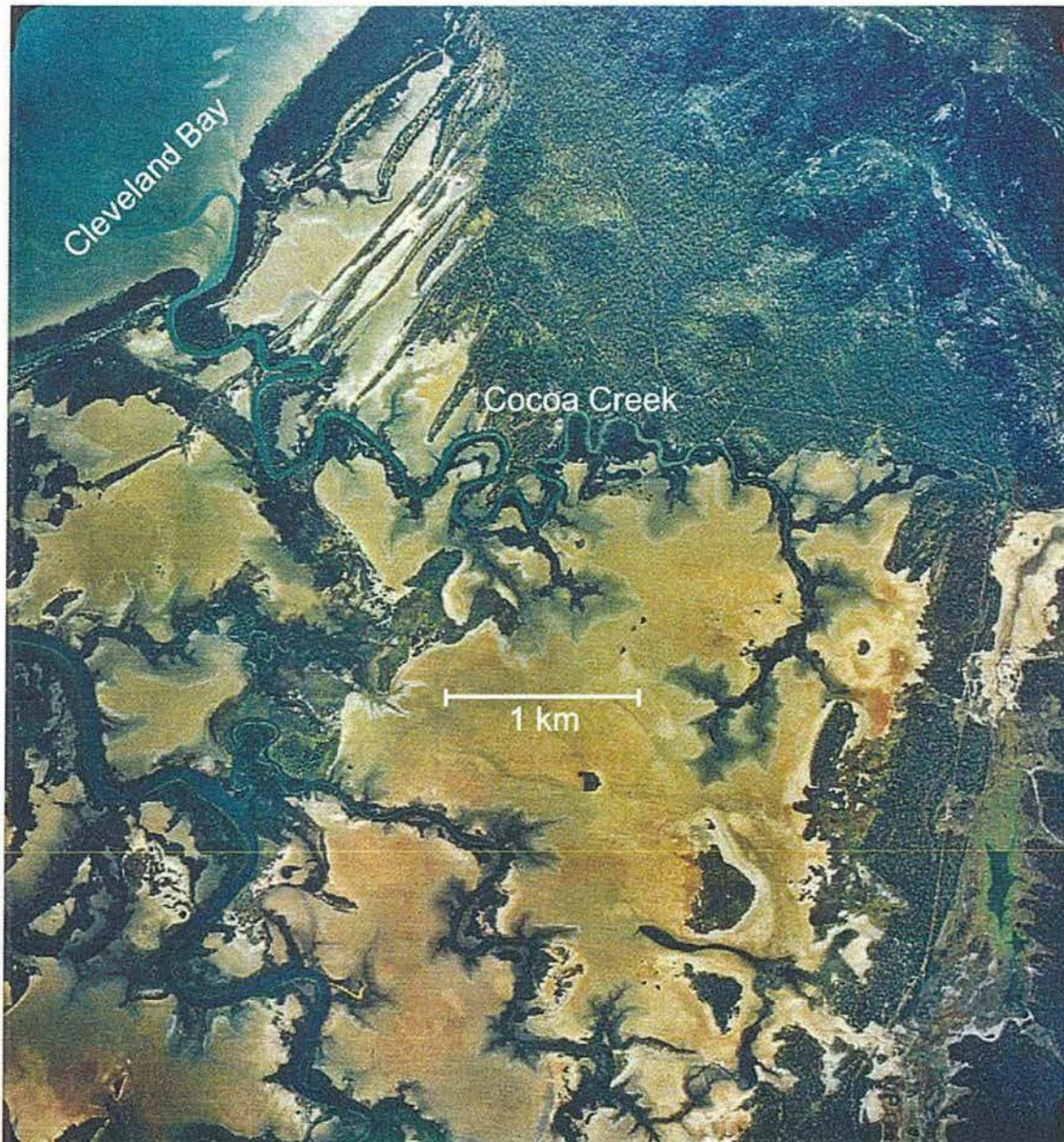


Figure 2.4: Cocoa Creek, one of the field sites, is one of the important creeks that flow into Cleveland Bay.

Modern sedimentation processes in the Cocoa Creek area have been investigated by Bryce (2001) and Bryce *et al.* (2003), which showed that suspended sediment concentration and sediment transport were primarily controlled by tidal currents. The sediment transport in this creek occurred in a two-way process, i.e. the net movement of gravel and sand is in the seaward direction, whilst the net movement of fine sediment occurs in the landward direction (Bryce, 2001). During all neap and intermediate tides, suspended sediment fluxes are oriented landward towards the head

of the creek, and these fluxes become a local supply of sediment for the overbank tides to come. During overbank tides, tidal currents are strongest during the ebbing period when SSCs (Suspended Sediment Concentrations) increase significantly all along the creek with a complex distribution pattern. Bryce *et al.* (2003) found that during within-channel tides, the suspended sediment transport is small (20 to 50 tons per tidal cycle), mostly landward directed. On the contrary, a significant seaward net transport of sediment takes place (from 50 up to 200 tons per cycle) during overbank tides, i.e. for tidal height above 2.9 m above LAT (Lowest Astronomical Tide). This pattern is accentuated during the largest tides (around 3.25 m LAT).

Besides the study of sedimentation processes, measurements of groundwater salt concentration were conducted across the mangrove swamps, cheniers, side creeks (streams that are lower than the surrounding area and that drain tidal waters back to the creek), salt flat and salt grass areas (Sam & Ridd, 1998; Ridd & Sam, 1996b; Sam, 1996) close to the estuary of Cocoa Creek (area B in Figure 2.5). Groundwater conductivity was obtained by Sam & Ridd (1998) by measuring the electromagnetic induction (EMI) and the resistivity of the ground immediately after tidal inundation, when the sediment was still water saturated. It was found that groundwater salt concentration depended on depth and area of the sediment. The concentration in the mangrove forest and near the edges of the salt flats (50 g/l) was lower than in the salt flats area (up to 150 g/l). In addition, at a depth greater than 0.8 m from the surface in all areas, salt concentration in the soil was more homogenous than at a depth less than 0.8 m. For example, at a depth *ca.* 2 m, the groundwater salt concentration varied from 75 g/l to 125 g/l, while at a depth of *ca.* 0.4 m, the variation ranged from 75 g/l to 175 g/l. Despite these differences with depths and environments, the overall pattern remained that the highest groundwater salt concentration occurred in the salt flat area, whilst the lowest salinity was found in the mangrove sediment.

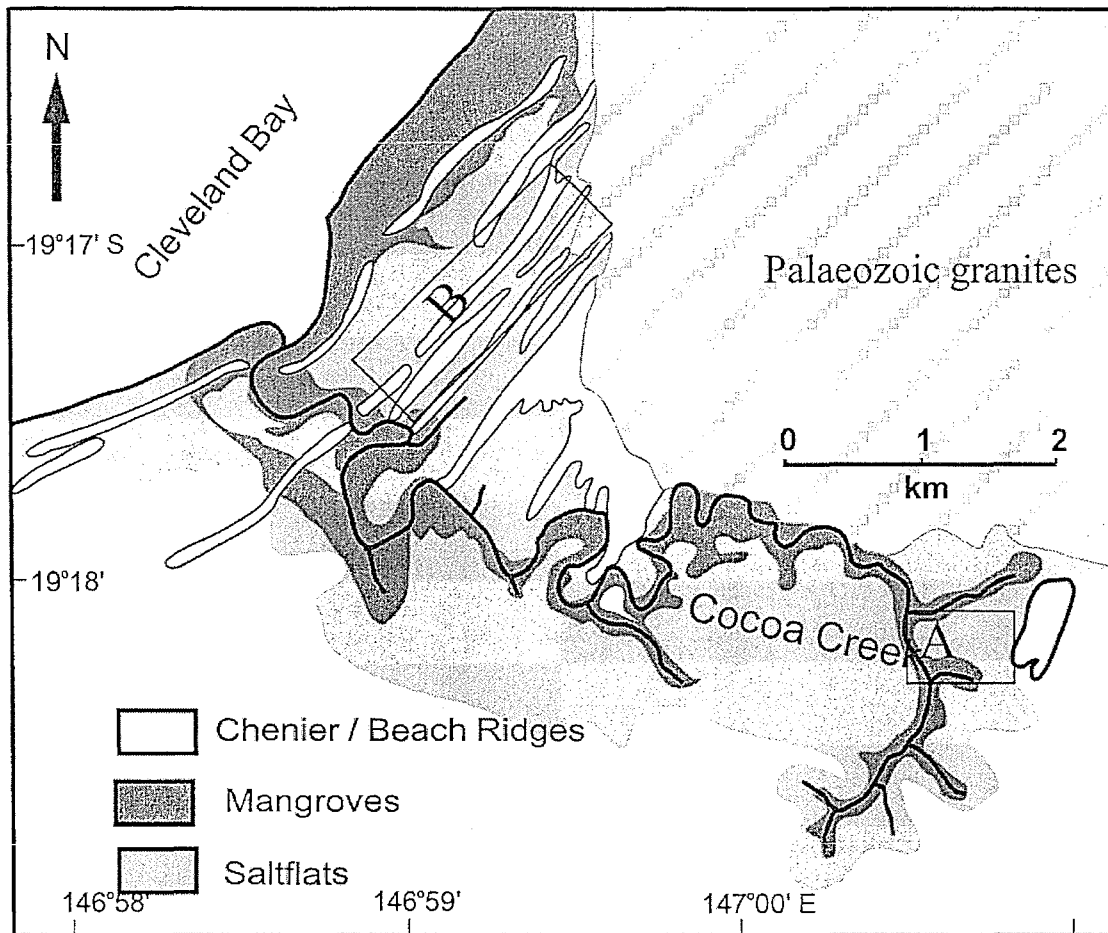


Figure 2.5: Cocoa Creek topography and vegetation. B is the area where electromagnetic induction and resistivity methods were used to measure groundwater salt concentration and groundwater salinity by Sam & Ridd (1998), Ridd & Sam (1996b) and Sam (1996). A is the field area of this study.

The field area, chosen in the upper reaches of Cocoa Creek (A on Figure 2.5), comprises a thin fringe of mangroves (*ca.* 9 m wide), an area of dead mangroves (*ca.* 20 m wide), and an extensive area of salt flats (*ca.* 160 m wide). The overall slope of the area is approximately 1:1200, with a maximum and minimum slope of 1:300 (mangrove area) and 1:1500 (salt flat) respectively. Cheniers occur in the area with the chenier ridges *ca.* 25 cm higher than the salt flat, and these ridges are therefore never inundated by tidal waters. Mangroves and salt flats are flooded for tidal range greater than 3.4 m above LAT, and the average inundation frequency of the field site is *ca.* 6 inundations/month for the salt flat area, with the maximum number of

inundation in March (approximately 13 times) and the minimum number in November (approximately 2 times) (Queensland Department of Transport, 2001).

2.2.2 Gordon Creek

Gordon Creek, a tributary of the Ross River that flows through Townsville and into Cleveland Bay, is a small creek *ca.* 5 km south of Townsville (see Figure 2.6). It is *ca.* 3 km long, and 16 m wide at the mouth and 4 m wide at the head. The entire catchment of this area is undisturbed with no commercial landuse. This creek is a mesotidal mangrove creek, has a seasonal freshwater input, and is subject to a semidiurnal tidal regime with a maximum high tide of *ca.* 4 m above LAT and a minimum high tide of *ca.* 2 m above LAT. At low waters, the bed of the creek, which is formed of silty sand (Larcombe and Ridd, 1996), is exposed, especially in the middle and lower reaches of the creek.

Mangrove forests grow along Gordon Creek. *Rhizophora stylosa* dominate and reach up to 8 m high at the edge of the creek. *Ceriops* are found further landward from the creek and reach a few meters high before rapidly becoming stunted (1 m high). Beyond this area lies a salt grass area (1 – 3 m in width), which finally joins with a bare salt flat. Mangrove forests and salt flats along the creek occupy *ca.* 1.5 km².



Figure 2.6: Gordon Creek area, *ca.* 5 km south of Townsville. Mangrove forests grow along the creek and salt flats lie beyond the mangrove forest.

Gordon Creek hydrodynamic regime is ebb-dominated, with maximum depth-mean current velocity of 0.62 m/s for flood tide and 0.98 m/s for ebb tide (Larcombe and Ridd, 1995c). The relative elevation of the mangrove sediment influences the sediment transport in the creek. The lower the elevation of the sediment is, the more often the sediment will be inundated, and the more sediment mass will be flushed during flooding and ebbing tides. Overbank tides that inundate the mangrove sediment/flat create strong ebb currents, flushing bedload to the seaward direction

with a rate up to 0.3 kg/s per meter of creek width. This rate is the same as the maximum suspended sediment flux occurring during flood tide in the landward direction. The tide in Gordon Creek is asymmetric, therefore the total sediments flushed during flood and ebb tide is different. During the dry season, annual bedload discharged seaward is up to 400 tons, which is much higher than at Cocoa Creek (up to 200 tons) (Larcombe and Ridd, 1996).

The creek margins lie at an elevation of *ca.* 2.9 m above LAT. This causes the entire mangrove fringe to be inundated during high tides with a range greater than *ca.* 3.0 m above LAT. The sediment of this mangrove forest is composed of a thick organic mud, which is burrowed by crustaceans. The average annual number of inundations is 19/month, with a maximum and minimum in March and November with approximately 26 and 11 times/month respectively (Queensland Department of Transport, 2001).

The study area lies in the middle part of Gordon Creek in the mangrove forest (see Figure 2.7) on the Eastern side of the creek. *Rhizophora stylosa* is the main mangrove species growing in this area, from the edge of the creek to *ca.* 36 m to the East, but *Ceriops* is also found beyond the field site and continues landward up to a small road. Burrows in this mangrove forest are mainly inhabited by the crab *Sesarma messa* *Alpheus cf. macklay* (Stieglitz *et al.*, 2000a).

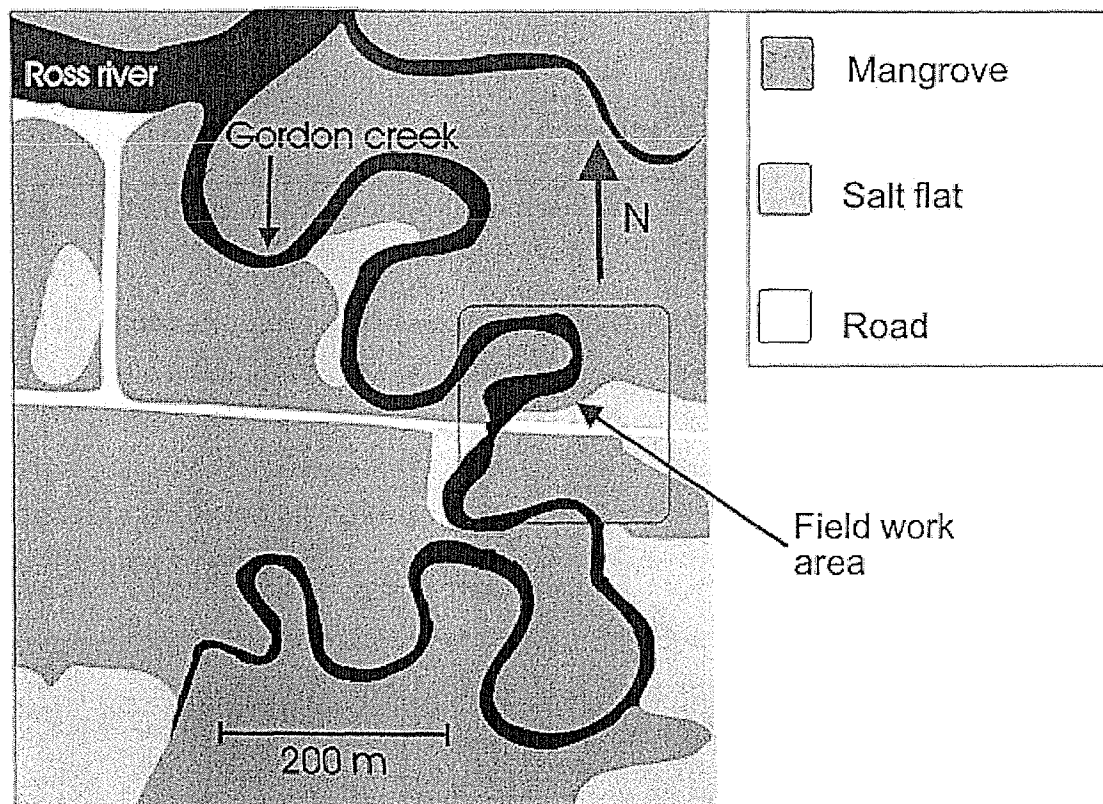


Figure 2.7: Gordon Creek is a tributary of Ross River, flowing into Cleveland Bay. The experimental site was located in the mangrove forest within the middle section of the creek.

Some geophysical studies relevant to groundwater flow dynamics occurring in the sediment have been conducted in this area by various authors. Heron (2001a) measured the dissolved nitrate concentration and salinity of the groundwater at three burrows and at different depths (5 cm, 39 cm and 50 cm depth). No significant variation of the nutrient concentration was found throughout the depth of the burrow, but the salinity was lower at the top than at the bottom of the burrow. Hollins (2001) and Hollins and Ridd (accepted) measured the concentration and consumption of oxygen in the burrow water of *Sesarma messa* *Alpheus cf. macklay*. They found that the oxygen concentration during neap tides remains close to zero but briefly rises during spring high tides. Stieglitz *et al.* (2000a) compared the volume of one burrow system to the total volume of sediment using resin casts. The volume of the burrow was ca. 10 % of the total volume of the sediment.

2.2.3 Three Mile Creek

Rowes Bay is located between Townsville city and Many Peaks Range, just North of Townsville and is orientated North-Northwest. The entire catchment of this area is undisturbed with no commercial landuse. Four streams discharge into Rowes Bay. The northernmost stream is located at the base of Many Peaks Range (see Figure 2.3 on the sign “N”) and is unlikely to deliver sediment to Rowes Bay (Aziz, 1992), except in the rain season. A second stream, Three Mile Creek (see Figure 2.3, Figure 2.8, and Figure 2.9), discharges near the center of the bay and is often responsible for delivering sediment to the northern sector of the bay. Two more streams (see Figure 2.3 on the sign “S”) that discharge in the southern section of the bay are believed to occasionally contribute to the sediment budget of the bay. There is no information on whether these streams contribute more to the sediment budget of the beach than Three Mile Creek does. But during the rain season, when the rain water volume of these two streams is enough to reach the ocean, the runoff will bring some sediment from around these creeks to the beach area. These streams are also responsible for carrying large volumes of water from Townsville during storms (Aziz, 1992).



Figure 2.8: Aerial photograph of Three Mile Creek, located *ca.* 15 km Northwest of Townsville.

Three Mile Creek is the only one of the four streams flowing into Rowes Bay that flows through the year. The total length of the creek is *ca.* 2.5 km. The creek flows through salt flats and mangrove areas (Figure 2.8 and Figure 2.9) to the South and West of the suburb of Pallarenda. The creek width is *ca.* 20 m at the mouth and less than 5 m at the head. The bed is mainly composed of quartz beach sediment, especially near the mouth of the creek.

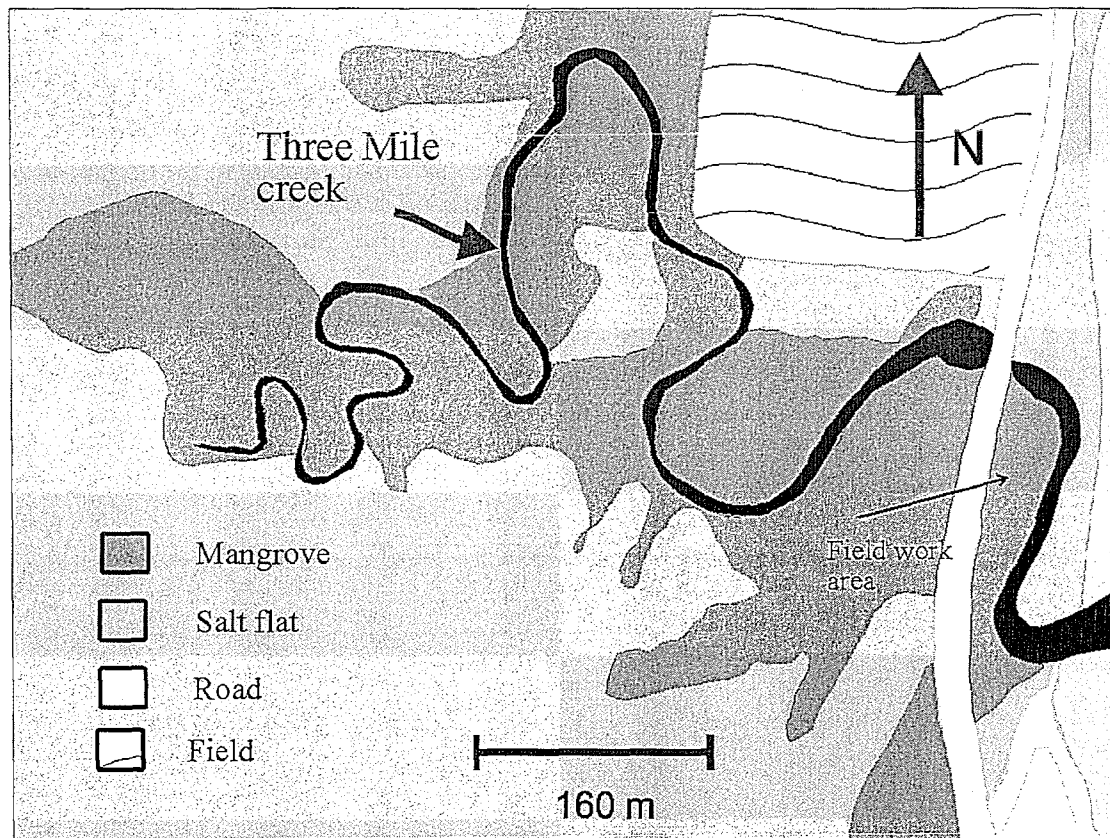


Figure 2.9: Three Mile Creek flows along the mangrove area, salt flat and finally enters Rowes Bay. The study area was in the mangrove sediment, on the East side of the road.

Mangrove forest grows on both sides of Three Mile Creek, dominated by *Rhizophora stylosa* along the creek edge, and *Ceriops* forest farther landward where the sediment surface rises. The *Rhizophora* forest is inundated by tides of *ca.* 2.5 m to 3 m above LAT and the *Ceriops* forest is inundated by tides greater than 3 m. The maximum number of inundation occurs in March and the minimum in November. Unfortunately, information about Three Mile Creek is very sparse compared to Cocoa and Gordon Creeks, and the description of this creek is therefore limited.

Chapter 3: Investigations of physical characteristics of sediment and groundwater in mangrove and salt flats.

3.1 Introduction

The difference in sediment type of each area reflects the historical and present sedimentation processes at work in mangrove forests and salt flats. A difference in mangrove forest sediment is expected from dead mangrove and salt flat, due to the presence of live or dead mangrove roots, and due to the presence or absence of mangrove trees, which will influence the organic content of each type of sediment. As a consequence of the sediment structure, groundwater characteristics and processes will also vary from place to place. In salt flat areas, where evaporation is high and macropores are absent, the movement of groundwater is more restricted than in the mangrove area. The seawater inundating the mangrove forest and salt flat during high tide has the same salinity, which is *ca.* 35. However, because physical characteristics of these sediments such as porosity and hydraulic conductivity are different, characteristics of the groundwater will also be different. Therefore, the salinity and density of the groundwater in the mangrove and salt flat sediment are expected to be different from each other.

In this chapter, we describe investigations that were carried out at Cocoa and Gordon Creeks to determine the sediment physical characteristics, including its electrical conductivity. A reconstitution of sedimentation layers was deduced from sediment cores, using visual and particle size analysis (it is noted that the age of the sediment was not taken in consideration in this study and there was a compaction when the vibrocoreing occurred). The electrical conductivity of the sediment was measured using resistivity probe developed by Ridd & Sam (1996b). Salinity and density variations of the groundwater along mangrove forest, dead mangrove and salt flat areas were also observed at the Cocoa Creek field site by taking groundwater from

piezometers at different times. Experiment methods and results are reported here. Finally, hydraulic conductivity of salt flat sediment from the Gordon Creek study site was measured in the laboratory using a falling-head permeameter and results were used to explain the characteristics of the groundwater in salt flat area. This survey is described at the end of the chapter.

3.2 Physical characteristics of the sediment

3.2.1 Method

Physical characteristics of sediment were observed based on vibrocores. This sampling technique, which consists in driving a tube with a vibrating device (or “vibrohead”), is used to collect core samples in unconsolidated sediments (Rossfelder, 2000). Vibrocores were collected at Cocoa Creek on 18th and 19th October 2000 along living mangrove forest, dead mangrove and salt flat areas (see Figure 3.1).

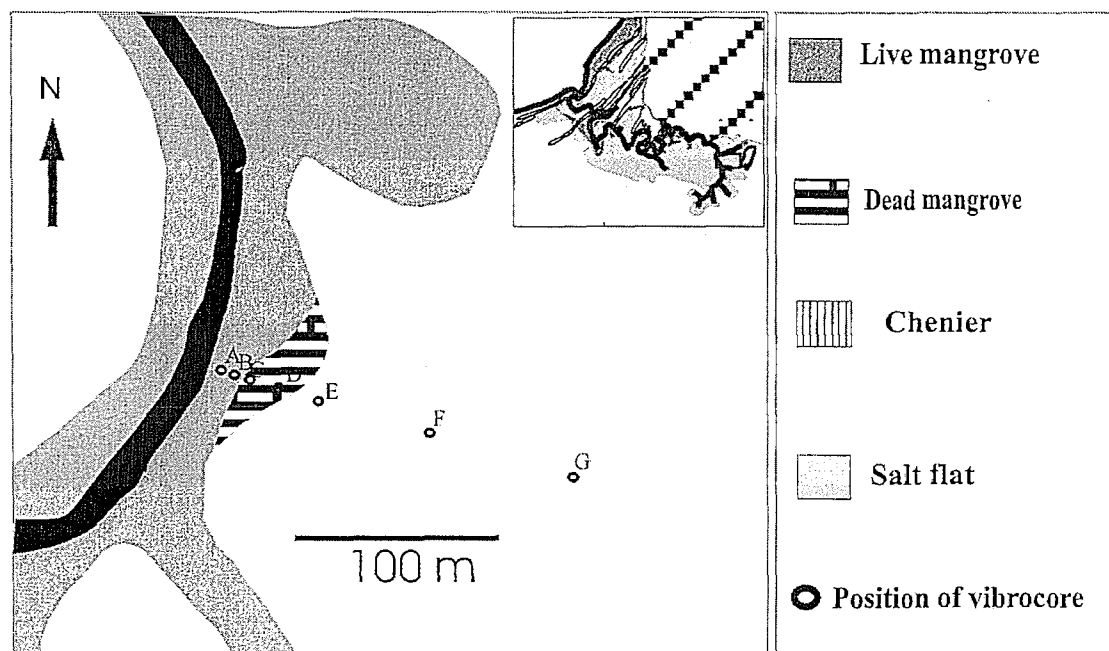


Figure 3.1: Drilling locations in the upper reaches of Cocoa Creek. Two cores were collected at locations A, D and E at two different depths (2m & 4 m, 2 m & 3.35 m, and 2 m & 2.91 m, respectively), and one core was collected at 2 m depth at all other locations.

The drilling device of the Earth Sciences Department of James Cook University was used to obtain cores in this field study (see Figure 3.2). An aluminum coretube of 70 mm in radius and 2.3 or 4.3 m in length (for cores of 2 and 4 m, respectively) was held by a clamp at the top of this coretube. A vibrohead of *ca.* 25 kg, 30 cm and 10 cm in weight, length and radius respectively was attached to the clamp at the top of the tube. The vibrohead was connected by a thick cable to a Honda petrol engine of *ca.* 3.5 HP (Horse Power). The engine rotation caused the vibrohead to vibrate, and this vibrating energy was imparted to the coretube. Two or three people holding and pushing down the coretube ensured a vertical penetration of the coretube (aluminum) into the sediment. The penetration of the core in the mangrove area was very easy for the depth of 2 m and 4 m, because the sediment was soft. However, the penetration of core in the dead mangrove and salt flat areas was sometimes made difficult by very hard sediment especially in salt flat area, in which case we poured water around the coretube whilst shaking and continually pushing the coretube to the maximum possible depth. The aim was to drill cores down to 2 m and 4 m in depth, which was possible in the mangrove area, but not in the two other areas due to the very hard sediment (only 2 m, 2.9 m and 3.3 m cores were obtained in these types of sediment).

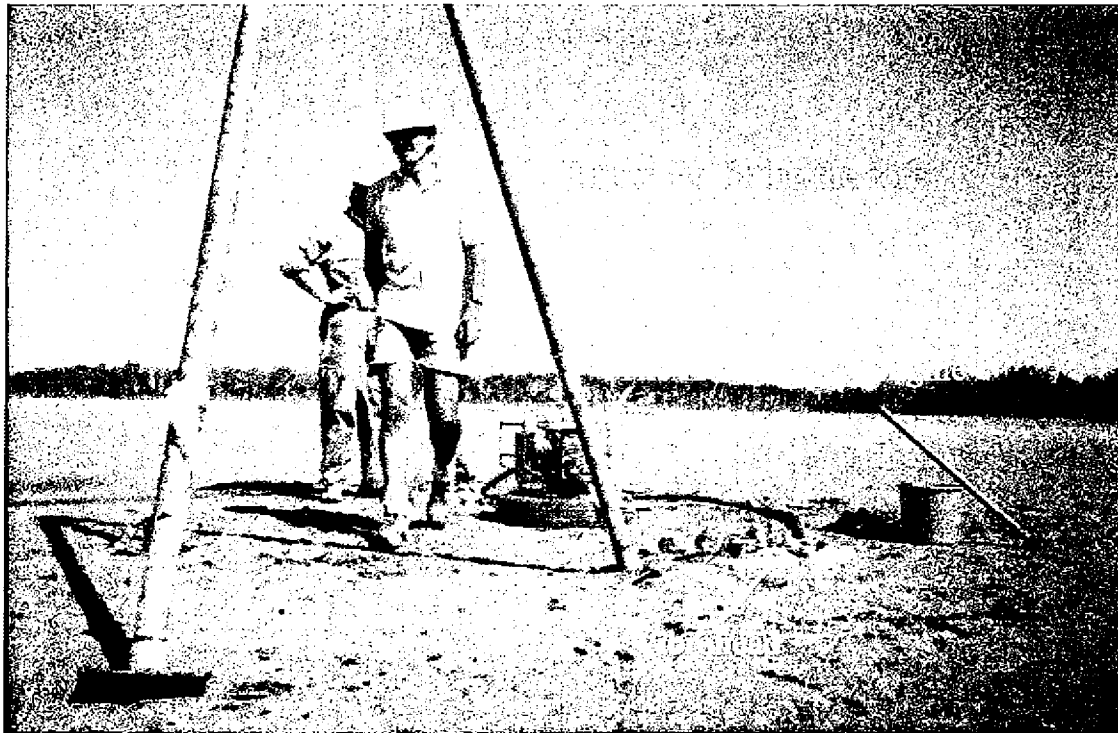


Figure 3.2: Vibrocoreing conducted on a salt flat in the upper reaches of Cocoa Creek, on October 18th and 19th 2000.

To prevent cores from releasing from the coretube after drilling was completed, the remaining space in the coretube was filled with water and sealed with a cap, whilst the tube was still in the sediment. This prevented the sediment core from falling down when the coretube was lifted from its hole with a tripod. The coretube was laid down, the sealing cap was removed and the water on top of the coretube was released. The empty part of the coretube was cut off. Both ends of the coretube were sealed using caps and tightened with tape before transporting the core from the field to the laboratory.

During the vibrocoreing, friction between the wall of the coretube and the sediment could cause compaction of the sediment inside the tube, resulting in a difference of length between the core itself and its hole. The degree of compaction varied for each core, depending on the sampling location. However, there was no fixed rule as to the degree of compaction of each area (mangrove, dead mangrove and salt flat). Lengths of cores and of drilling holes, and compaction factor are presented in Table 3.1.

Site	Depth of sediment (m)	Length of the core (m)	Compaction factor
A2 (mangrove)	2	0.85	2.4
A4 (mangrove)	4	3.04	1.3
B2 (mangrove)	2	1.31	1.5
C2 (mangrove)	2	1.5	1.3
D2 (mix, mangrove and dead mangrove)	2	1.87	1.1
D4 (mix, mangrove and dead mangrove)	3.35	1.60	2.1
E2 (salt flat)	2	0.46	4.3
E4 (salt flat)	2.91	1.76	1.7
F2 (salt flat)	2	1.51	1.3
G2 (salt flat)	2	1.70	1.2

Table 3.1: Depth of core into sediment (column 2) and actual core length (column 3), showing compaction at the drilling sites of Cocoa Creek. The compaction factor (column 4) was not constant.

3.2.1.1 Analysis of sediment cores

Two types of analysis were carried out on the sediment cores: visual analysis through observations of sediment contents, colour group and colour photography; and particle size analysis with a laser particle sizer (McIntyre, 1996).

To this end, each coretube was split in two halves along its vertical axis with a circular saw, after being cut on a board into 1-m long sections maximum (length of the board). To split the core, a sharp thin steel rod was pulled from the top end to bottom end of the core between the two halves of the core. One half was used for visual analysis, whilst the other half was stored in the fridge in a custom-designed wooden crate for particle size analysis at a later stage.

A. Visual analysis

One half of each core was laid on a bench for visual analysis. The analysis was done based on the type, colour and presence of organic matter in the core sediment. The core was divided into several sections based on colour changes and presence of organic matter, where the length of each section ranged from a few cm to over 1 m. If the difference of visual appearance between two sections was too small, two cores collected close to each other were laid side by side and were compared to decide on the length of each section. This method relied on the fact that between two adjacent field sites (or cores), the sedimentation process would not be significantly different, except if there were a spectacular geological process (such as a fault for instance).

B. Colour photography

After visual analysis, the same cores were photographed in colour for comparison with the visual analysis. A photo was taken of each 1-m section of the core by lying a graduated tape alongside the coretube and illuminating the latter with two halogen lights (60 watt each) positioned *ca.* 50 cm above the bottom and top end of the

coretube. The camera was clamped to the bench above the center of the coretube at *ca.* 1 m high. Each coretube was photographed twice for duplication purposes. After film processing, the processed film were scanned with a scanner, and saved the result in jpg file.

The pictures composing one core were then assembled thanks to image processing software (Corel Draw) and the resulting image was stretched to compensate for the compaction factor as measured in the field. Compaction factor was computed as the difference between the hole length and the core length (see Table 3.1). This resulted in an image of what the sediment would have looked like before coring. This method assumed that the compaction of the core was uniform in each core, which was not tested but seems a reasonable assumption.

3.2.1.2 Particle size analysis.

A. Selection of sediment sample to be analysed.

The second halves of the coretubes (that were not photographed) were kept in a cool room (2°C) and used for particle size analysis. Samples taken from the core depended on the length of the core. All sections of the cores were sampled at the top, middle and bottom, regardless of the degree of compaction. Therefore, samples for particle size analysis were collected based on arbitrary positions and not based on the visual characteristics of the sediment (McIntyre, 1996).

B. Laser Particle sizing processing.

Prior to particle size analysis, each sample was sieved through a 1 mm mesh, then diluted with tap water in a plastic container. The solution was introduced into the chamber of a Malvern Mastersizer laser particle size. Before a measurement was conducted, each sample was submitted to *ca.* 15 seconds of ultrasound in the Malvern Mastersizer chamber to disperse any potential floc. The set up of this equipment was a

lens of 1000 mm focal length that allows particles in the range 7 to 1000 μm to be measured. The accuracy of this equipment is $\pm 2\%$ of the volume median diameter (McIntyre, 1996).

3.2.1.3 Bulk electrical conductivity measurement

Bulk soil electrical conductivity was measured using a conventional resistivity method described by Ridd & Sam (1996b) (see Figure 3.3).

The resistivitymeter consists of a steel pipe (2.10 m long, 5 cm diameter), whose top is a T handle made of steel. The bottom end of the pipe is mounted in a hollow rod filled with glass-fibre epoxy resin. Prior to mounting, the rod is equipped with four copper electrodes spaced by 3.5 cm from each other. These electrodes are used for measurement of voltage (two top ones) and current (two bottom ones) through the soil when the electrical conductivity probe is deployed. Four thin cables fed through the pipe connect the electrodes to a control box that consists of an oscillator, a voltmeter and an ampere meter. An A.C. signal of approximately 1 V RMS (Root Mean Square) is generated by the oscillator to stimulate the two voltage copper electrodes. The resulting current I passing through the current electrodes was measured with a conventional multimeter, like the A.C. signal. The ratio between current and voltage (I/V) was calculated and considered to be equal to the bulk electrical conductivity of the soil close to the electrodes.

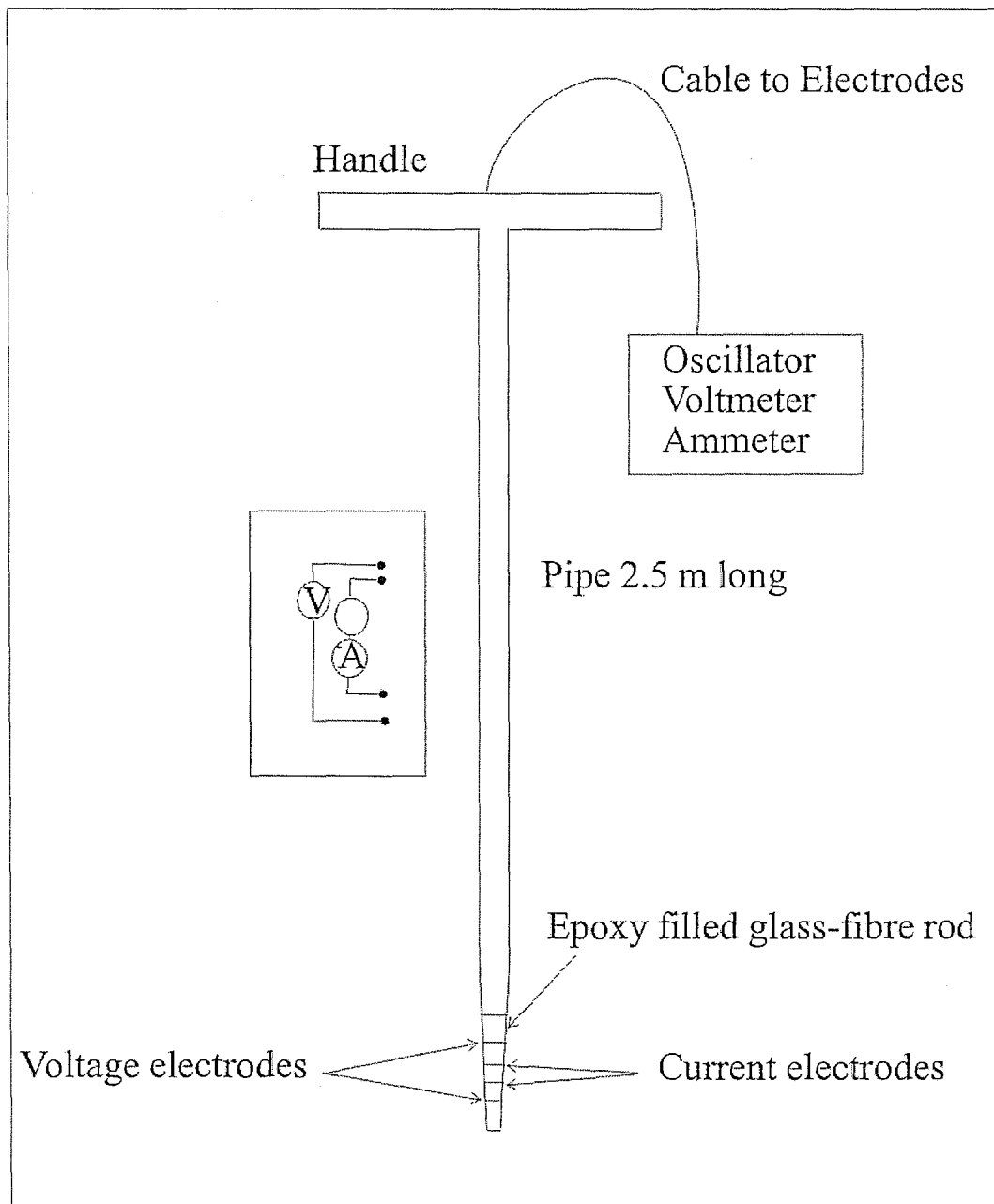


Figure 3.3: Schematic diagram of the resistivity probe used for measuring electrical conductivity of the sediment (after Ridd and Sam, 1996b).

In this study, measurements of the bulk electrical conductivity of the sediment were undertaken 1 to 3 days after spring tide, on 19, 20 and 21 of August 2001 and thus all the sediment was water saturated and it was assumed that the properties (salinity, electrical conductivity and density) of the water covering the sediment were uniform over that period. During these three days, the maximum height of the tide was 3.90 m,

3.77 m and 3.50 m above LAT, respectively. Measurements were taken between 9 am and 4 pm.

Over the 3-day period of the experiment, the soil bulk electrical conductivity was measured along 36 vertical profiles at various distances from the creek. All measurements were taken every 10 cm from the surface down to 2 m deep, which was the bottom of some of the drilling holes. The spacing between profiles in the mangrove forest, dead mangrove and salt flat was 1 m, 3 m and 8 m, respectively (some profiles were 10 m apart in the salt flat area).

The probe was calibrated in the creek water to check for instrument drift before and after each profile. At the same time, a sample of the creek water was collected in order to take an electrical conductivity measurement with a laboratory salinometer (Model WP-84, Conductivity-Salinity-Temp.), which was used as a reference. Before using this salinometer to measure electrical conductivity of the creek water, this salinometer was calibrated against the reference water which the salinity was 35. The conversion factor from field reading electrical conductivity to reference electrical conductivity was calculated as follows:

$$k = \sigma_1 \frac{V_1}{I_1} \quad (3.1)$$

(Hollins, 2001)

where:

σ_1 = electrical conductivity of creek water measured in the laboratory in
mSiemens

k = constant factor (unitless)

I_1 = current (mA) during the electrical conductivity measurement of creek
water in the field

V_1 = voltage (mV) during the electrical conductivity measurement of creek
water in the field

Based on this calculation, k was obtained as a characteristic of the field electrical conductivity probe, and the bulk electrical conductivity of the soil was calculated as follows for each field measurement:

$$\sigma_2 = k \frac{I_2}{V_2} \quad (3.2)$$

Where:

σ_2 = bulk electrical conductivity of soil (mSiemens)

I_2 = current (mA) of soil (using conventional resistivity probe)

V_2 = voltage (mV) of soil (using conventional resistivity probe)

3.2.2 Results

3.2.2.1 Core analysis.

An example of the comparison between visual analysis and colour photographing is shown in Figure 3.4, whilst the complete set of results is shown in Appendix 1.

Figure 3.4 is the result of three photographs of the core, which all have a middle part brighter than the top and bottom ends. This may be due to variations in light intensity. This image shows that the changes in colour are generally smooth. On this photograph, the colour of the top *ca.* 1 m is quite uniform with small red dots, indicating the presence of organic matter in this section. Between 1 m and *ca.* 2.8 m, the colour is dark grey/black, indicating the presence of clay and smooth sediment. Below this section, which is the lowest section, the colour is brown again, which is laminations of sand and clay. As explained above, that results of colour photographing analysis were also compared to visual analysis.

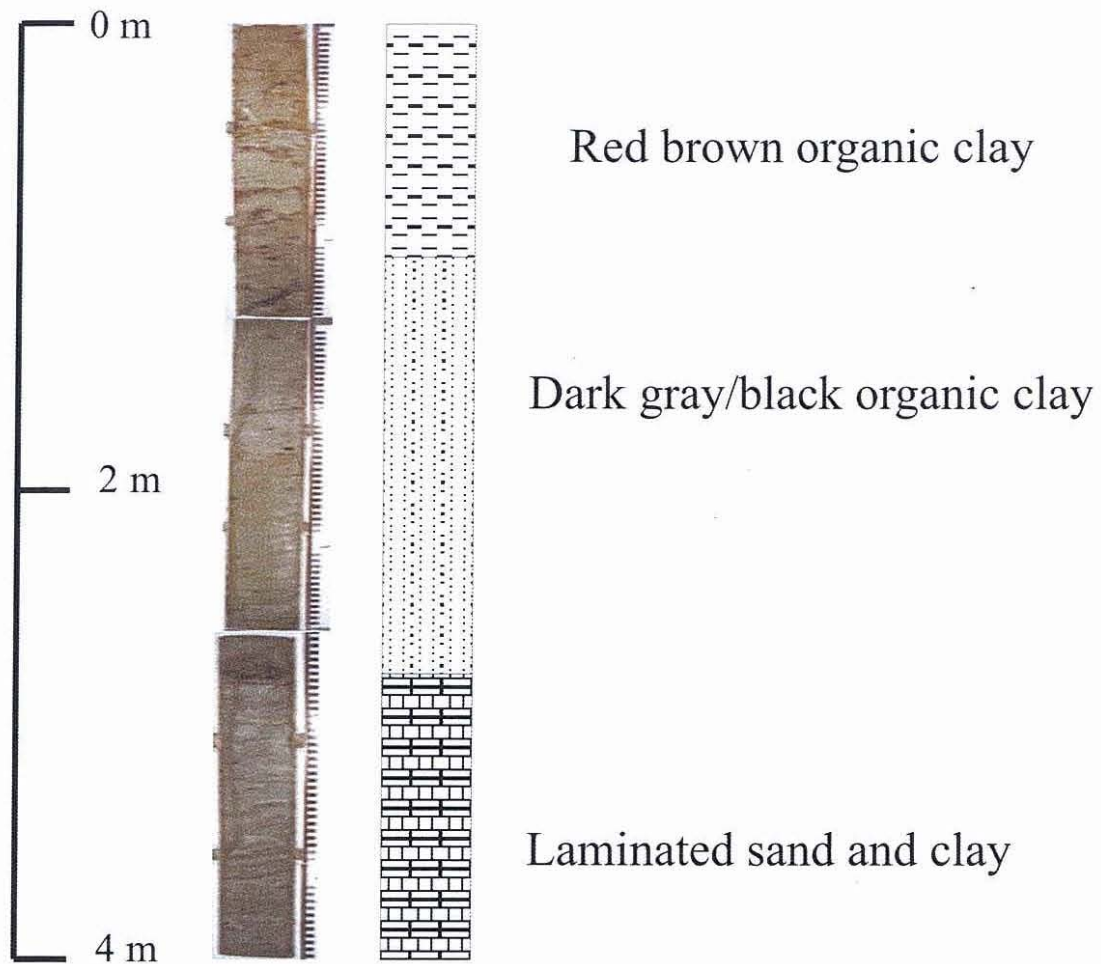


Figure 3.4: Comparison between colour photographing and visual analysis for core from site A4. The length of the core is 3.04 m, but original length in the filed is 4 m. The core is stretched to become 4 m length (depth).

3.2.2.2 Particle size distribution

An example of the distribution grain size results is shown on Figure 3.5, whilst the complete data set is shown in Appendix 2.

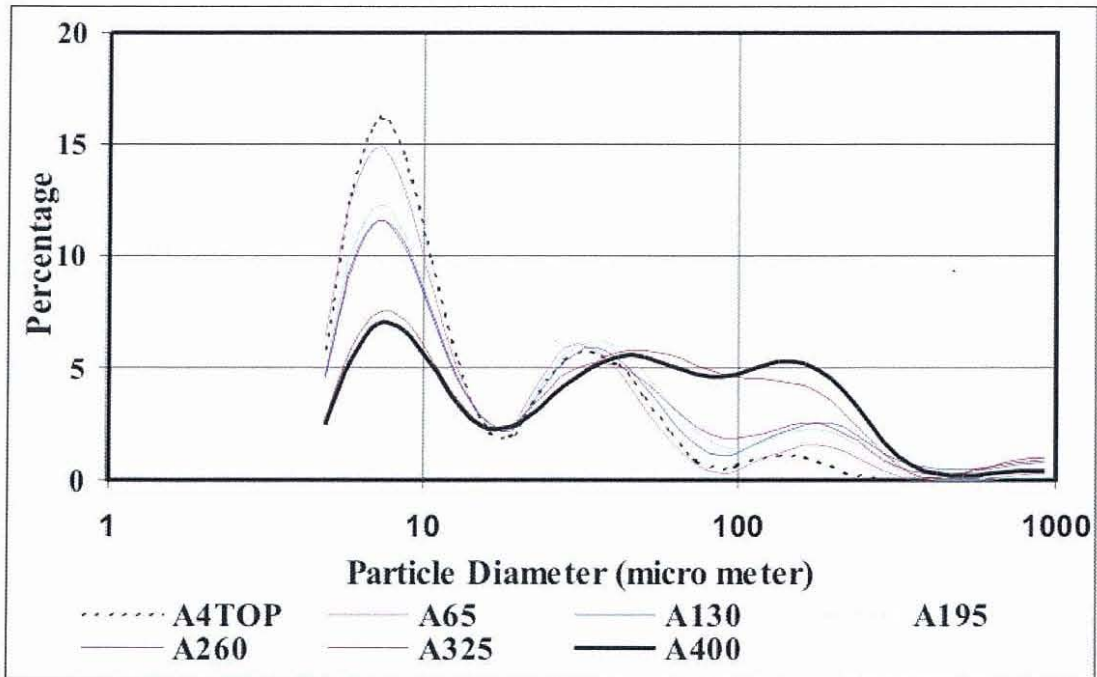


Figure 3.5: Particle size analysis for site A4. A4Top means the sample is taken from the top of the core, and A65 means the sample is taken from 0.65 cm depth in the core, etc.

Figure 3.5 shows that grain size distribution is not unimodal but instead all sediment samples show 3 modes, which are below 10 mm, between 10 and 100 mm, and above 100 mm. Wilson (1994) divided the particle size range of each material; clay (< 10 mm), silt (between 10 mm and 60 mm), and sand (between 60 mm and 2 mm). According to these definitions, Figure 3.5 shows that clay dominates the top layer of the core, whilst sand dominates the bottom of the core. This pattern is found in almost all cores and more generally, we can conclude that the deeper sediment layers are, the less dominant the clay is.

Reconstruction of the *in-situ* sediment stratigraphy was based on the results of the visual analysis, the colour photographing and the particle size analysis, as seen in Figure 3.6.

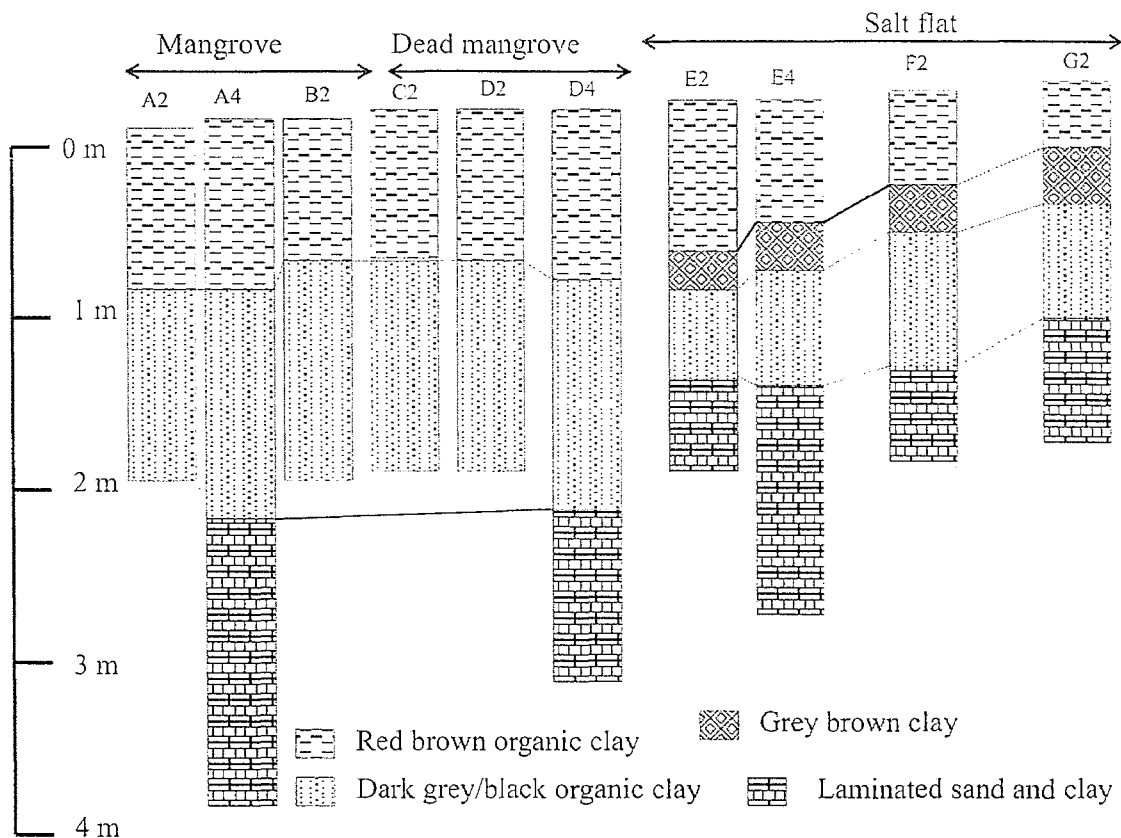


Figure 3.6: Reconstruction of *in-situ* sediment stratigraphy based on visual analysis, colour photographing and particle size analysis for mangrove area, dead mangrove area and salt flat areas at upper reaches of Cocoa Creek.

Figure 3.6 shows that the top sediment layer in the mangrove area and dead mangrove appeared to contain red brown organic clay, with a thicker layer in mangrove area than in dead mangrove. The top layer of salt flat area was similar to the mangrove and dead mangrove top layer, though its organic content was lower and it was dominated by fine silt instead. Sediment below the organic clay in the mangrove and dead mangrove areas was dark grey/black organic clay. This layer was also found in salt flat area but a thin layer of grey brown clay was present in between that organic layer and the top one. Below the grey/black organic clay, a lamination of sand and clay layer was present for both areas (dead and alive mangroves).

3.2.2.3 Bulk sediment electrical conductivity.

The sediment electrical conductivity was measured at depth intervals of 10 cm at Cocoa Creek. This transect took 3 days to complete. The resulting electrical conductivity contour plot is shown in Figure 3.7.

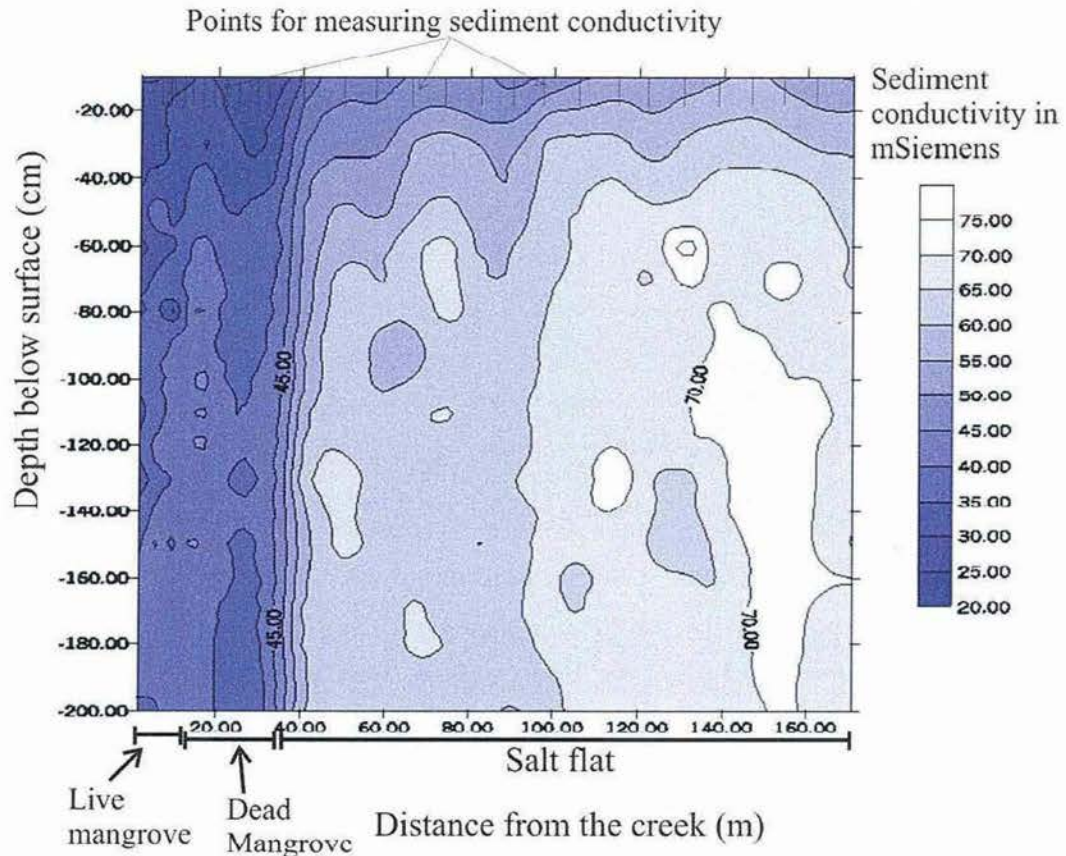


Figure 3.7: Depth contour plots of sediment bulk electrical conductivity along the transect that crossed mangrove, dead mangrove and salt flat sediments.

The sediment electrical conductivity pattern shown on Figure 3.7 can be described in 2 ways: horizontally (based on the distance from the creek), and vertically (based on the depth). Horizontally, the electrical conductivity increased as the distance from the creek increased and as the mangrove forest turned into a salt flat area. The electrical conductivity in the mangrove, dead mangrove and salt flat area ranged from *ca.* 30 mS (milliSiemens) to 40 mS, 40 mS to 50 mS, and 50 mS to 70 mS, respectively. Vertically, the deeper the sediment, the higher the electrical conductivity. However,

the increase was not linear. In mangrove areas (live and dead), the electrical conductivity changed from 30 to 40 mS between the surface and 0.5 m deep, but remained relatively constant below this depth (0.5 to 2 m). At the border between dead mangrove and salt flat, the electrical conductivity was homogeneous at *ca.* 45 mS for the whole depth. However, the electrical conductivity in the salt flat area ranged between 45 and 60 mS between the surface and 0.7 m at the area close to the dead mangrove, and between 55 to 70 mS between the surface and 0.4 m at the area farthest from the creek. The electrical conductivity remained relatively constant below 0.7 m in the dead mangrove area and below 0.4 m for area farthest from the creek.

3.2.3 Discussion

From the point of view of groundwater hydraulic conductivity, it is unlikely that the sediment characteristics between the live, dead mangrove and salt pan areas are significantly different as all regions have a very high proportion of very fine grained material. Thus while statistical difference between the sediment types may be present, the hydraulic conductivity, in the absence of macropores is likely to be very small.

Results from visual analysis and colour photographing show that the top layer was mainly composed of organic clay, although the colour could vary from black to brown. This result was also supported by particle size analysis of the mangrove and salt flat sediment, which showed that the top layer was dominated by clay. This organic matter is probably the result of decay of mangrove roots.

Overall, the deeper the sediment, the coarser the material in every area. The deepest sections of the cores (more than 2 m for the mangrove area and *ca.* 2 m for the salt flat area) show a laminated pattern of sand and clay. The sandy material could only have been brought by relatively strong currents, and suggest these layers may have been the past bed of Cocoa Creek. The modern bed of Cocoa Creek is composed of sand. Another explanation of sand layer is that they represent storm deposits.

The bulk electrical conductivity of a wet soil or rock depends on several parameters such as the electrical conductivity of the water present between particles in the soil,

the percentage of porewater in the sediment, and how water is distributed in the soil (Keller and Frischknecht, 1996). If the soil is fully saturated, i.e. when the water content is equal to the porosity, the bulk electrical conductivity of the sediment will depend on the three above parameters. However, if the soil is dry, and pore spaces are not interconnected by water, the soil may not conduct electricity. Usually, the drier the sediment is, the lower the electrical conductivity is, and vice versa.

Field measurements taken over 3 days when the sediment was water saturated by tidal water show that the sediment electrical conductivity in salt flat area was in general higher than in the live and dead mangrove areas. One explanation for this observation is the presence of burrows in the mangrove areas, which were numerous in the live mangrove area, still present in the dead mangrove areas (although in fewer numbers), but absent in the salt flat area. A diffusion process of salt from the sediment towards crab burrows has been documented in the past (Hollins, 2001) and inundation of the sediment surface during high tide can flush part of the water present in the burrows (Ridd, 1996a), flushing at the same time some of the salt accumulated from the above mentioned diffusion process. The end result is that sediment near crab burrows contains less salt than sediment deprived of burrows. Since sediment salinity and electrical conductivity are positively correlated (Sam and Ridd, 1996), this explains the increase in soil electrical conductivity in the salt flat area.

Another cause for the reduction in salinity and electrical conductivity of the sediment in the mangrove area compared to the salt flat area is a higher groundwater flow, which is believed to partly flush salt from the sediment. Groundwater flow depends on the hydraulic conductivity of the sediment. The hydraulic conductivity is likely to be heavily influenced by macropores such as the crab burrows and thus the groundwater flow in the salt pans, which has few burrows, will probably give much less than in the mangrove areas.

3.3 Salinity and density of the groundwater

3.3.1 Method

During this study, salinity and density of the groundwater were measured using different equipment. Approximately 1 liter of groundwater was pumped from every hole, which is 2 m depth (we did not include other than 2 m depth). Samples were collected on 24/10/00, 04/01/01, 12/07/01, 09/09/01, 27/09/01, and 18/10/01. These dates were all in the dry season, except the 04/01/01, which was in the wet season.

3.3.1.1 Salinity of the groundwater

Salinity was measured with a conductivity-salinity-temperature sensor (TPS model WP-84). Before measurement, the sensor was calibrated against a reference water sample of salinity 35 in the laboratory with a constant temperature ($\approx 20^{\circ}$ C). If the sensor gave wrong result (more or less than 35), then it was set up to be 35.

3.3.1.2 Density of the groundwater

The density of the groundwater was measured using a density hydrometer, which offers three scales: 1000 to 1050 kg/m³, 1050 to 1100 kg/m³, and 1100 to 1150 kg/m³. Before measuring the density of the groundwater, the hydrometer was calibrated against a reference of standard water. Groundwater samples with the lowest salinity were measured first (for density), followed by the higher salinity samples. The density measurement was repeated three times for each sample.

3.3.2 Results

3.3.2.1. Groundwater salinity

Groundwater salinity results are shown in Figure 3.8. The general pattern of the groundwater salinity can be described in terms of spatial and temporal variations. The results on the spatial distribution of salinity showed that the further the distance from the creek, the higher the salinity of the groundwater. On average the groundwater salinity at the salt flat was the highest, followed by dead mangrove and the least saline groundwater was found in the live mangrove area. The increase in salinity per unit of length from live mangrove to dead mangrove, and from dead mangrove to salt flat was *ca.* 1.3/m and 0.23/m, respectively. For a given site, there is no significant variation in salinity with time. The average and standard deviation of groundwater salinity measurements in the dry season at sites A2, B2, C2, D2, E2, F2 and G2 were (50.0 ± 2.5) , (60.0 ± 2.4) , (73.3 ± 1.6) , (86.5 ± 2.7) , (128.2 ± 3.4) , (141.8 ± 4.8) and (146.1 ± 4.8) , respectively.

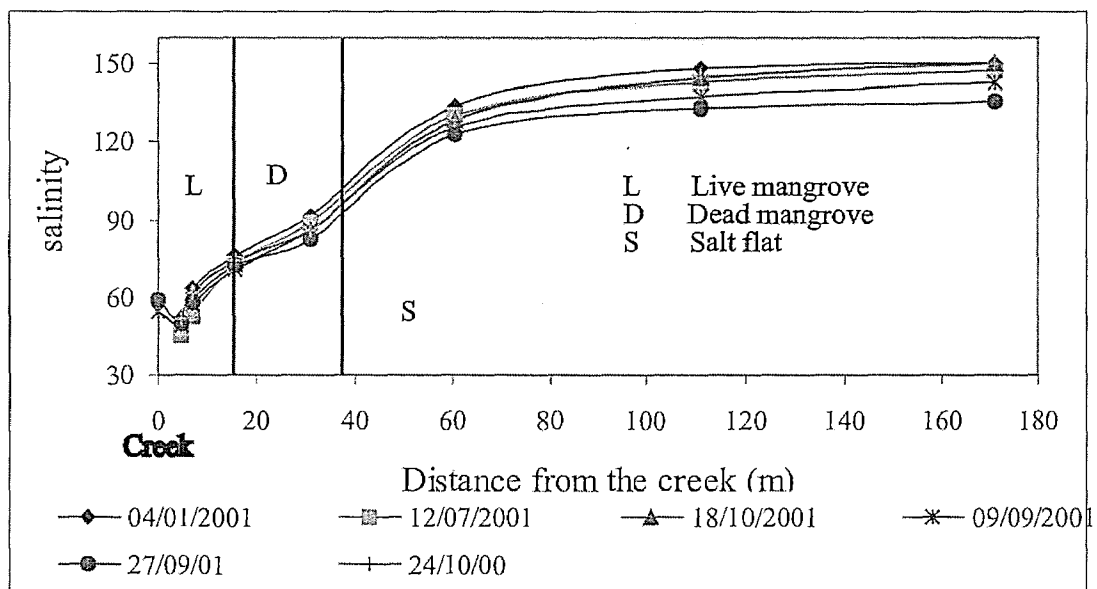


Figure 3.8: The horizontal variation of groundwater salinity in Cocoa Creek study area. The data at the 0 m position was taken from water in the creek.

3.3.2.2. Groundwater density

Groundwater density results are shown in Figure 3.9. The general pattern of groundwater density can also be described in terms of spatial and temporal variations. Spatially, the greater the distance from the creek, the higher the density of the groundwater and on average, the groundwater density at the salt flat was the highest, followed by dead mangrove and the least dense water was found in the live mangrove areas. The increase of the density per unit length between live and dead mangrove appears to be linear with distance. The increase in density between live mangrove and dead mangrove, and between dead mangrove and salt flat in two dimensional was *ca.* $\frac{1.2(kg/m^3)}{m}$ and $\frac{0.24(kg/m^3)}{m}$, respectively. For a given site, there is no significant variation in density with time. The average and standard deviation of the groundwater density at sites A2, B2, C2, D2, E2, F2 and G2 were $(1034.0 \pm 3.3)kg/m^3$, $(1042.3 \pm 2.6)kg/m^3$, $(1051.7 \pm 1.7)kg/m^3$, $(1065.8 \pm 1.7)kg/m^3$, $(1104.7 \pm 1.2)kg/m^3$, $(1122.5 \pm 0.8)kg/m^3$ and $(1129.3 \pm 1.5)kg/m^3$, respectively.

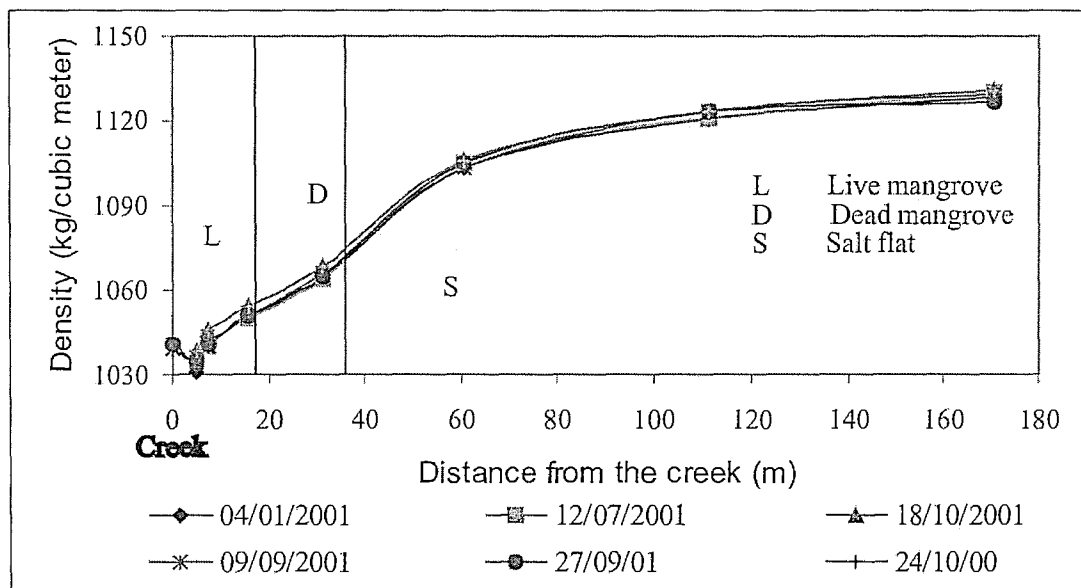


Figure 3.9: The horizontal variation of groundwater density in Cocoa Creek study area. The data at the 0 m position was taken from water in the creek.

3.3.3 Discussion

Groundwater salinity and density measurements of this study show that in general, salinity and density in salt flat areas were higher than in mangrove and dead mangrove areas, which was partly explained by the presence of burrows in mangrove sediment. These burrows allow part of the salt to be flushed from the sediment during high tide inundation and ebbing tide (Ridd, 1996a). Therefore, the water salinity in the burrows is lower than if there were no flushing from tidal water (as in salt flat areas that are deprived from burrows).

Another factor that is likely to emphasize this condition is that evaporation over the salt flat area during the dry season is about 5 mm/day (Hollins and Ridd, 1997), while evapotranspiration is only *ca.* 2 mm/day in the mangrove area (Wolanski and Ridd, 1986).

3.4 Hydraulic conductivity of salt flat sediment: laboratory measurements

3.4.1 Method

Laboratory measurements of sediment hydraulic conductivity can be conducted using two basic principles. Firstly, if the hydraulic conductivity of the medium is high enough, gravity pressure may be used to indicate the hydraulic head of the water. This technique is used by two types of instruments; called a constant-head permeameter and a falling-head permeameter (De Marsily 1986, Bouwer 1978). For samples such as sands and gravels with a hydraulic conductivity of ($10^{-1} - 10^{-5}$) m/s, a constant-head permeameter is used (Bouwer, 1978). If the hydraulic conductivity of a sample is less than 10^{-5} m/sec however, the falling-head permeameter must be used. Secondly, if the hydraulic conductivity is very low (lower than 10^{-9} m/sec, De Marsily 1986), pressure pumps are used to create a hydraulic head and induce flow through

the sediment sample. In this study, gravity-based instruments were used (see Figure 3.10) and the latter method will thus not be discussed.

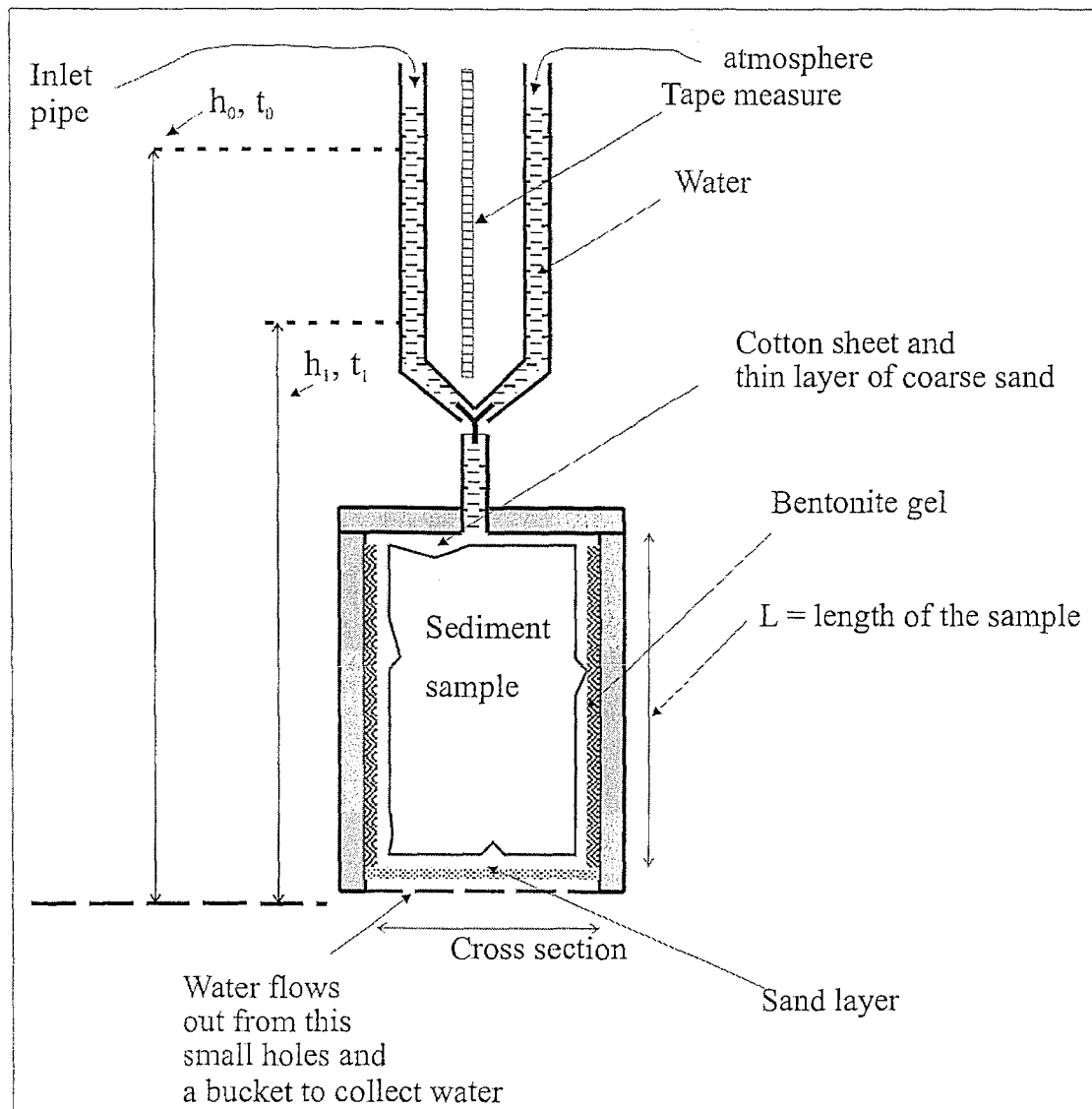


Figure 3.10: Sketch of a falling-head permeameter as used in this study, after modification of a design by De Marsily (1986).

The permeameter was made of a PVC tube of diameter, length and thickness 15 cm, 20 cm and 1.5 cm, respectively (see Figure 3.10). The bottom of the cylinder was closed with a sheet of PVC, in which small holes were drilled to allow the water to drain from the sediment sample. A sheet of transparent cotton was placed at the bottom of the sample to prevent the erosion of the sediment. A cylindrical sediment

sample was placed in the middle of the PVC tube and jelly bentonite gel was poured around the sample to prevent the water from infiltrating down around the PVC wall. Bentonite gel is an impermeable gel that is usually used in geotechnical drilling applications as it can diminish fluid loss and reduce seeping of the fluid into permeable formations. The top of the sediment was covered by a sheet of transparent cotton and coarse sand to prevent erosion of the sediment. The tube was then closed using another circle sheet of PVC, which was 1.5 cm thick. A small hole (diameter = 1 cm) was made in the middle of this PVC sheet, and a short siphon (about 7 cm length and the 1 cm diameter) was inserted in this hole. A T shape small tube (diameter inside 4mm) was connected to the top part of this siphon. Two other vertical long siphons (diameter 6 mm) were joined to the T tube, and then hung on the frame from *ca.* 1.5 m high. Water was filled through one siphon (inlet pipe, see Figure 3.10). This water flowed down to the sample and some amount flowed up through the other siphon. Since the siphons were both open to atmospheric pressure, the water level in both siphons was the same. Calculation of hydraulic conductivity from these measurements is detailed later on in this section.

Measurements of hydraulic conductivity were conducted in the Wet Laboratory of the School of Mathematics and Physics Sciences, JCU (James Cook University), Australia. The samples were taken from the salt flat area at Gordon Creek field sites. Three sediment samples were used in total, from depth of 0.25 to 0.5 m, 0.5 to 0.75 m and 0.75 to 1m from the surface. Samples were collected by carefully digging around the sample on sediment surface to avoid disturbing the condition of the soil. This sampling procedure was preferred to coring to avoid the compaction of the sediment.

Prior to laboratory measurement of the bulk soil hydraulic conductivity of the samples, it was necessary to ensure that the sample was water saturated. If the sample was not water saturated, the amount of water that infiltrated into the sample during the experiment, would not be the same as the water coming out from the sediment. First of all, one of the two siphons was filled with tap water. Some amount of water would flow down and infiltrate to the sample, and some would flow into the other siphon. If the sediment was not water saturated, the water in the siphon would flow down

quickly. This operation was repeated about ten times and took ca. 3 to 4 hours for each sample. By the time the sediment was water saturated, the down flow of water would remain stable and the amount of water coming into the sediment was the same as the water coming out of the sediment. Finally, water was filled into one siphon once more and the water level in the other siphon (parallel to a tape measure) was noted as h_0 (at the beginning of the experiment) and h_1 (at the end of the experiment). The time required for the water to flow down from one level to another level was also noted (as t_0 and t_1 , respectively) for every 10 cm increment between h_0 and h_1 .

The calculation of the sediment hydraulic conductivity (K) can be calculated based on equation 3.3 and 3.4 below:

$$Q = K Ah/L \quad (3.3)$$

where:

Q = volume rate of flow

K = hydraulic conductivity of sediment sample

A = cross section area of the sample (the sample is a vertical cylinder)

h = vertical distance between constant water level above sample and water level outflow cylinder

L = height (length) of the sample

From the Figure 3.10, the volume rate flow of the water (Q) can also be determined as follows:

$$Q = -a \Delta h / \Delta t \quad (3.4)$$

where:

a is the cross section of the siphon

A is the cross section of the sample

Δh is the position of the water level from h_0 to h_1

Δt is the time needed for the water to flow down for h_0 to h_1

If Δh and Δt are small, we can write equation 3.4 to become:

$$Q = -a \frac{dh}{dt} \quad (3.5)$$

Equation 3.3 and 3.5 can be merged into equation 3.6 as follows:

$$\frac{dh}{h} = - \frac{K A}{a L} dt \quad (3.6)$$

The integration of equation 3.6 between the initial and final time of the experiment (t_0 and t , respectively, with a corresponding water level of h_0 and h) gives:

$$\ln \frac{h}{h_0} = - \frac{AK}{aL} (t - t_0) \quad (3.7)$$

or

$$K = - \ln \left(\frac{h}{h_0} \right) \frac{aL}{A(t - t_0)} \quad (3.8)$$

3.4.2 Result

The parameters used in this measurement were: $A = 150 \text{ cm}^2$; $L = 13.5 \text{ cm}$ and $a = 1 \text{ cm}^2$. The results of the measurement can be seen in the table. 3.1.

No.	$-\ln(h/h_0)$	$(t-t_0)$ (second)	K (m/day)
1	0.1186	1980	0.004
2	0.1346	1980	0.005
3	0.1557	2040	0.005
4	0.1845	2160	0.006
5	0.2264	2280	0.007
6	0.4139	3000	0.009

Table 3.2 Hydraulic conductivity of salt flat sediment

Chapter 4. The bulk hydraulic conductivity of mangrove soil perforated with animal burrows.

4.1 Introduction.

The salinity of the groundwater has a significant influence on the growth of mangrove trees. Mangroves that grow in areas that are frequently inundated by the tide, or that grow in lower salinity regions of the estuary, are likely to grow more rapidly than those living in swamp regions, which are rarely inundated, and where groundwater salinity is very high (Tomlinson, 1986).

Mangrove trees can increase soil salinity around their roots (Passioura *et al.*, 1992). Freshwater evaporates at the leaf but, unlike terrestrial plants, the roots are surrounded by saltwater. The removal of the excluded salt is an important mechanism that must occur if the groundwater salinity is to remain below lethal levels. Two mechanisms exist which can remove the salt accumulated within the mangrove soil. The first process is diffusion of the salt across the short distance from the root to an animal burrow, where upon it is flushed by lower salinity water during tidal inundation (Stieglitz *et al.* (2000a), Hollins *et al.* (2000) and Heron and Ridd (2001b)). The other process that can reduce local groundwater salinity is groundwater flow back to the creek or estuary. The flow of groundwater back to the creek is also affected by the presence of animal burrows as they significantly increase the hydraulic conductivity of the soil (Hughes *et al.*, 1998a).

In this chapter, measuring bulk hydraulic conductivity of the soil is primary concerned (i.e. the hydraulic conductivity including the influence of burrows and macropores). Hughes *et al.* (1998a) found from laboratory experiments that surface hydraulic conductivity of the sediment in the estuarine wetland without crab holes and macropores was approximately 0.01 m/day. Because of the presence of crab holes, it was estimated by Hughes *et al.* (1998a) that the average hydraulic conductivity

increased to become 0.1 m/day to 1 m/day or 1 to 2 orders of magnitude bigger than without crab burrows and macropores.

Animal burrows in mangrove swamps act as low resistance pathways for water flow. Burrow systems can be deep and occupy a significant fraction of the soil volume. For example, Stieglitz *et al.* (2000a) found that the overall depth of burrows to be up to 1.2 m and that the total volume to be about 10 % of the swamp soil volume.

The measurement of hydraulic conductivity including the influence of the burrows, must ideally be carried out *in-situ* because it is usually impossible to take a sufficiently large sample of soil that would include a significant number of burrow systems. Stieglitz *et al.* (2000b) found that burrow systems may have horizontal and vertical scales of over a meter and a sample significantly bigger than this would need to be extracted for analysis. In this chapter a new method is presented for measuring hydraulic conductivity *in-situ*, that takes account of the animal burrows, and which does not disturb the soil. In addition the method can be applied rapidly and does not require the use of piezometers that are difficult and costly to install in mangrove swamps.

4.2 Methods

4.2.1 Measurement of the bulk hydraulic conductivity of mangrove soils using crab burrows.

Bulk hydraulic conductivity was determined by utilising crab burrows as natural piezometers. This involved pumping a *small* quantity of water out of the burrows and measuring the flow rate back into the burrow from the sediment porewater. This is similar to the traditional method of pump testing of piezometers (De Marsily, 1986) but in this case, it uses the natural burrows that are already in the system. Pump testing involves pumping water from a piezometer and noting the rate at which water returns to some fraction of its original level

It is common in mangrove swamps that the crab burrow systems overlap and intermingle with each other as shown in Figure 4.1. Because of this intermingling of the burrows, the distance through the sediment from one burrow chamber to another chamber in an adjacent burrow system may be only a few centimeters. Figure 4.1a shows three separate burrow systems. If water is pumped from burrow B, water will return through the mangrove soil from the surrounding burrow systems, burrow A and burrow C. This will occur in a similar manner to the way that water will flow during natural groundwater flow i.e. due to a pressure gradient (Figure 4.1b). Although the adjacent burrow systems intermingle, the water level in each of the burrows will be slightly different between adjacent burrow systems. Essentially the water flow from one burrow to another is determined by the sediments with high resistance to flow. It should be noted that Figure 4.1b represents the case during neap tides when the swamps are not inundated by high tides.

The flux of water into the burrow domain is given by:

$$q = K \frac{\Delta z}{\Delta r} \quad (4.1)$$

where

K = bulk hydraulic conductivity of the sediment (to be determined) (m/day)

Δz = drop in water level compared to adjacent burrows (m)

Δr = characteristic distance between centers of adjacent burrow domains (m)

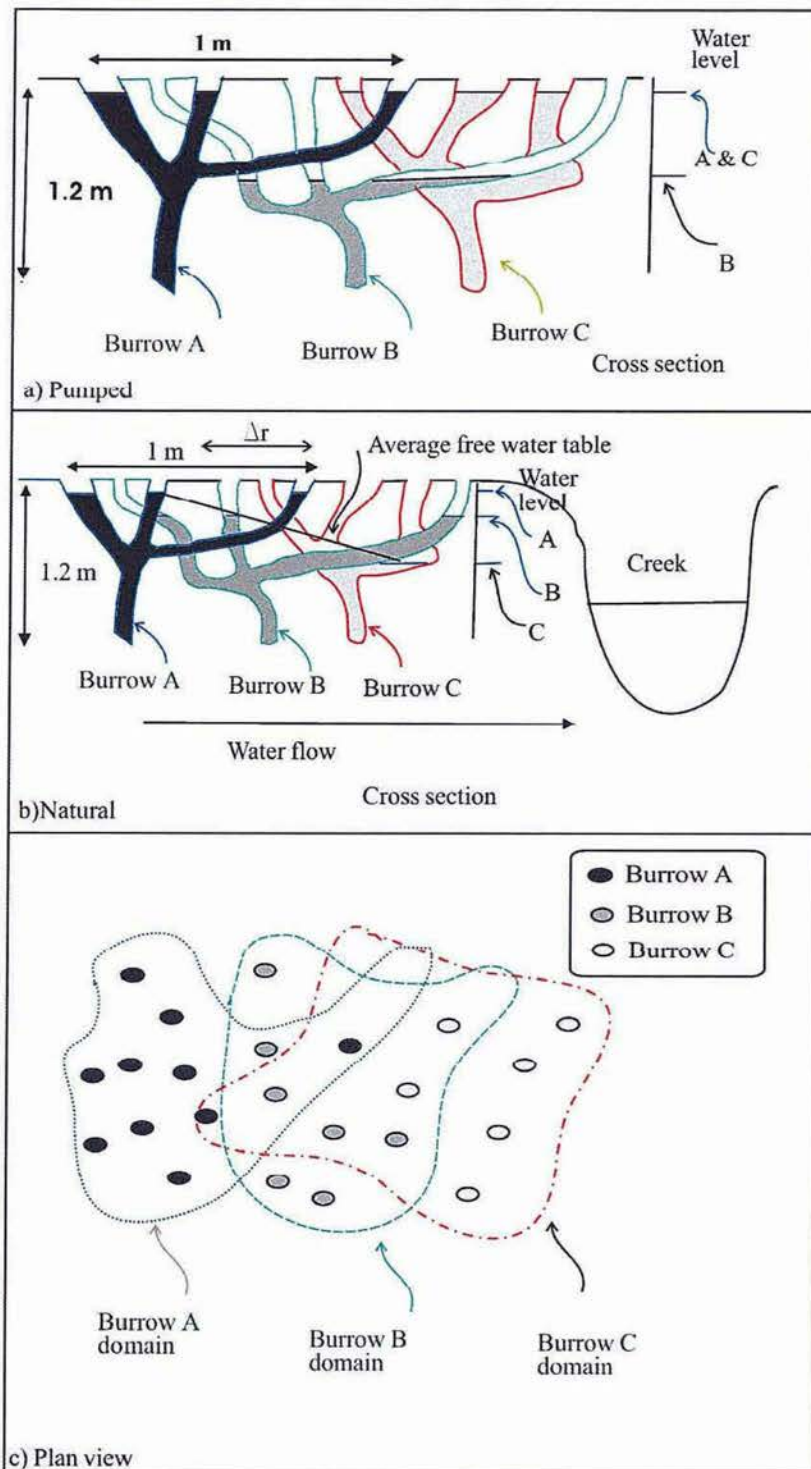


Figure 4.1: Schematic diagram of crab burrows that are intermingled with, but separate from each other. (a) shows the case when a quantity of water is pumped from burrow B. (b) shows the normal relative water levels in the burrows, i.e. where the closer the burrow to the creek, the lower the water level in the burrow. Note the burrows size is greatly exaggerated compared to the size of the creek. (c) shows the plan view of three burrows systems that intermingle with each other.

The parameter Δr requires some further explanation. As the water naturally flows through the ground towards the creek, in the direction of the hydraulic gradient, it will pass from one burrow to another (Figure 4.1b). Because flow within the burrow chambers has effectively zero resistance, the net flow rate is determined by the resistance to flow in the sediment between chambers of adjacent burrow systems. As the water flows towards the creek, it experiences a succession of discrete water pressure drops as it passes from one burrow system to another, i.e., the water level drops by Δz in the distance between the burrows (Δr). This value of Δr has a scale equivalent to the horizontal scale (radius) of the burrow systems (see Figure 4.1c). In practice this can be easily estimated when the water is removed from the burrow because the burrow openings will have a lower water level than the surrounding burrow systems. By noting the positions of the burrow openings where the water level drops, measurements of the horizontal extent of these burrow can be made, thus, giving an estimate of Δr .

Equation 4.1 allows the calculation K . A small quantity of water is pumped from a burrow and the drop in water level Δz (in the order of centimetres) is measured with a ruler to an accuracy of 1 mm. Δr can be determined from the geometry of the burrow, and can determine the flux by measuring the time and the amount of the water that returns to the burrows. The flux of the water q is determined using the equation

$$q = \frac{\Delta V}{\Delta t} \frac{1}{A} \quad (4.2)$$

where ΔV is the volume of water that flowed into the burrow in time Δt , and A is the area of the curved surface surrounding the burrow domain. This surface is assumed to be a cylinder of radius Δr and height equal to the burrow depth H . The area A is given by

$$A = 2\pi\Delta rH \quad (4.3)$$

$\Delta V/\Delta t$ is the rate of flow into the burrow. Ideally $\Delta V/\Delta t$ must be measured instantaneously but in practice it is measured over some time interval (usually a few minutes). In this work, a convenient period of averaging was to set Δt to the time for the water to return halfway back to its original position. Δt can not be determined since the different burrows and type of sediment will be different for the time to return halfway back to its original position. ΔV is thus approximately half the volume of water removed.

The burrow depth H was determined using the method described by Stieglitz *et al.* (2000b). This involves using a small conductivity sensor mounted on the end of a glass fibre rod that is progressively inserted into the mangrove soil. When the conductivity sensor passes through an animal burrow, the conductivity reading rises by roughly a factor of three. By inserting the sensor into the soil a large number of times at different locations, a good indication of the burrow depth, typical chamber dimensions, and inter-burrow spacing, can be made. This methodology was also corroborated in one of the field areas by taking a resin cast of the burrow (Stieglitz *et al.*, 2000a).

The procedure for measuring K was carried out 1 or 2 hours after tidal inundation to ensure that the burrows are full of water and was repeated on numerous burrows in order to get an average bulk hydraulic conductivity for the region in question. Because these mangroves are only inundated during spring tides, all measurement were taken during spring tides. In this work, approximately 5 burrows were used in each region, each burrow being within a few tens of metres of each other.

4.2.2 Measurement of Bulk Hydraulic Conductivity using a Piezometer Array.

In order to verify the method described above to measure hydraulic conductivity, an independent method is required. In our case this is done using an array of piezometers in a transect perpendicular to a mangrove creek. Piezometers consist of a pipe that is

inserted into the soil with an opening near the bottom of the pipe (Hughes *et al.*, 1998a and Hughes, 1998b). Groundwater flows into the pipe and the water level in the pipe gives a measure of the water pressure. Provided that there are no significant vertical water flows, or impermeable layers, the water level in the piezometer also represents the free water table height.

In this work, three piezometers were installed by using a vibro-corer to extract a cylindrical core of sediment of radius 70 mm. A plastic pipe of radius 50 mm and length 2 m was then inserted into the cylindrical hole. Near the bottom of the pipe, slots are put into the plastic to allow water to flow into, or out of the pipe. Around these slots was placed a linen bag filled with coarse sand. The purpose of the sand is to allow water to percolate into the pipe without allowing the sediment to block the slots. Water level fluctuations in the piezometers were measured using pressure sensors attached to a data logger (Dataflow System PTY LTD, 1999). The data loggers recorded the water level every 30 minutes with an accuracy of 3 mm. Pressure sensors were calibrated both before and after deployment to achieve this accuracy.

By taking measurements of water table level (from the piezometers) during neap tides (when there is no surface recharge), conservation of mass can be used to infer the fluxes of groundwater between each piezometer. In addition, the piezometers also give measurements of water table surface slope and thus pressure gradient. With flow rate and slope, equation 4.1 can be used to determine the hydraulic conductivity.

In order to apply the above method to calculate the hydraulic conductivity from the data from the three piezometers, it is made the assumption that the bulk of the water flow occurs in the upper zone of the sediment that is perforated by animal burrows (Figure 4.2). Consider the slab of sediment shown in Figure 4.2 that is (a) above the impermeable lower layer, (b) between Piezometers A and B, and (c) has a dimension parallel with the axis of the creek of Δy . The volume of water in this slab below the water table is dependent on h , the distance from the water table to the impermeable layer; p , the porosity of the soil; and F_b , the fraction of this layer that is occupied by burrows, which are full of water in this zone. It will presume that for small water

slopes, h will be a constant over the length, Δx_1 , of the slab. The volume of water above the water table will depend upon the degree of saturation of this layer, $F_s(t)$, and also the fraction of this layer, F_b that is occupied by animal burrows, which are empty of water in this zone. F_s will be equal to 1 for fully saturated soil and equal to zero for completely dry soil. Hence the volume of water in the slab is given by the following equation:

$$V = h \Delta x_1 \Delta y p (1 - F_b) + (H - h) \Delta x_1 \Delta y F_s(t) p (1 - F_b) + h \Delta x_1 \Delta y F_b \quad (4.4)$$

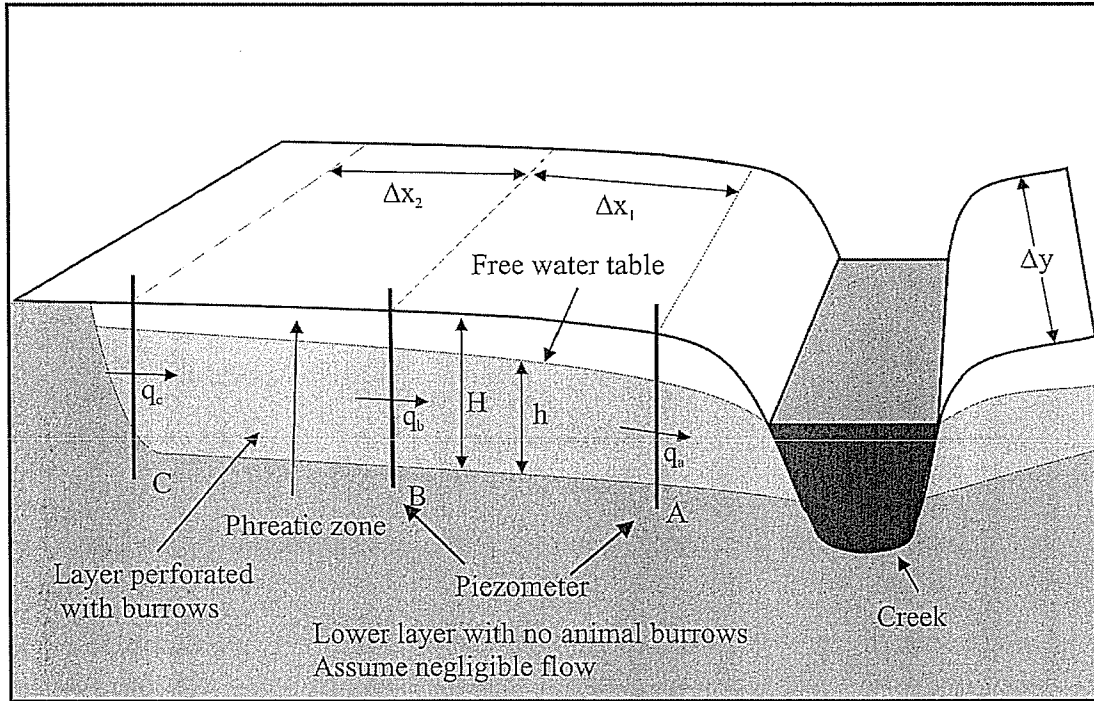


Figure 4.2: Model of groundwater flow in the mangrove swamp during neap tides.

Equation 4.4 is derived by considering the volume of water contained in the porewater and in the burrows. The first term on the right hand side of equation 4.4 represents the pore water in the region below the water table surface, the second term represents the pore water in region above the water table, and the third term represents the water in the burrow.

By considering the flux entering and leaving the slab, the rate of change of water volume in the slab of sediment between piezometer A and B is given by the following equation:

$$\frac{\Delta V}{\Delta t} = -q_a h \Delta y + q_b h \Delta y - E \Delta y \Delta x_1 \quad (4.5a)$$

and similarly for the sediment between piezometers *B* and *C*

$$\frac{\Delta V}{\Delta t} = -q_b h \Delta y + q_c h \Delta y - E \Delta y \Delta x_2 \quad (4.5b)$$

where *E* is the evapotranspiration rate. On the right hand side of equations 4.5(a) and 4.5(b), the first term represents the groundwater flowing out of the sediment matrix towards the creek, the second term represents the flow into the volume, and the third term represents the loss of water due to evapotranspiration. Hollins and Ridd (1997) found *E* to range from 1 to 5 mm/day with a typical value for mangroves of around 2 mm/day.

It was assumed in this analysis that the flux $q_c = 0$ because of field conditions (discussed later) with presumed low hydraulic conductivity due to the absence of animal burrows. Equation 4.4 is used to calculate the volume of the stored water in the sediment between piezometer sites *C* – *B*. q_b is calculated from equation 4.5b, i.e.

$$q_b = -\frac{\left(\frac{\Delta V}{\Delta t}\right) - E \Delta x_2 \Delta y}{(h \Delta y)} \quad (4.6)$$

Using Darcy law, and assuming that the flux midway between piezometers *B* and *C* is the average of the fluxes q_c and q_b , the value of *K* between site *C* and *B* was determined using

$$K = \frac{q_b}{2} \frac{\Delta x_2}{\Delta h_{CB}} \quad (4.7)$$

where Δh_{CB} is the water level difference between piezometers C and B.

However, to calculate q_a , the value of q_b must be taken into account, i.e..

$$q_a = \frac{-\left(\frac{\Delta V}{\Delta t}\right) + q_b h_b \Delta y - E \Delta x_1 \Delta y}{h_a \Delta y} \quad (4.8)$$

Finally, the calculation of K value between site B and A is accomplished using

$$K = \frac{(q_b + q_a)}{2} \frac{\Delta x_1}{\Delta h_{BA}} \quad (4.9)$$

where Δh_{BA} is the water level difference between piezometers B and A.

In order to use this method it is necessary to determine F_s , F_b , and p . This is described below.

4.2.2.1 Determining degree of saturation F_s

F_s is defined as the ratio of the water content of the sediment to the water content when the sediment is fully saturated. When the sediment is inundated by a spring tide, the sediment will be fully saturated, and therefore the degree of saturation will be 1. After the last inundation of the spring tides, the sediment will slowly dry, and therefore the degree of saturation will decrease. F_s was determined experimentally by measuring the reduction in the wet bulk density of samples of sediment taken from the unsaturated layer. This was done by digging a small hole in the sediment and removing a cylindrical sample of sediment of roughly 3 cm in diameter and 3 cm in length from the walls of the hole. The weight of these samples was determined on an electronic mass balance and then the sample volume was measured by immersion in a measuring cylinder of water and noting the change in water level. The bulk density of

the sample could thus be calculated and compared with density of fully saturated samples (ρ_{bw}) taken during spring tide inundation. This was performed on 15 samples every second day during periods when the mangroves were not inundated. The reduction in density of the samples were assumed to be due to the water loss of the sediment and thus the degree of saturation could be determined. It was found that on average, during neap tides the sediment samples were 85% saturated, i.e. $F_s = 0.85$.

4.2.2.2 Determining the fraction occupied by burrows, F_b

F_b was determined from previous experiments conducted by Stieglitz *et al.* (2000a) and found to be approximately 0.1 as explained in the Chapter 1, section 1.2.2.

4.2.2.3 Determining porosity p

Porosity (p) of the sediment is determined based on the equation,

$$p = \frac{\rho_g - \rho_{bw}}{\rho_g - \rho_f} \quad (4.10)$$

where ρ_g is the average density of the sediment particles, ρ_{bw} is the saturated bulk density, and ρ_f is the water density (Rieke and Chilingarian, 1974). The value of ρ_{bw} from our measurements was $1.61 \pm 0.023 \text{ g/cm}^3$. ρ_f ranges from 1.028 g/cm^3 for water of salinity 35 to 1.052 g/cm^3 for water of salinity 50. The value of these densities are also dependent on the temperature. The value of ρ_g for most sediments range from 2 to 2.2 g/cm^3 (Allen, 1985). Therefore, porosity of the sediment ranges from 0.41 to 0.51.

4.2.3 Description of field sites

The field sites were chosen in the upper reaches of Cocoa Creek, Gordon Creek and Three mile Creek, which are all small mangrove fringed estuaries in tropical North Queensland, Australia (see Figure 4.3).

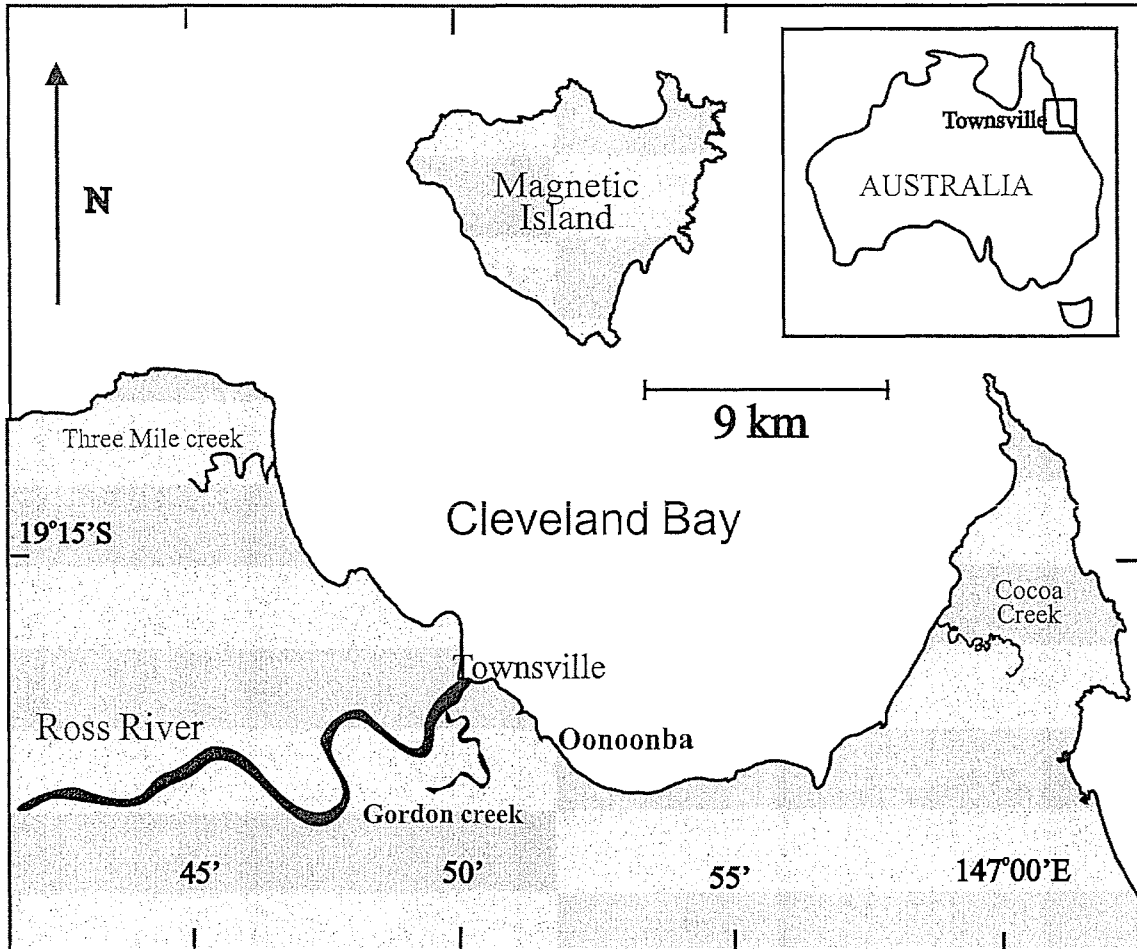


Figure 4.3: The location of experiments at Cocoa Creek, Gordon Creek and Three mile Creek. Piezometer experiments were carried out at Cocoa Creek only, while burrow experiments were at all three locations.

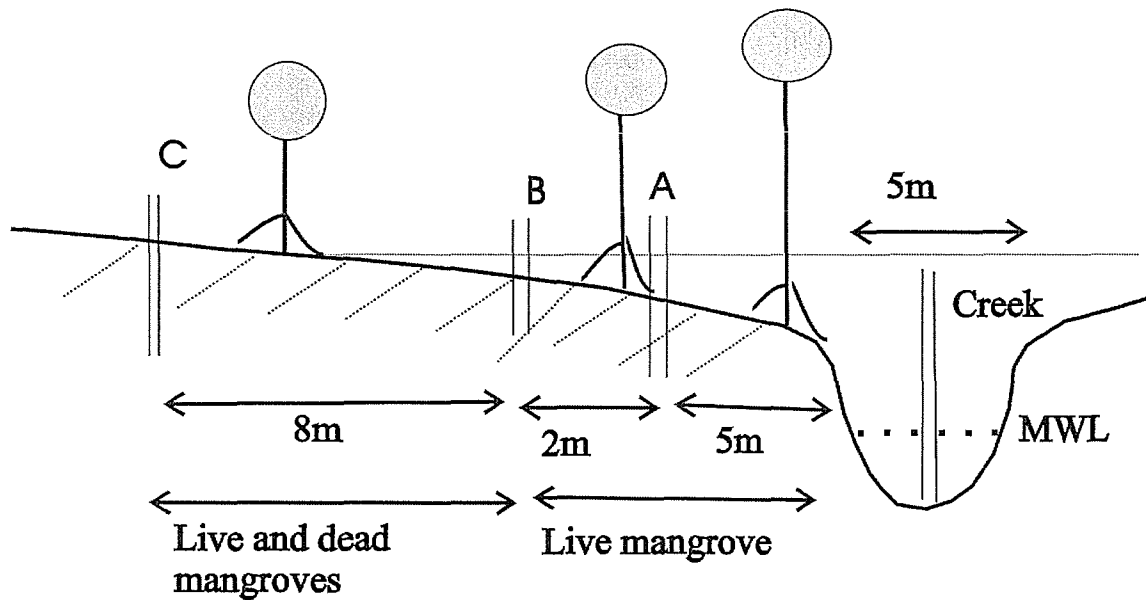


Figure 4.4: Piezometer array in the upper reaches of Cocoa Creek.

The first site is Cocoa Creek area (see Figure 2.5 on Chapter 2). The piezometer transect in Cocoa Creek area passes from the creek through a thin fringe of mangroves and an area of live mangroves mixed with dead mangroves as shown in Figure 4.4. The width of the band of mangroves is around 7 m from the creek and the width of live and dead mangroves is around 10 meters. Burrows also occur along this transect and were pumped to determine the hydraulic conductivity of mangrove sediment. Burrow density in this area is about 10 to 13 holes/m² of sediment surface.

The second site is Gordon creek area (see Figure 2.7 on Chapter 2). At the study site there are two types of mangrove plants, i.e. *Rhizophora stylosa* and *Ceriops spp.* The *Rhizophora stylosa* forest grows close to the creek and its sediment surface is relatively lower (290 cm above LAT) than *Ceriops spp.* area (300 cm LAT). Another difference between the *Rhizophora stylosa* and *Ceriops spp.* forests in this area is that the *Rhizophora stylosa* trees are generally taller (ca 8 m) than the *Ceriops spp.*, (1 – 6 m) (Hollins, 2001). The density of the number of crab burrow openings in the *Rhizophora stylosa* forest is about 14 holes per m², which is higher than in the *Ceriops spp.* forest which has around 6 holes per m².

The final experimental area was conducted at Three Mile Creek (see Figure 2.9 on Chapter 2). Only burrow experiments were conducted. The number of burrows openings for each burrow system in this area ranges from 5 to 15 holes and the density is about 25 holes/m².

4.3 Results.

4.3.1 Sediment Physical Properties in the field area

Material composing the sediment affects the effective porosity of the sediment and is a relatively important factor in determining the hydraulic conductivity. Effective porosity is the porosity of the bulk sediment, which can be less than or the same as true porosity. For coarse material, such as gravels, effective porosity is not different to true porosity, but for fine material, effective porosity is less than true porosity. Particle size analysis of the sediment at each site was determined using a Malvern Instruments Mastersizer analyzing the 7 μm to 1000 μm size fraction. The results are shown in Figure 4.5. It can be seen that the particle size at Three Mile Creek is significantly coarser than at the other sites. Cocoa Creek had the finest sediment. The mean for each site was 10 μm , 25 μm , and 53 μm for Cocoa Creek, Gordon Creek., and Three Mile Creek, respectively.

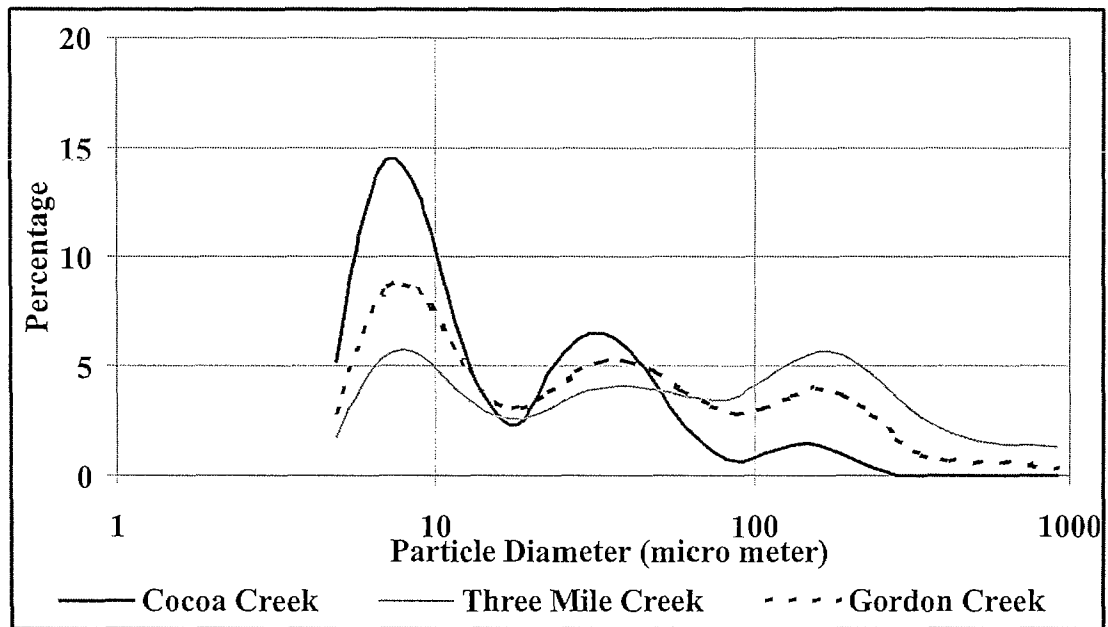


Figure 4.5: Sediment particle size distribution at the study sites. The samples were taken at the mangrove forest of *Rhizophora stylosa* at Cocoa and Three mile Creeks and *Ceriops spp.* at Gordon Creek.

4.3.2. Measurement of hydraulic conductivity of sediment using animal burrows.

The results of measurement of hydraulic conductivity for the four different field sites are shown in Table 4.1. The size of the error was determined from the variability of individual measurements and is a very large fraction of the measured value.

Location	Average Hydraulic Conductivity K (m/day)	Standard error (m/day)	Number of measurements
Gordon Creek Rhizophora	7.4	3.5	7
Gordon Creek Ceriops spp.	0.8	0.6	4
Cocoa Creek Rhizophora	3.7	2.7	5
Three Mile Creek <i>Rhizophora</i>	9.9	5.4	4

Table 4.1: Hydraulic conductivity at different field sites measured by removing water from the animal burrows .

4.3.3. Calculation of hydraulic conductivity using the piezometer array.

In order to confirm the accuracy of the results of hydraulic conductivity determined from the burrow experiments shown in Table 4.1, hydraulic conductivity was also determined using the piezometer array at Cocoa Creek (Figure 4.4). Groundwater level recordings were used to calculate volumes (V), fluxes (q) and hydraulic conductivity (K) in the mangrove area (between sites C and B, and A and B).

The water level from the piezometers at the Cocoa creek site from 25 July to 10 August 2001 (Julian day, from 206 to 222) are shown in Figure 4.6. During this period the neap and spring tides are evident. The neap tides are characterized by a slow and monotonic reduction in the water level, in this case from days 207 to 210 and from day 218 to 222, except for 218 and 220 for site A. The data from Figure 4.6 gives a measure of the change of h with time.

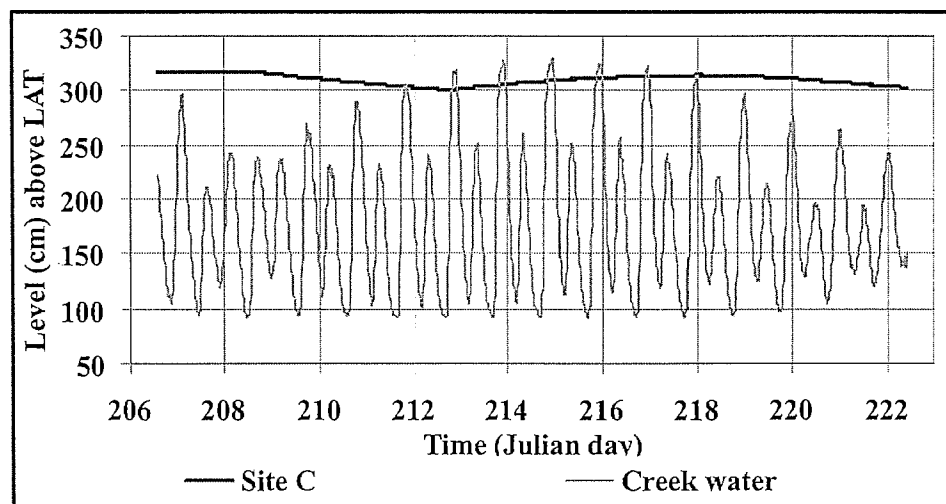
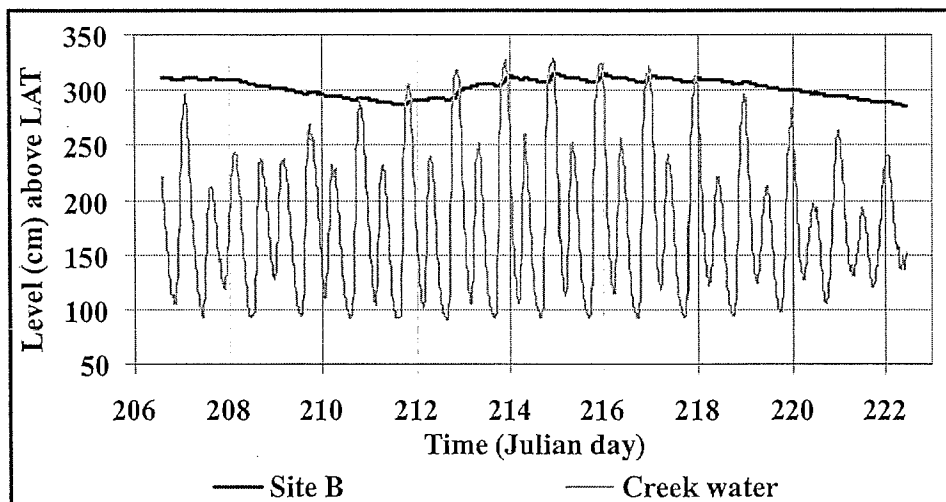
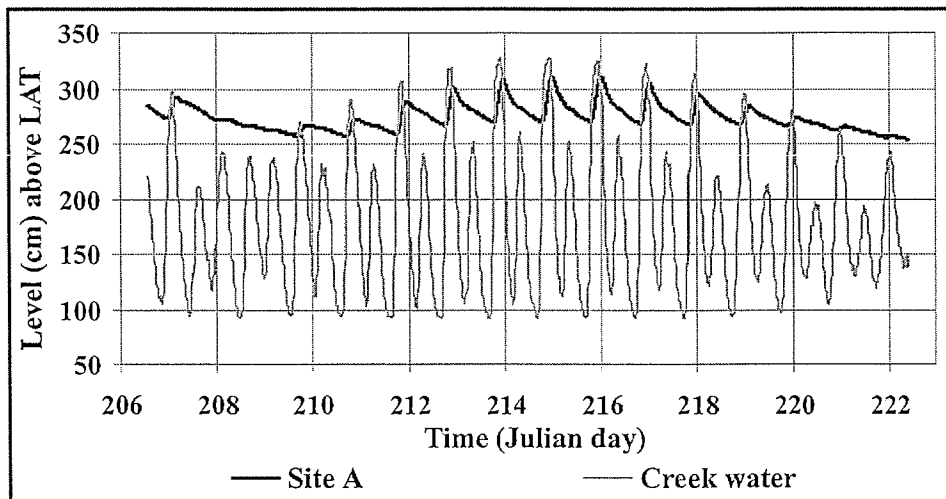


Figure 4.6: Fluctuation of groundwater and creek water level at site A, B and C at Cocoa creek recorded using pressure sensors. Of particular note is the water level at the site closer to the creek (A), shows a very pronounced tidal signature. At site C there is no tidal signature at the

diurnal and semidiurnal frequency but the spring-neap oscillation is evident the tidal signature is so small.

Hydraulic conductivity using groundwater level was calculated for data from piezometer sites A, B and C. Days processed were 208, 218 and 220, i.e. when there was no inundation due to neap tides except for site A. During each of these days, the value of K , was estimated over four 6 hour time intervals. In order to give an idea of the dependence of the calculation on evaporation rate E , calculations were done with two values of E i.e. 1 mm/day and 2 mm/day, the latter probably representing a typical value whereas 1 mm/day would be an extremely low value (Hollins and Ridd, 1997).

The results of K from this calculation is shown in Table 4.2

Julian days	K_{CB} (m/day)		K_{CB} (m/day)		K_{BA} (m/day)		K_{BA} (m/day)	
	$(E = 2 \text{ mm/day})$		$(E = 1 \text{ mm/day})$		$(E = 2 \text{ mm/day})$		$(E = 1 \text{ mm/day})$	
208	1.27	(0.24)	1.45	(0.24)	0.28	(0.06)	0.32	(0.06)
218	1.29	(1.15)	1.49	(1.17)	0.38	(0.23)	0.40	(0.23)
220	1.58	(0.43)	1.78	(0.43)	0.89	(0.25)	3.74	(0.78)

Table 4.2: Average and standard deviation (in brackets) of hydraulic conductivity calculation of mangrove sediment using Evapotranspiration 1 mm/day and 2 mm/day and porosity, p , of 0.46 ± 0.05 .

It can be seen that a wide range of values of K calculated from this method using $E = 1 \text{ mm/day}$ ranges from 1.1 to 3.4 m/day and using $E = 2 \text{ mm/day}$ ranges from 1.0 to 3.0 m/day. Based on these results the average value of K is $K = (2.5 \pm 0.8) \text{ m/day}$ and $K = (2.2 \pm 0.7) \text{ m/day}$ for $E = 1 \text{ mm/day}$ and $E = 2 \text{ mm/day}$, respectively.

4.4 Discussion

The results of the measurements of the bulk hydraulic conductivity, K , using the new method indicated that K is highly variable spatially at any one site. At Gordon Creek in a *Rhizophora stylosa* forest, measurements of K varied from 2.5 to 10.5 m/day over 7 samples with an average value of 7.4 m/day and a standard deviation of 3.5 m/day. In an adjoining *Cerriops spp.* forest the calculated values of K averaged 0.81 m/day with a standard deviation of 0.61 m/day. This significant reduction in the average value of K seems reasonable as the burrow density in the *cerriops spp.* forest is much less than in the *Rhizophora* forest (14 and 6/m²) respectively. An area of *Rhizophora* forest in Cocoa Creek yielded an average K of 3.7 m/day with a standard deviation of 2.7 m/day (5 samples). At Three Mile creek a very high value of K was found (average 9.9 and standard deviation of 5.4 m/day). This may have been the result of the coarser, and therefore more permeable sediment found at the Three Mile Creek site. However a more extensive experimental program would need to be carried out to confirm this with enough samples to do rigorous statistical analysis.

At the Cocoa Creek site, measurements of K using piezometer data were also carried out. Assuming an evapotranspiration rate of 1 mm/day, this method yields the result that K was 2.5 ± 0.8 m/day. If the evapotranspiration was 2 mm/day, the corresponding value of K was 2.2 ± 0.7 m/day. This compares with the result from the burrow method of 3.7 m/day and standard deviation of 2.7 m/day.

It is inevitable that any method for determining K will have relatively large error bars. In the burrow method, because of the complicated shape of the burrows, the dimensions of the burrow system are not exactly known and the geometry used in the calculation is a simplification of the real geometry. In addition large spatial variations in K may well be real. Though the error bars in this work are large, natural variations in the value of K for different material may vary by many orders of magnitude. For example, for sand (particle size 0.06 to 2 mm), K is in the order of 1 to 100 m/day, whereas for silt (2 to 60 μm particle size) K may fall to 0.01 to 0.1 m/day (Wilson, 1994). Relative to such enormous natural variation in K , the error bars reported here are modest and the burrow method gives a useful estimate of K .

The measurement of hydraulic conductivity of sediments is problematic requiring piezometers which are expensive and difficult to install. This paper presents a new and innovative method that allows the rapid assessment of hydraulic conductivity using existing crab burrow networks. Each measurement on one burrow takes approximately 20 minutes and typically five to 10 burrows should be measured to allow averaging of a significant area of the swamp. Field results show that the new method compares well to more traditional estimates using piezometers. Thus estimation of hydraulic conductivity may be made relatively quickly and with a minimum of equipment, especially compared with the methods using piezometers. The method also does not in any way disturb the sediment matrix.

Field measurements of hydraulic conductivity of the mangrove sediment were considerable higher than would be expected with sediment with no macropores, with values ranging from 1 m/day to 10 m/day.

Chapter 5. Comparison between tidally-driven groundwater flow and flushing of animal burrows in tropical mangrove swamps.

5.1 Introduction

Groundwater flow processes vary with seasons, in particular in the tropics. Groundwater flow typically decreases in absolute volume over the dry season, and nutrient concentrations in a mangrove creek in Brazil were reported to also decrease towards the end of the dry season (Lara and Dittmar, 1999; Cohen *et al.*, 1999), which may be linked to the reduced groundwater flow dynamics. However, Kitheka *et al.* (1999) estimated that the contribution of groundwater seepage, including nitrite and nitrate components, was highest during the dry season in Mida Creek, Kenya, showing an increase of the relative importance of groundwater flow in the dry season. For instance, groundwater seepage due to the tide passing through mangrove swamps has been found to maintain mangrove trees during the dry season, although nutrient shortage and high salinity were occurring in the mangrove forest (Kitheka *et al.*, 1999). Hence groundwater flow can potentially contribute to the nutrient cycle of a mangrove swamp, which is thought to be important for the ecology of mangrove ecosystems (Wolanski, 1992).

Besides affecting the nutrient cycling and water properties, groundwater flow in mangrove swamps also influences the porewater salinity of the soil. Mangrove trees exclude large quantities of salt at their roots (Hollins *et al.*, 2000). If accumulated salt is not removed, hypersaline conditions can be fatal (Passioura *et al.*, 1992). Two mechanisms have been identified by which salt can be removed from the root zone. Firstly, it may be dissolved and carried to the mangrove creek by direct groundwater flow through the sediment. Secondly, it can diffuse through the soil to nearby crab burrows (Stieglitz *et al.*, 2000a; Hollins *et al.*, 2000), from where it may be flushed

during tidal inundation (Ridd, 1996a; Stieglitz *et al.*, 2000a; Heron, 2001a). The latter mechanism is known as “burrow flushing”.

Burrow flushing during inundation may be an important factor in exchanging solutes (oxygen, nutrients, toxins and salt) between surface water and burrow water (Heron, 2001a), and recent research has investigated the mechanism driving this process (Aucan & Ridd, 2000) and has attempted to quantify it (Hollins and Ridd, accepted). Flushing of burrow water occurs during tidal inundation and is caused by a pressure difference across the numerous openings of the burrow due to the surface water slope (Aucan & Ridd, 2000). It was estimated that about 30% of burrow water was flushed per tide during that process (Hollins and Ridd, accepted). This proportion may represent a significant absolute volume of exchanged water for the swamp since burrows have an overall depth (D_{burrow} on Figure 5.1) up to 1.2 m (Stieglitz *et al.*, 2000a). Each burrow is a discrete system that may represent about 10 % of the swamp soil volume, but because systems intermingle, the actual proportion of burrow volume in the mangrove soil is thought to be greater than this value, which also increases the volume of flushed water.

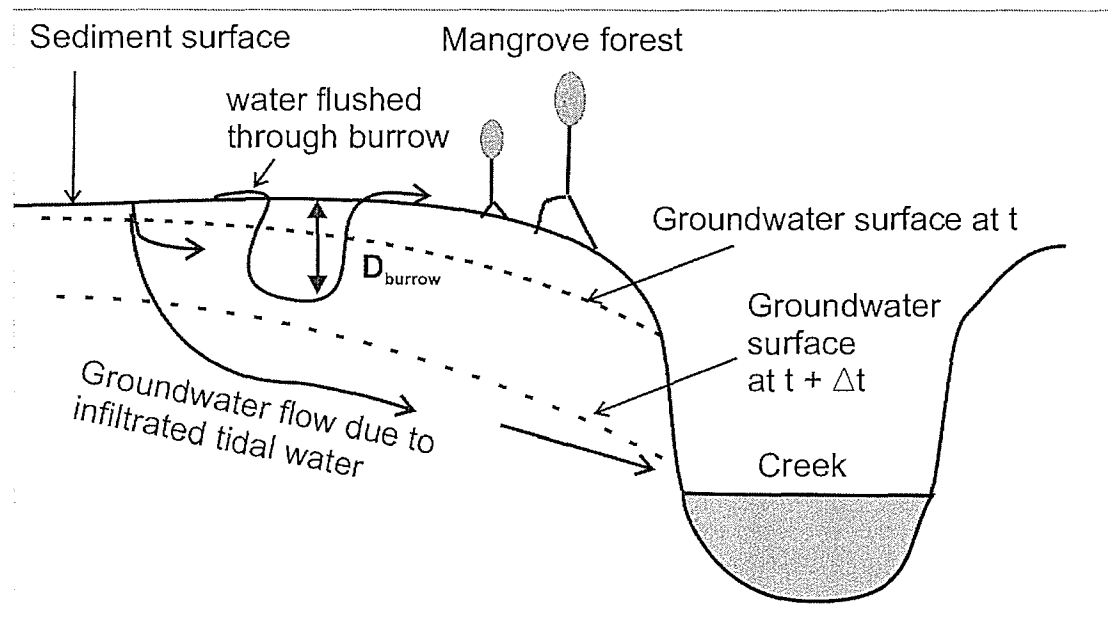


Figure 5.1: Groundwater flow paths through a mangrove swamp during tidal inundation, via direct flow caused by infiltration and via burrow flushing.

As outlined above, tidal water in a mangrove swamp can flow to the creek by two mechanisms illustrated on Figure 5.1: (a) groundwater that flows through the sediment as interstitial pore-water from the swamp to the creek due. This flow is a consequence of water infiltration, especially during and after tidal inundation, and is due to the hydraulic gradient between the swamp and the creek. Hereafter it will be called “direct groundwater flow”. And (b) flushing of free water through animal burrows during tidal inundation, that will be called “burrow flushing flow” hereafter.

In this chapter, we compare the importance of water flow rates due to direct groundwater flow and due to burrow flushing in mangrove swamps, assuming that both mechanisms occur. This chapter is the first attempt to compare these processes quantitatively.

5.2 Methods

5.2.1 Study sites

The two study sites were located in mangrove forest area at the upper reaches of Cocoa Creek and Gordon Creek (see Figure 2.5 and 2.7 on Chapter 2). These sites were selected because they contained extensive mangrove communities and well developed creek network. Besides, experiments on the hydraulic conductivity of mangrove sediment had been carried out previously in both areas (see Chapter 4). Finally, investigations on the morphology of burrows (using resin casts (Stieglitz *et al.*, 2000a)) and on the proportion of burrow water flushed during each inundation (Hollins and Ridd, accepted) had also been conducted in the *Rhizophora stylosa* mangrove forest at Gordon Creek.

The first measurements (Cocoa Creek) were taken along a 16 m transect outward from the creek through a thin fringe of living and dead mangroves. Living mangroves occur immediately adjacent to the creek and span over a width of *ca.* 7 m, followed by dead mangroves over a width of *ca.* 8 m and salt-flat areas.

The second study site, Gordon Creek (see Figure 2.7 on Chapter 2). The mangrove forest growing along Gordon Creek is mainly composed of *Rhizophora stylosa* at the edge of the creek and *Ceriops spp.* The latter are found further landward from the creek and reach a few meters high before rapidly becoming stunted (1 m high) at the fringe with the bare salt flat. The total width of the mangrove forest at the study site is *ca.* 36 m and it is entirely flooded by tides greater than 3.0 m above LAT. Although there is some human disturbance of the region around Gordon Ck, the area selected to carry-out the groundwater flux study was not impacted and one can be confident that both the groundwater and surface water dynamics at the site have not been altered.

5.2.2 Piezometer arrays

Four piezometers were installed at Cocoa Creek amongst the living and dead mangrove trees at irregular intervals, at 2 and/or 4 m depth depending on the site, and water level was logged continuously from 14 June through to 27 September 2001 (Table 5.1 and Figure 5.2).

Sites no.	Site name	Level of the screen (PVC) above LAT (cm)	Distance from the Creek (m)	Level of the soil surface above LAT (cm)
Cocoa Creek				
1.	A2	104	5	309
2.	A4	-82	6.1	313
3.	B2	114	7.1	319
4.	C2	114	15	319
Gordon Creek				
5.	O1	190	1	285
6.	O2	190	6	257
7.	O3	195	13	258
8.	O4	197	23	276
9.	O5	200	36	287

Table 5.1: Position and name of piezometers used for recording groundwater level.

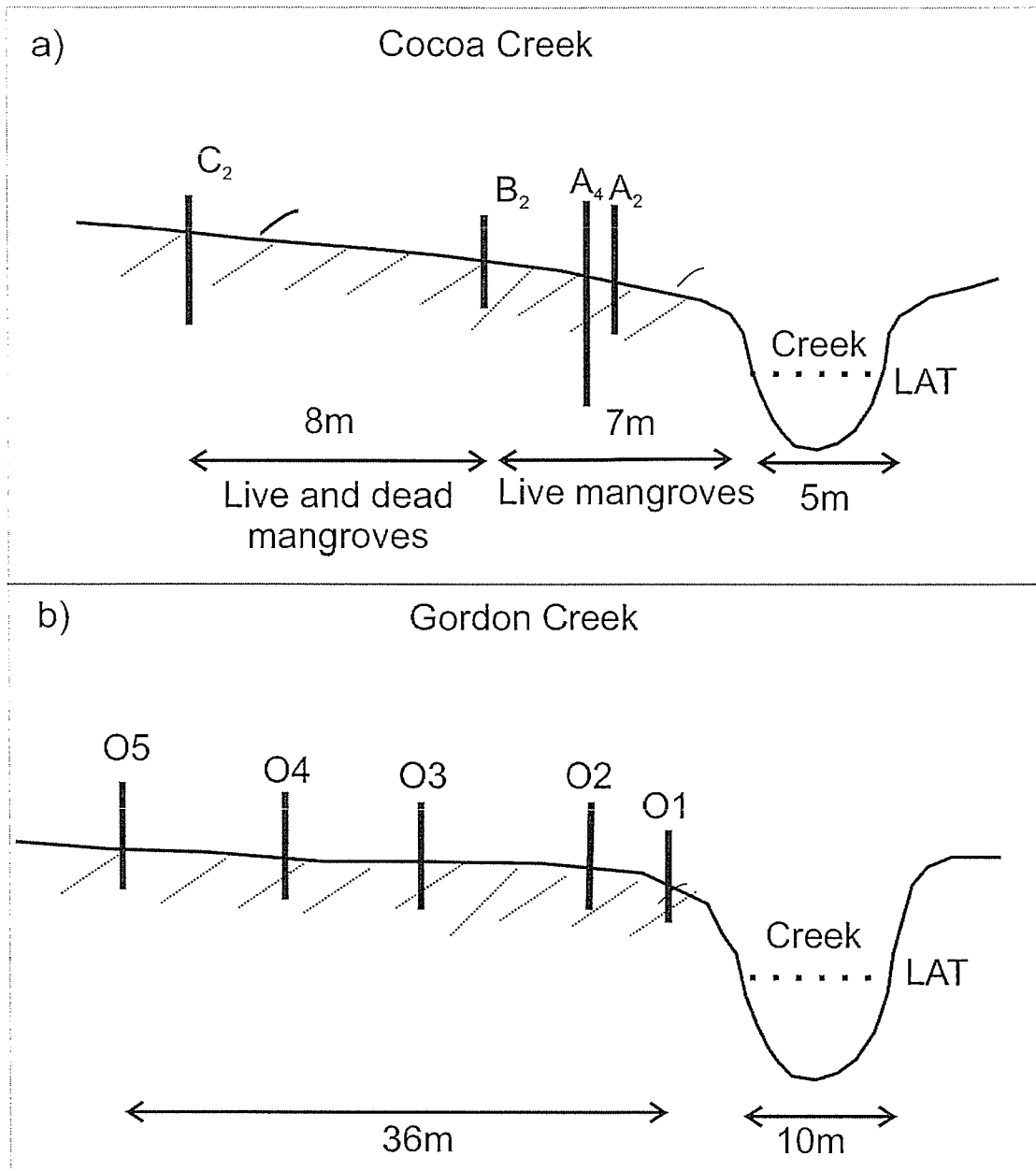


Figure 5.2: Piezometers transects as installed: (a) in the upper reaches of Cocoa Creek, with three instruments amongst live mangroves, and one in a mixed zone of dead and live trees; and, (b) at Gordon Creek.

A fifth piezometer was deployed in the middle of Cocoa Creek for 2 weeks in order to compare tidal variations on site with tidal predictions at Townsville. Observations and predictions appeared to coincide, and predictions were used from then on to determine tidal elevation at the field site. Each piezometer was deployed by drilling a 70 mm diameter hole in the mangrove sediment with a vibrocore barrel and placing a 50 mm

diameter PVC tube in the hole. Dataflow Systems Pty Ltd (Australia) pressure sensors were then mounted inside the PVC tubes (Figure 5.3) and the data logger was attached on top of a stand approximately 1.5 m high from the sediment surface to avoid flooding at high tide.

At Gordon Creek, 5 piezometers were installed from October 2001 to April 2002, at approximately 1 m depth mostly in the *Rhizophora stylosa* area, except for one piezometer that was installed at the border between *Rhizophora stylosa* and *Ceriops spp* (Figure 5.2b and Table 5.1). A depth of 1 m was chosen to position the bottom of each piezometer in a burrow and to record water level inside burrows. The deployment site was also the area where Stieglitz *et al.* (2000a) determined the depth and the volume of the burrows to be 1.2 m and 70 l respectively. With hindsight of the data recorded, piezometers were positioned inside burrows at sites O3, O4 and O5, but probably not at sites O1 and O2.

5.2.3 Piezometer description

Approximately 200 holes of 2.5 mm diameter were drilled 5 to 20 cm from the bottom of a PVC tube to create a screen encasing the pressure sensor (Figure 5.3). The screen was surrounded by a cotton bag filled with coarse sand to allow free groundwater flow from the surrounding soil into the PVC tube. To ensure that the water flowing into the PVC tube enters at the level of the screen, an impermeable bentonite gel barrier was placed above the sand screen. This prevented water from flowing down the side of the piezometer. A second bentonite gel barrier was made around the top 70 cm below the surface to prevent surface water flowing directly to the screens during tidal inundation or rainfall. The piezometer configuration at Gordon Creek was similar except that no bentonite barrier was placed above the sand screen, since the intention was to measure water levels inside burrows. It was possible to confirm that the water level in the PVC tube was the same as in adjacent burrows by removing water from the tube and watching to see if the water level in the burrows dropped. Bentonite was placed at the top to avoid surface water from flowing into the piezometer along the pipe. It should be noted that the free water table in the burrows,

as measured by the piezometer is likely to be similar to that in the sediment surrounding the burrows as the burrows are hydraulically in close contact with the sediment.

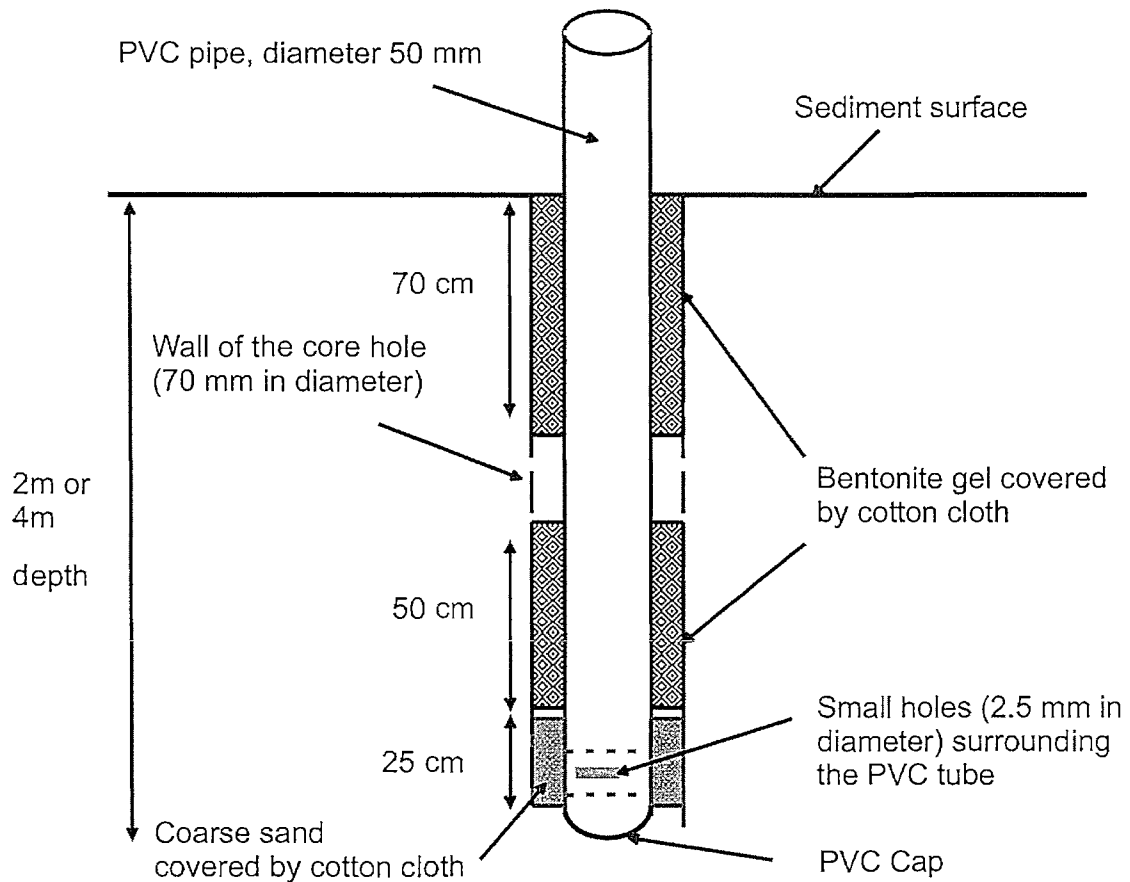


Figure 5.3: Schematic view of the PVC tube used to install piezometers in the field at Cocoa Creek. The same setup was used at Gordon Creek, except that no bentonite barrier was used above the sand screen.

Each pressure sensor was calibrated in a tank before field deployment. In addition, further calibration was carried out every 4 weeks in the field. This was done by immersing every sensor at 20 cm, 40 cm, 60 cm, 80 cm and 100 cm below the groundwater level in the piezometer holes for 4-minute periods, with a sampling rate of 30 second. The piezometer response to these known water depths was used to calibrate depth versus pressure response. The water level in each piezometer was then recorded at 30-minute intervals and downloaded every 2 weeks.

5.2.4 Model description

Upon tidal inundation, a certain amount of tidal creek water with a salinity of *ca.* 35 inundates the mangrove forest. Some of this water infiltrates the mangrove sediment pores and becomes groundwater that will flow back to the creek due to the pressure gradient difference between mangrove forest sediment and creek. Flushing of salt in mangrove sediment will affect the salinity of the groundwater, which will be:

$$S = 35 + \Delta s$$

where Δs is positive, depending on the salt concentration in the sediment. The infiltration process occurs until the whole sediment is water saturated.

When tidal height is lower than the swamp sediment surface and there is no tidal inundation, the water table level in the mangrove forest is located below the swamp sediment surface and infiltration will not occur. However, the tidal influence is still present in the sediment body, as the water level in the sediment will follow the tidal signature, up to a certain distance from the creek. Further away from the creek, groundwater level in the sediment will slowly fall because it will be out of range of the horizontal pressure caused by tidal fluctuations.

Regardless of the tide height, level with respect to the swamp sediment surface, the water table level will gradually fall during ebbing periods until the next flooding tide. Moreover, in both cases where the water level is lower than the sediment surface (i.e. at ebbing tide of high tides, and during flooding and ebbing of small high tides), the rate of groundwater loss from the mangrove sediment pores to the creek over a period Δt can be calculated from the piezometer water level (see Equation 5.1 referring to Figure 5.4).

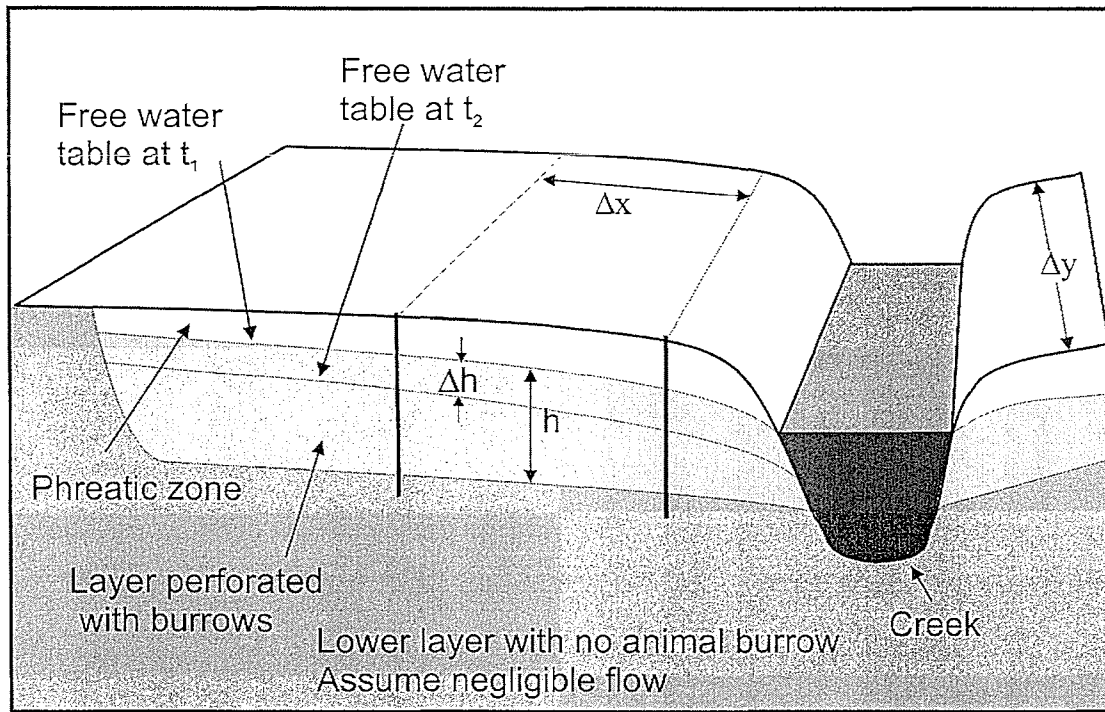


Figure 5.4: Position of the underground water table during ebb tide. During a few hours (days), when ebb or small high tides occur, the water table in the sediment body will drop in relation with the porosity of the sediment.

Based on Figure 5.4, the equation for direct groundwater flow can be defined as:

$$\frac{\Delta V}{\Delta t} = \left(\frac{\Delta h}{\Delta t} - E \right) \Delta x \Delta y (1 - F_s(t)) p (1 - F_b) + \left(\frac{\Delta h}{\Delta t} - E \right) \Delta x \Delta y F_b \quad (5.1)$$

where $\frac{\Delta V}{\Delta t}$ = rate of change of volume of water stored in the sediment (m³/day);

$\frac{\Delta h}{\Delta t}$ = rate of change of the water table level (measured with the piezometers)

(m/day);

E = evapotranspiration rate (m/day);

Δx and Δy are defined in Figure 5.4 (m);

$F_s(t)$ = degree of saturation of the sediment (%);

p = porosity of the sediment (%);

F_b = fraction of sediment layer that is occupied by animal burrows (%).

The first term on the right hand side of equation 5.1 is the rate of change of water volume stored in the sediment pores, and the second term is the volume of free water that is stored in the burrows. Both terms refer to a period Δt . Hence Equation 5.1 expresses the total amount of tidal water that is stored in a slab of sediment of surface area $\Delta x \Delta y$ over a period Δt .

The groundwater fluctuations recorded by the piezometers were used to determine the value of $\frac{\Delta V}{\Delta t}$ in equation 5.1 and to calculate the rate of change of water volume stored in the sediment. The water level was calculated and averaged for each piezometer over periods of hours or days, depending on the data available. During times within the spring-neap-tidal cycles that no inundation occurs (neap tides), an averaging interval of a few days was possible. During periods of daily tidal inundation, an averaging periods of greater than a few hours is not possible. For example, the slope at Cocoa Creek site was averaged over a few hours at sites A2 and A4, and over 3 or 4 days at sites B2 and C2. Such differences in the time period over which the calculation is done does not introduce any additional error, provided that the drop in water level over that period is not too small (i.e. greater than *ca.* 1 cm), so that Δh is clearly significantly greater than the piezometer resolution. This calculation was also conducted at Gordon Creek sites, where the slope was averaged over periods of a few hours at site O2 and a few days at the other sites.

Tidal flushing of the burrow was also modeled for the same slab of surface area $\Delta x \Delta y$, over a period of time Δt , based on the configuration presented on Figure 5.1. The average volume of water that is removed from the burrows over approximately a lunar cycle period ($Dt = 1$ month) was calculated. Since water is removed from the burrows at each inundation of the swamp, the number of inundations per month (N) was first determined. Different mangrove swamps will undergo different numbers of inundations over a lunar cycle, depending on the level of the swamp sediment surface and characteristics of the tide. From the physical characteristics of the mangrove

swamp, the flow rate of the water flushed from a burrow, Q_{wf} , can be described as follows:

$$Q_{wf} = \Delta x \Delta y D_b F_b F_{wf} \frac{N}{\Delta t} \quad (5.2)$$

where: D_b = depth of the burrow;

F_b = fraction of burrow volume compared to sediment volume;

F_{wf} = fraction of burrow water flushed per inundation;

This flow rate is expressed in m^3/day , but it can be reduced to a rate in (m of depth/day) or in (m of depth / s) by considering 1 m^2 of sediment surface.

5.3 Results

5.3.1 Fluctuations of groundwater levels at Cocoa Creek.

Figure 5.5 shows the results of groundwater fluctuations recorded at Cocoa Creek over approximately 2 weeks (14 - 28 June 2001) during the dry season (no rainfall occurred during that period). Although measurements were recorded over 3.5 months in total, only a 2-week subsample covering a spring-neap cycle is presented here for clarity. Other spring-neap cycles nor presented in the figures displayed a similar pattern. Because the swamp sediment surface of the mangrove forest at Cocoa Creek is relatively high (3.2 m above LAT), the sites were rarely inundated with only 9 inundations occurring per month on a yearly average, with the maximum number of inundations in March (15), and the minimum number in June (5, including the period shown on Figure 5.5).

Groundwater surface fluctuations in the mangrove area closest to the creek (Figure 5.5a and 5.5b) followed the daily fluctuations of the tide during spring tides. However, the shallower site (A2, 2 m depth) only shows one fluctuation per day, whilst the deeper site (A4, 4 m depth) shows two. Further away from the creek at sites B2 and C2, water level fluctuations do not follow the daily tidal pattern, but a weak

spring-neap cycle envelope is visible (Figure 5.5c and 5.5d). This water level cycle is as follows: a) the water level drops slowly during neap tides; b) the water level increases up to the swamp sediment surface with the first inundation of the swamp; c) the water level remains approximately at the swamp sediment surface level during the spring tides with small daily drops during ebbs; and d) the water level starts dropping continuously again when the high tide level does not exceed the swamp sediment surface level anymore. This pattern is also visible at site C2, the site furthest away from the creek (15 m), although without any daily signal, even during spring tides.

Groundwater levels are generally very close to the sediment surface during the spring tides and fall gently by about 30 cm by the end of neap tides. Groundwater rises rapidly after rainfall, by an amount determined by the rainfall. Generally there is little difference between the wet and dry season data, as the recharge due to rainfall is very small compared to the tidal inundation

The delay of water level fluctuations in the piezometers over the tidal cycles was 3 to 5 hours, depending on the distance of the piezometer from the creek and on the depth of the piezometer. The greater the distance from the creek, the longer the time lag between tide height and groundwater response. This happened because the tidal forcing needed more time to reach the longer distance from the Creek, and tidal water inundating the sediment needed time to infiltrate the layer of the sediment. In addition, at sites A4 and A2 which are close to each other but at different depths, the time lag was the same for both piezometers, but the deepest piezometer (A4) followed the tidal signature more closely in terms of amplitude of response. Sediment core analysis showed that the sediment at 4 m depth was coarse sand, whilst it was fine sand at 2 m depth. This difference in hydraulic conductivity may explain the difference in amplitude of responses at those two depths, as well as the fact that the record from site A4 shows 2 peaks per day as opposed to one (during spring tides) or none (during neap tides).

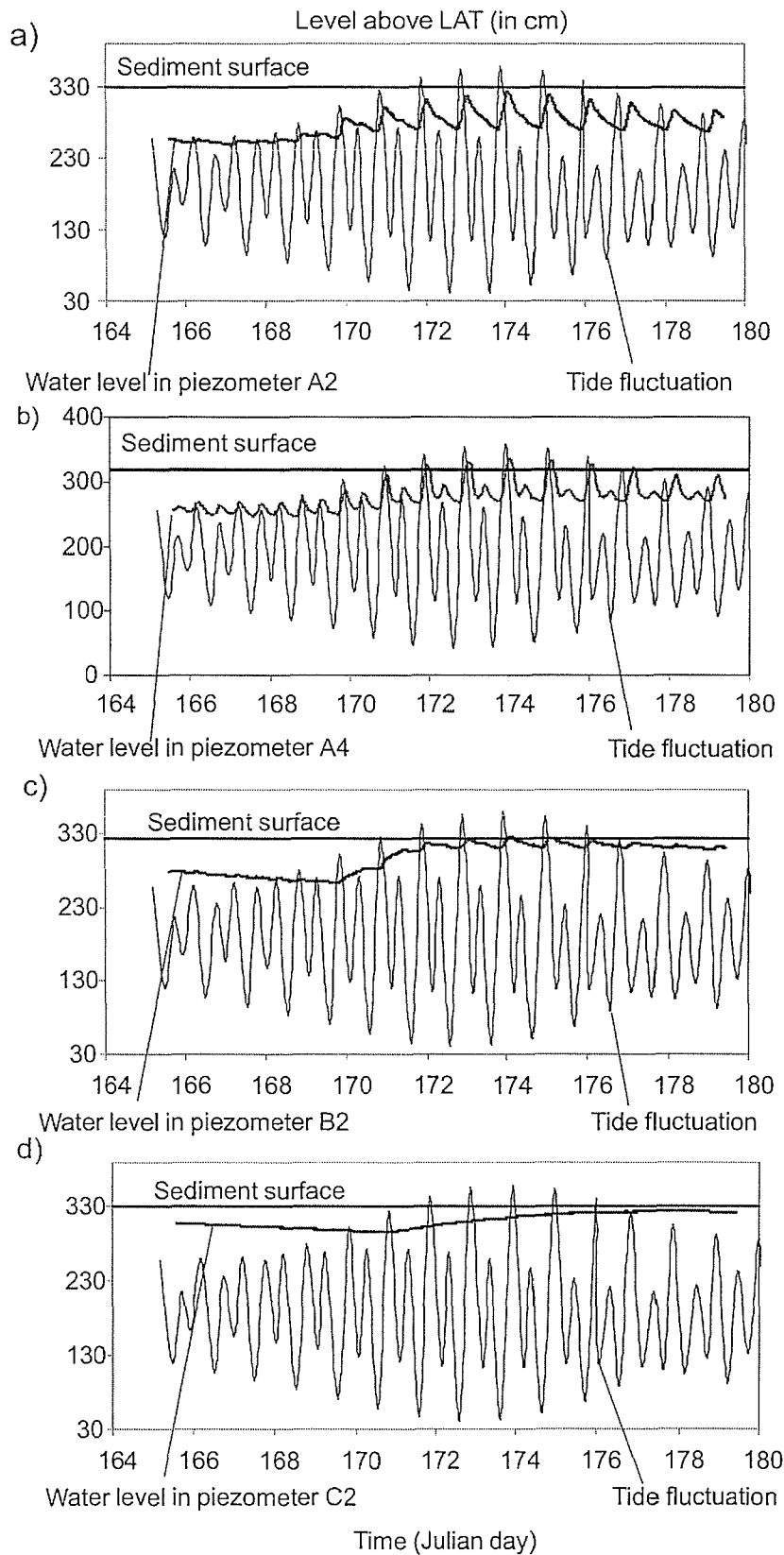


Figure 5.5: Fluctuations of groundwater level and tides at Cocoa Creek sites with respect to the sediment surface level. Swamp sediment surface level at each site and tidal levels taken from tide tables at Townsville are also shown.

5.3.2 Fluctuations of groundwater levels at Gordon Creek.

There was no period over which reliable data was recorded simultaneously at all sites at Gordon Creek, due to battery failure, faulty pressure sensors, and PVC screens not touching the burrows. Therefore, the data presented in Figure 5.6 covers different periods for different sites, but there was no rain throughout the duration of the study and thus conditions were consistent. All sites were inundated by the tide 19 times per month on average, which is therefore also the frequency at which the crab burrows were flushed.

Water level fluctuations at Gordon Creek show a similar pattern at sites O3, O4 and O5 (Figure 5.6c, 5.6d and 5.6e). This pattern is that the water level fluctuations followed the tidal signature when the tide was higher than the swamp sediment surface. In contrast, fluctuations disappeared when the tide did not reach the swamp sediment surface. There was no delay between tidal height and groundwater level peaks, which indicates that the piezometers were well connected to burrows.

At site O1, groundwater fluctuations followed tidal variations only for the highest tides, and without a time lag. A lag occurred only when the tide was below the swamp sediment surface, with a *ca.* 1 hour lag. During the rest of the study period, water height fluctuations display only one oscillation per day with a sharp rise and a slow fall, which were least pronounced at the end of the neap period. Site O2 showed two oscillation per day, on Julian days 318 and 320, and the rest were only one oscillation per day, which also tended to disappear at the end of the neap period. The time lag in groundwater level for this site was *ca.* 1 hour, similar to site O1. This lag suggests that sites O1 and O2 were not connected to a burrow.

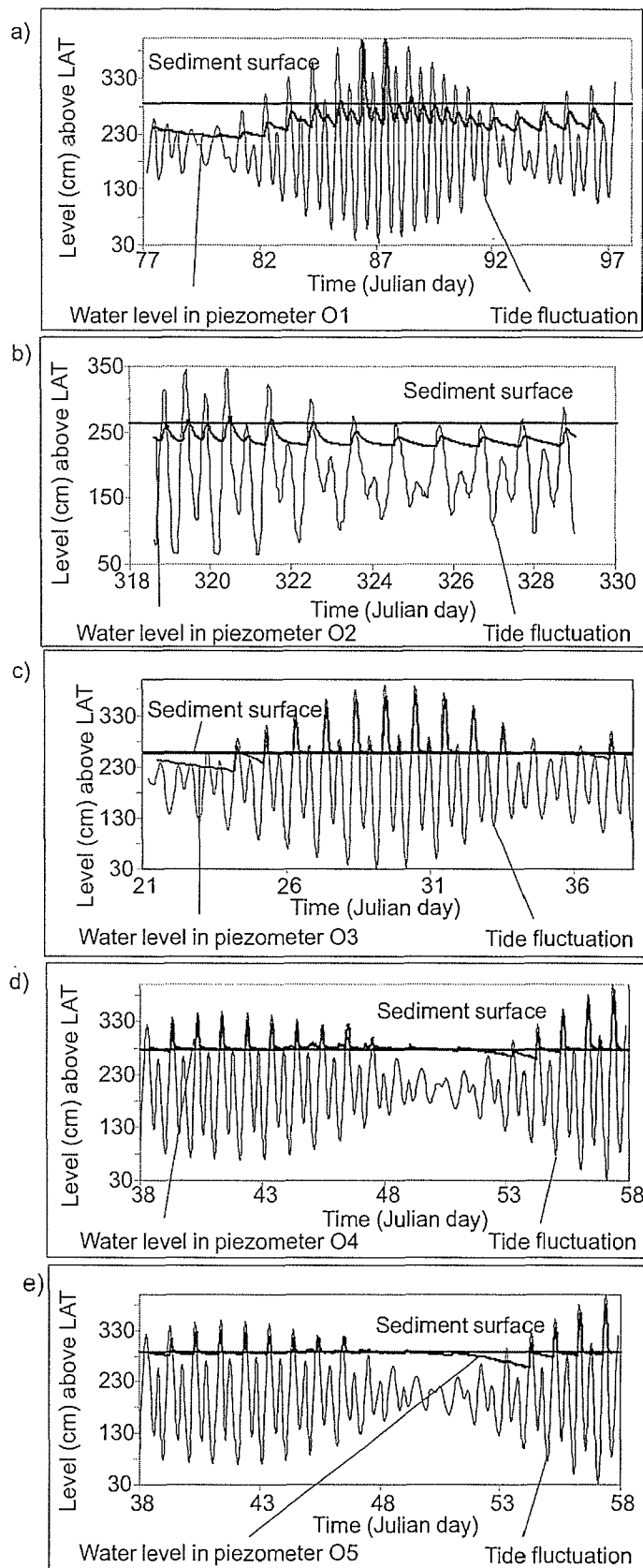


Figure 5.6: Fluctuations of groundwater level (from piezometer records) and tides (from tide table) at the Gordon Creek sites.

5.3.3 Direct groundwater flow.

Calculation results based on Eq. 5.1 for direct groundwater flow and for rate of change of water volume stored in the sediment are shown in Table 5.2. At both field sites, the area closest to the creek has a higher rate of change in water volume than the area farther from the creek. The only exception is at site O1 in Gordon Creek area, where the infiltration is less than site O2. This may be explained by the fact that the swamp sediment surface at site O1 was rising locally and caused the sediment surface to be higher than at O2 (285 cm above LAT at O1 and 257 above LAT at O2).

Sites	Rate of change of the water table level $\Delta h / \Delta t$ in (m/day)	Rate of change of water volume stored in the sediment per unit of sediment surface area $m^3/(m^2 \text{ day})$
A2 (Cocoa Ck)	0.13 ± 0.03	0.02 ± 0.004
B2 (Cocoa Ck)	0.05 ± 0.01	0.007 ± 0.002
C2 (Cocoa Ck)	0.03 ± 0.01	0.005 ± 0.001
O1 (Gordon Ck)	0.12 ± 0.09	0.02 ± 0.004
O2 (Gordon Ck)	0.18 ± 0.02	0.03 ± 0.005
O3 (Gordon Ck)	0.09 ± 0.02	0.015 ± 0.003
O4 (Gordon Ck)	0.11 ± 0.02	0.017 ± 0.003
O5 (Gordon Ck)	0.10 ± 0.02	0.016 ± 0.003

Table 5.2: Average and standard deviation of speed of infiltration obtained from each piezometer in two areas (Cocoa and Gordon Creeks, column 2), and volume of infiltrated water at each site (column 3).

From the above result, the average rate of change of water volume stored in a slab of sediment per unit area is $0.016 \pm 0.003 \text{ m}^3/(\text{m}^2 \text{ day})$. The maximum rate of groundwater stored in the sediment body per unit area is $0.02 \pm 0.004 \text{ m}^3/(\text{m}^2 \text{ day})$ and $0.03 \pm 0.005 \text{ m}^3/(\text{m}^2 \text{ day})$ for Cocoa and Gordon Creek area respectively, and both occur at *ca.* 5 m from the creek. Further away from the creek, the rate is about half of these values and seems to stabilise after the maximum point.

5.3.4 Calculation of burrow flushing during tidal inundation

The burrow flushing flow was calculated based on equation 5.2 with the following parameters: the average monthly number of tides that inundate the sediment surface in our field experiment at Cocoa Creek and Gordon Creek is 9 and 19 respectively; $D_b = 0.9 - 1.3$ m and $F_b = 0.05 - 0.15$ (Stieglitz *et al.*, 2000a); and $F_{wf} = 0.25 - 0.35$ (Hollins & Ridd, accepted). Hence, the average amount of water flushed per day through burrows, per 1 m^2 , is $0.01 - 0.04 \text{ m}^3/(\text{m}^2 \text{ day})$. We assume in this calculation that parameters are constant for the entire swamp area. From the results above, we can draw the comparison between direct groundwater flow and burrow flushing flow rates in both areas, as is in Figure 5.7.

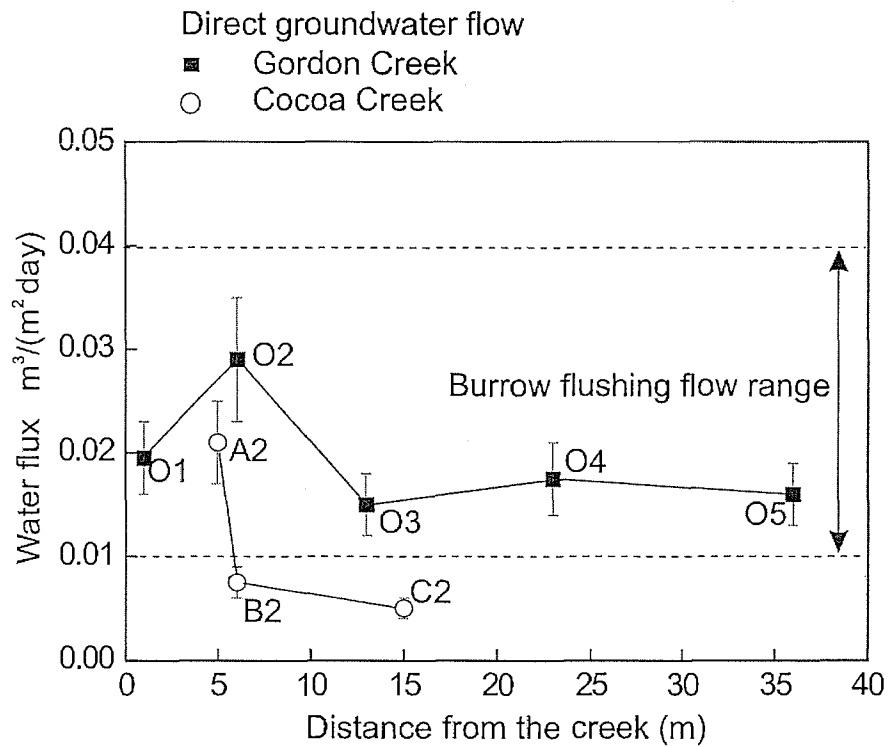


Figure 5.7: Comparison of direct groundwater flow and burrow flushing flow rates.

5.4 Discussion

Direct groundwater flow to the creek occurs everyday and the amplitude of this flow depends on the physical characteristics of the sediment including porosity, burrow fraction, evapotranspiration, degree of saturation of the sediment, and slope of the water level. Burrow flushing flow occurs only during tidal inundation of the swamp, and it depends on the fraction of burrows in the soil, the depth of the burrows, the number of tidal inundations, and the fraction of water in the burrow flushed for each inundation.

Using data from this and previous experiments in the same field areas (Susilo & Ridd, in press.; Stieglitz *et al.*, 2000a and b; Hollins & Ridd, accepted), both mechanisms were compared. More specifically, the amount of groundwater returning to the creek appeared to decrease by half at a distance of *ca.* 5 to 10 m from the creek compared to the section within the first 5 m from the creek. This decrease in flux with distance from the creek is perhaps expected as this is the region where water table slopes are the highest. In comparison to the groundwater flux range (0.007 - 0.03 m³/(m²day)), the burrow flushing flux was found to have a similar range of flux (0.01 - 0.04 m³/(m²day)). Considering the errors involved in the experiments and calculations, which are considered to introduce an error margin in the order of 50-100%, these ranges can be considered as being similar, and neither process can be considered dominant. Instead, both seem to be significant in terms of flow, and as a consequence in terms of their potential contribution to the flushing of salt and nutrient from the swamp sediment to the creek.

This result suggests that a new approach to studies of groundwater processes in mangrove swamps is required. In the past, direct groundwater flow has been considered the most important factor in transporting nutrients and flushing salt in mangrove environments (Wolanski & Gardiner, 1981; Cohen *et al.*, 1999; Kithika *et al.*, 1999). However most researchers (Lara & Dittmar, 1999; Mazda *et al.*, 1990; Wolanski, 1992) have drawn this conclusion qualitatively rather than quantitatively. One exception is a study by Hughes *et al.* (1998a) that provides calculation from

piezometer measurements of groundwater flux caused by tidal water. This earlier study shows that the groundwater flux was dependent on the rainfall and therefore season, with a variation by a factor three between dry and wet season.

Over recent years, studies have revealed that tidal water flushes some water in and out of animal burrows (Ridd, 1996a) that contain high salt concentration, as a consequence of a diffusion process from the mangrove sediment to crab burrows (Hollins, 2001). Burrow flushing processes are therefore also very important in the mangrove environment and Stieglitz *et al.* (2000a) stated that this process was an efficient mechanism for removing salt accumulated in the mangrove soil. The authors suggested from their experiment of conductivity measurements of burrow water that the burrow water was flushed completely in one hour (during a single tidal event) whilst Hollins and Ridd (accepted) found from oxygen concentration measurements that approximately 30 % of the burrow water was flushed during one tidal inundation. Hence flushing of burrows, whether complete or partial only, is increasingly recognised as an important process to flush salt from burrows.

In this chapter, we quantify both mechanisms (groundwater flow and burrow flushing) in two areas, and compare their relative importance for the first time. It appears that both have the same order of magnitude, with burrow flushing showing a slightly wider range than groundwater flow. As a consequence, surveys of groundwater processes in mangrove areas, and more generally in swamp and tidal areas where animal burrows are present, will need to consider both mechanisms. Investigations of the influence over flushing mechanisms of different residence times of the water in burrows and in the sediment body would also be recommended in order to establish salt and nutrient budget in mangrove swamps.

Chapter 6: Groundwater flow model in the mangrove forest

6.1 Introduction

The ability to predict groundwater fluxes with a minimum of effort and measurement is an important objective. Numerical modeling is one approach to obtain such a prediction. Predictions of groundwater fluxes can be used to determine fluxes of other materials such as salt and nutrients provided the concentrations of these materials are known independently. In this chapter an analytical model is developed to predict the flow of groundwater from the mangrove forest to the creek. The model will make use of the geometry and hydraulic conductivity determined in previous chapters. The model will be validated by comparing the model results of net flow rate of the groundwater with data collected from Gordon and Cocoa creeks, as described in Chapter 5.

The model used will follow a similar methodology to that used by Gill and Read (1996). The solution for the groundwater flow is written in terms of an analytic series solution, based on two dimensional potential flow. The approach is basically to solve the hydraulic potential flow for steady state conditions using the Laplace equation. The advantages of this method are that it is simple but accurate, and the error in the computation can be readily calculated.

The model is a steady state model and thus it cannot predict the time evolution of the groundwater levels. Although this is a weakness of the model, it allows a much simpler numerical scheme to be applied. The geometry to which the model will be applied is shown in Figure 6. 1. The sediment in the mangrove forest is composed of two layers, the upper layer of which has a very high hydraulic conductivity due to the presence of animal burrows. The lower layer is effectively impermeable. The presence of a relatively impermeable salt flat adjacent to the mangrove swamp is also taken into account by forcing a no flow boundary condition at this interface.

6.2 Methods

6.2.1 Laplace equation

The general equation of steady state flow in the groundwater flow is (Rushton & Redshaw, 1979):

$$\frac{\partial}{\partial x} \left(k_x \frac{\partial \Phi}{\partial x} \right) + \frac{\partial}{\partial y} \left(k_y \frac{\partial \Phi}{\partial y} \right) + \frac{\partial}{\partial z} \left(k_z \frac{\partial \Phi}{\partial z} \right) = 0 \quad (6.1)$$

where:

k_x, k_y, k_z are hydraulic conductivity of the sediment to the x, y and z direction

Φ is hydraulic potential of the groundwater, which is the groundwater level (Wilson, 1994).

If the soil of the sediment is homogeneous and isotropic, equation 6.1 can be written as:

$$\frac{\partial^2 \Phi}{\partial x^2} + \frac{\partial^2 \Phi}{\partial y^2} + \frac{\partial^2 \Phi}{\partial z^2} = 0 \quad (6.2)$$

Equation 6.2 is well known for steady state flow, and is called the Laplace equation. If the geometry is two dimensional vertically with flow only in the x and y direction, equation 6.2 becomes (Strack 1989, Bouwer 1978):

$$\frac{\partial^2 \Phi}{\partial x^2} + \frac{\partial^2 \Phi}{\partial y^2} = 0 \text{ or } \nabla^2 \Phi = 0 \quad (6.3)$$

Equation 6.3 will be used to solve the problem of groundwater flow from the mangrove forest sediment to the creek.

6.2.2 Boundary conditions

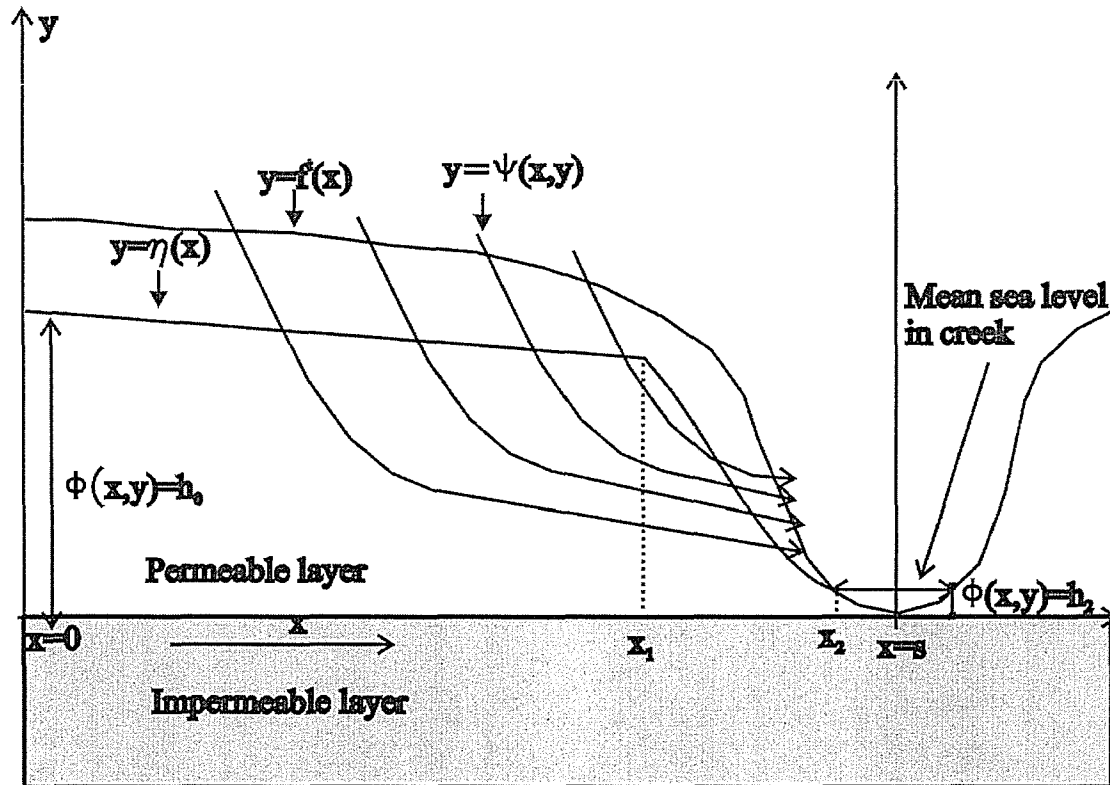


Figure 6. 1: Model of the groundwater seepage to the creek. In this model, h_2 is 0 m.

The symbols in Figure 6. 1 have the following definitions.

$\eta(x)$ represents the groundwater free surface.

$f'(x)$ represents the sediment surface

$\Psi(x, y)$ is the stream function of the groundwater

In order to solve the Laplace equation, the following boundary conditions are applied.

1. No flow across the vertical boundaries at $x = 0$ and $x = s$.

$$\left. \frac{\partial \Phi(x, y)}{\partial x} \right|_{x=0} = 0 \quad , \quad \left. \frac{\partial \Phi(x, y)}{\partial x} \right|_{x=s} = 0 \quad (6.4)$$

The above equations are velocity potential to the x direction.

2. No flow into the lower impermeable layer at $y = 0$.

$$\left. \frac{\partial \Phi(x, y)}{\partial y} \right|_{y=0} = 0 \quad (6.5)$$

3. The water level in the creek takes its tidally averaged value, i.e.

$$\Phi(x, y) = h_2 = 0, \quad x_2 < x \leq s \quad (6.6)$$

6.2.3 Solution for the hydraulic potential, $\Phi(x, y)$, of the groundwater

The method used to solve Laplace equation is separation of variables i.e. the hydraulic potential is written in the form (Gill & Read, 1996, Liggett & Philip, 1983):

$$\Phi(x, y) = X(x) Y(y) \quad (6.7)$$

Using the Laplace equation, equation (6.7) can be written as:

$$X'' Y + X Y'' = 0 \quad (6.8)$$

The solution of equation (6.8) is:

$$\frac{X''}{X} + \frac{Y''}{Y} = 0 \quad \text{then} \quad \frac{X''}{X} = -\frac{Y''}{Y} = -\sigma^2 \quad (6.9)$$

Equation (6.9) can be rewritten as:

$$X''(x) + \sigma^2 X(x) = 0 \quad (6.10a)$$

$$Y''(y) - \sigma^2 Y(y) = 0 \quad (6.10b)$$

Applying the boundary condition in equation (6.4), where there is no flow at $x=0$ and $x=s$, the solution of equation (6.10a) becomes:

$$X_n(x) = \cos(n\pi x/s) \text{ and, } n=0,1,2,\dots \quad (6.11)$$

Applying the bottom boundary condition (equation 6.5), the solution of equation (6.10b) is:

$$Y_n(y) = \begin{cases} \alpha_0, & n = 0 \\ \alpha_n \cosh(n\pi y/s), & n \geq 1 \end{cases} \quad (6.12)$$

The general equation can be written as (Gill and Read, 1996):

$$\Phi(x, y) = \sum_{n=0}^{n=\infty} [\alpha_n u_n(x, y)] \quad (6.13)$$

where:

$$u_n(x, y) = \cosh(n\pi y/s) \cos(n\pi x/s) \quad (6.14)$$

Equation (6.14) is a time independent function, and represents the steady hydraulic head (or hydraulic potential) throughout the saturated part of the soil beneath the mangrove forest.

6.2.4 The stream function, $\Psi(x, y)$, of the groundwater

In this model, where the sediment is homogeneous and isotropic, the direction of the flow will be normal to the equipotentials (Bouwer, 1978), and therefore the streamlines of the groundwater flow must be orthogonal to the equipotential or water table. The stream function $\Psi(x, y)$ is thus defined as:

$$v_x = -\frac{\partial \Psi}{\partial y} \quad , \quad v_y = \frac{\partial \Psi}{\partial x} \quad (6.15)$$

where v_x and v_y are velocities of flow (Rushton & Redshaw, 1979) in the x and y directions.

The equation of continuity is defined as:

$$\frac{\partial v_x}{\partial x} + \frac{\partial v_y}{\partial y} = 0 \quad (6.16)$$

Substituting equation (6.15) to (6.16), yields:

$$\frac{\partial^2 \Psi}{\partial x \partial y} - \frac{\partial^2 \Psi}{\partial y \partial x} = 0 \quad (6.17)$$

In homogeneous isotropic soil, where the hydraulic conductivity of the sediment is constant, v_x and v_y are (Rushton and Redshaw, 1979):

$$v_x = -\frac{\partial \Phi}{\partial x} \quad , \quad v_y = -\frac{\partial \Phi}{\partial y} \quad (6.18)$$

Therefore, the relationship between the hydraulic potential and stream function (Strack, 1989 page 222) is:

$$\frac{\partial \Phi}{\partial x} = \frac{\partial \Psi}{\partial y} \quad , \quad \frac{\partial \Phi}{\partial y} = -\frac{\partial \Psi}{\partial x} \quad (6.19)$$

Equation 6.19 is well-known Cauchy – Riemann equation.

Using equation (6.19), which is applied to equation (6.14), the stream function of the groundwater will be:

$$\Psi(x, y) = c + \sum_{n=1}^{n=\infty} \alpha_n \sinh\left(\frac{n \pi y}{s}\right) \sin\left(\frac{n \pi x}{s}\right) \quad (6.20)$$

Where c is an arbitrary constant. In this model, c is zero along the impermeable boundary.

The dimension of the stream function is $[L^2T^{-1}]$

6.2.5 Solving for $\Psi(x, y)$

6.2.5.1 Calculation of α_n coefficient

When the sediment is water saturated, the free water table will be the sediment surface itself,

$$\eta(x) = f'(x) \quad (6.21)$$

If variable y in equation (6.14) is replaced by the function of the sediment surface, $f'(x)$, then the equation will only have 1 variable, i.e. x . The hydraulic potential, $\Phi(x, y)$, will also only vary in x . $\Phi'(x)$ is introduced as a hydraulic potential, equation (6.14) becomes:

$$\Phi'(x) = \sum_{n=0}^{n=\infty} \alpha_n \cosh\left(\frac{n \pi f'(x)}{s}\right) \cos\left(\frac{n \pi x}{s}\right) \quad (6.22)$$

To solve the equation (6.22), it is needed to calculate the coefficients α_n . It will use the least square method to calculate the A_n , the least squares approximation to α_n . e The series after $n = N-1$ terms needs to be truncated, so equation (6.22) is rewritten as:

$$\Phi'_N(x) = \sum_0^{N-1} A_n u'_n(x), \quad (6.23)$$

where $u'_n(x) = \cosh\left(\frac{n \pi f'(x)}{s}\right) \cos\left(\frac{n \pi x}{s}\right)$

The hydraulic potential along the upper saturation boundary is:

$$h^t(x) = \begin{cases} \eta(x) & , & 0 \leq x \leq x_2 \\ h_2 & , & x_2 < x \leq s \end{cases} \quad (6.24)$$

Equation (6.24) assumes that the location of water table, $\eta(x)$ is known. Therefore

$$h^t(x) \approx \sum_{n=0}^{n=N-1} A_n u_n^t(x)$$

The hydraulic potential along the saturated boundary must satisfy:

$$h^t(x) \approx \sum_{n=0}^{n=N-1} A_n u_n^t(x) \quad (6.25)$$

The least square method is used to calculate the coefficient A_n from equation (6.25),

$$u^t a_{\sigma'} = h^t_{\sigma'} \quad (6.26)$$

$$[u^t]_{ij} = \langle u_i, u_j \rangle \quad , \quad [u^t_{\sigma'}]_i = \langle u_i, h^t \rangle \quad (6.27)$$

Note: $\langle u_i, u_j \rangle \neq \|u_i\|^2 \delta_{ij}$

The first step in this process is to calculate:

$$[u^t]_{ij} = \langle u_i^t, u_j^t \rangle = \int_0^s u_i^t(x) u_j^t(x) dx \quad (6.28)$$

where,

$$u_i'(x) = \cosh\left(\frac{i\pi f'(x)}{s}\right) \cos\left(\frac{i\pi x}{s}\right) \quad (6.29)$$

$$u_j'(x) = \cosh\left(\frac{j\pi f'(x)}{s}\right) \cos\left(\frac{j\pi x}{s}\right) \quad (6.30)$$

Note, i and j are integers, which are 1, 2, 3 ..., n

In the second step

$$\left[\frac{u_i'}{\%}\right]_i = \langle u_i', h' \rangle = \int_0^s u_i'(x) h'(x) dx \quad (6.31)$$

is calculated, where $u_i'(x)$ is calculated from equation (6.29) and $h'(x)$ is taken from equation (6.26).

The value of A_n are obtained by solving numerically the matrix equation (6.27). These values are then used to calculate hydraulic potential (equation (6.14)) and stream function (equation (6.20)).

6.2.5.2 Error analysis

The root mean-square error (RMS error) is defined by the error between the approximate measurement of A_i and the true value of T_i (Scheid, 1968). For discrete data, the RMS error is defined as:

$$\varepsilon = \left[\frac{1}{N} \sum_{i=0}^N (T_i - A_i)^2 \right]^{\frac{1}{2}} \quad (6.32)$$

where T_i are known values and A_i are approximate values.

In this model, both the fixed value of hydraulic potential $h'(x)$ and the approximate value of hydraulic potential $\Phi(x, y)$, resulting from the calculation of the series solution are continuous. Therefore, the RMS error is defined:

$$\varepsilon = \left[\frac{1}{s} \int_0^s \left(f(x) - \hat{f}_N(x) \right)^2 \right]^{\frac{1}{2}} \quad (6.33)$$

where: $f(x)$ is a true value

$\hat{f}_N(x)$ is a calculated value.

With larger values of n , the error tends to zero (Scheid, 1968)

6.2.6 Calculation of the flux (q)

The flux per unit length normal to the plane of flow of the groundwater can be calculated using the result of the stream function (Rushton & Redshaw, 1979), i.e.:

$$q = \int_{y_1}^{y_2} v_x dy \quad (6.34a)$$

$$= \int_{\Psi_1}^{\Psi_2} d\Psi = \Psi_2 - \Psi_1 \quad (6.34b)$$

From equation (6.20) and (6.34b), the flux between two points of the stream values can be calculated. Because the stream value is flux per unit length, the unit is square length/time or m^2/day .

6.2.7 Programming

6.2.7.1 Determination of the sediment surface, water table and free surface water.

The upper saturated soil boundary consists of the soil surface when the aquifer is fully saturated, and the water table when it is partially saturated. The approximation of the saturated boundary is a series of three spline segments. The creek bank is approximated using a cubic, and a linear function is used for the upstream section. The function from the creek bank to the (linear) forest sediment is approximated using a quadratic. In this model, the water level in the creek is assumed to be zero or $h_2 = 0$.

6.2.7.2 Steps in the program

The programming tool used in this modeling is Matlab Release 6 version 12. The following steps are used in the model:

Three polynomials are used to represent the true value of sediment surface as measured with field data. The same approximation is used for the field data, when a water table is present.

Calculating of A_n by:

- Calculation of $\int_0^s u_i'(x) u_j'(x) dx$ (from equation 6.28)
- Calculation of $\int_0^s u_i(x) h'(x) dx$ (from equation 6.31)
- Calculation of A_n , $u'_{\sigma'} = h'_{\sigma'}$.

When A_n has been found, the calculation of $\Phi(x, y)$ and $\Psi(x, y)$ is undertaken.

Both the water table, $h'(x)$, and hydraulic potential of the groundwater, $\Phi(x, y)$, are plotted together along the saturated boundary. Basically, both of these functions must have the same value. However, because the value of n for the calculation is not infinite, there is an error, which is explained in the subsection 6.2.5.2.

N (capital n) is chosen, so that the RMS error is less than 10^{-3} . This ensures three figures accuracy in the solution for the stream function.

Using equation 6.38b, it will be calculated the flux of the groundwater of this model. The result of this model calculation will be compared to the flux of the groundwater from field measurement and calculation in Chapter 5.

6.3 Results

The model was applied to calculate the groundwater flow at the Cocoa Creek peizometer transect described in Chapter 5 and shown in detail in Figure 5.6. The distance between the impermeable salt flat to the creek is 11 m, and the slope of the creek bank is 45° . The elevation of the sediment at the salt flat is 1.1 m, and at the creek bank is 1 m. The slope of the mangrove sediment model is 0.6° or 0.01. Calculations were performed for neap tides i.e. when there was no tidal inundation of the swamps. From the peizometer data, the position of the free water table is known over this period and was used as an input to the model.

Because the model is not a time dependent model it is not possible to calculate the evolution of the free water table and water fluxes over the period of the neap tides. It is however possible to calculate the fluxes at particular times provided the position of the water table is known. The neap tide period, which will be defined as the period when no inundation of the mangroves occurs, usually lasts 5 days. In the analysis below, the fluxes are calculated on each of the 5 days of the neap tide period. Because the water table during spring tides is effectively at the sediment surface, the model can also predict the spring tide situation. The net flux of groundwater from the sediment is calculated by numerically integrating the flux of water passing into the creek. Therefore, the model of six days after inundation is the same as the day zero, i.e. the sediment is water saturated.

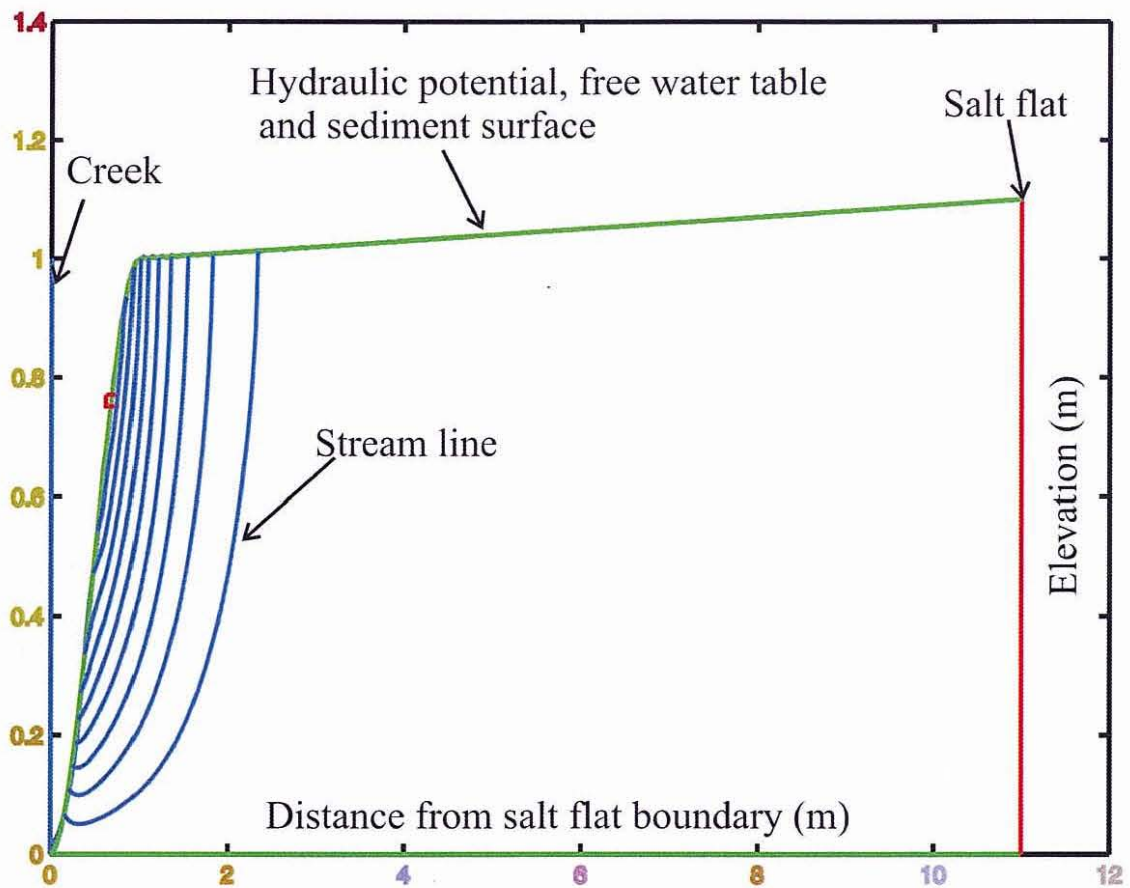


Figure 6. 2: The condition of the sediment, free water table and stream line, when sediment is water saturated or day zero.

Figure 6. 2 shows the results of the stream function immediately after the last tidal inundation of the spring tides, day 0, i.e. when the free water table was at the sediment surface. It should be noted that the result shown in figure 6.2 is also applicable for spring tides as the time of inundation is generally only a few hours per day even during spring tides. The water table for the rest of the period is at the sediment surface. Using piezometer data from successive days, the stream lines were calculated from day 1 to 5, after the last tidal inundation. These results are shown in Figure 6.3 to 6.7.

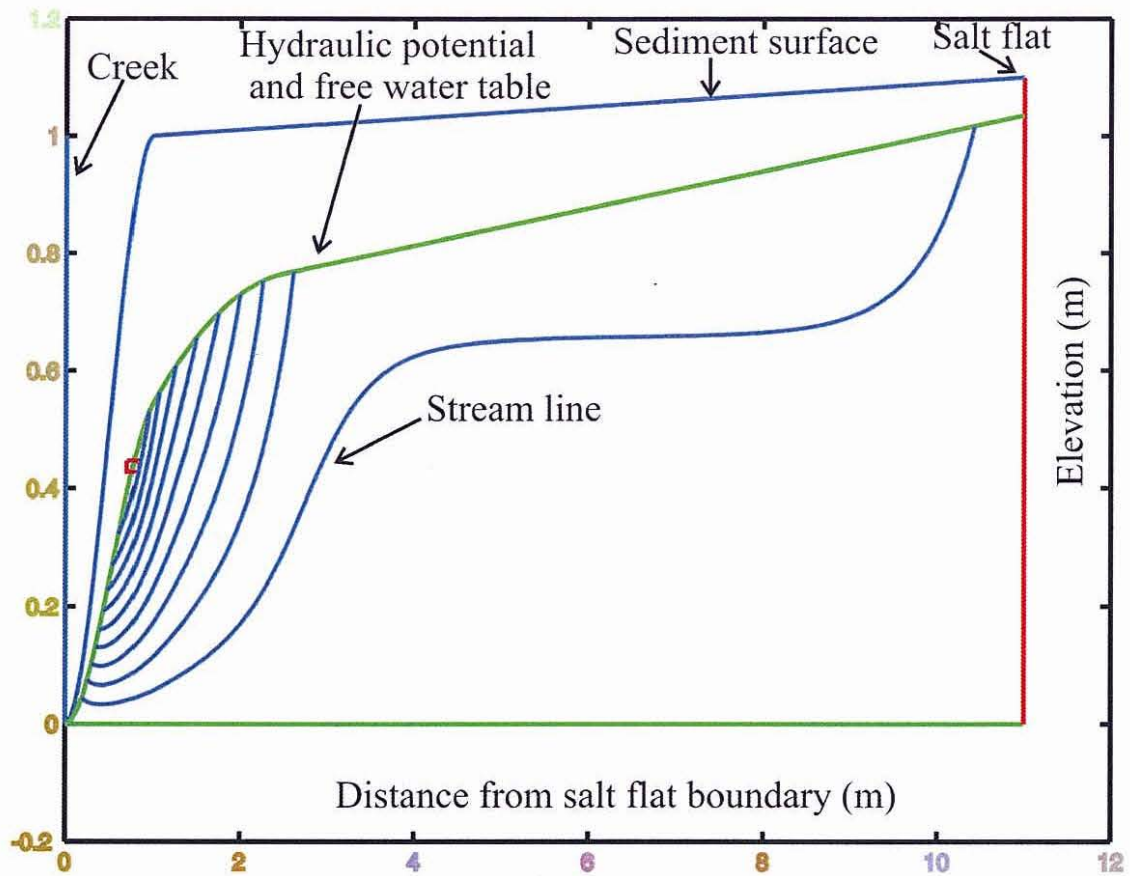


Figure 6.3: The condition of the sediment, free water table and stream line, when one day after inundation.

Figure 6.3 shows the condition of the model one day after inundation, where the slope of the water table increases, from 0.01 on the day zero to become 0.015 on the day one. The water table level is down by 0.065 m at the beginning of the sediment, to 1.035 m at the salt flat.

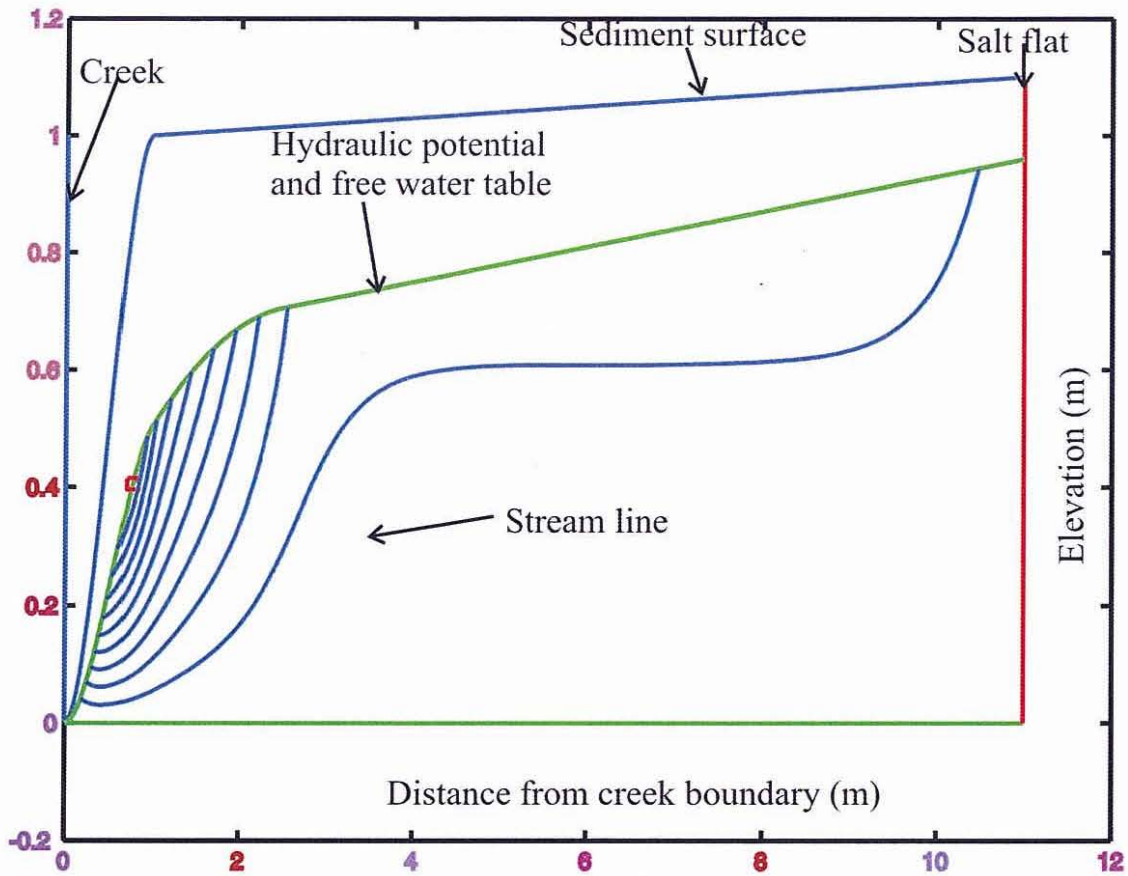


Figure 6.4: The condition of the sediment, free water table and stream line, on two days after inundation.

Figure 6.4 shows the condition of the model two days after inundation (day two), where the slope of the water table increases, from 0.015 on the day one to become 0.02 on the day two. The water table level is down by 0.14 m from the day zero at the beginning of the sediment, to 0.96 m at the salt flat.

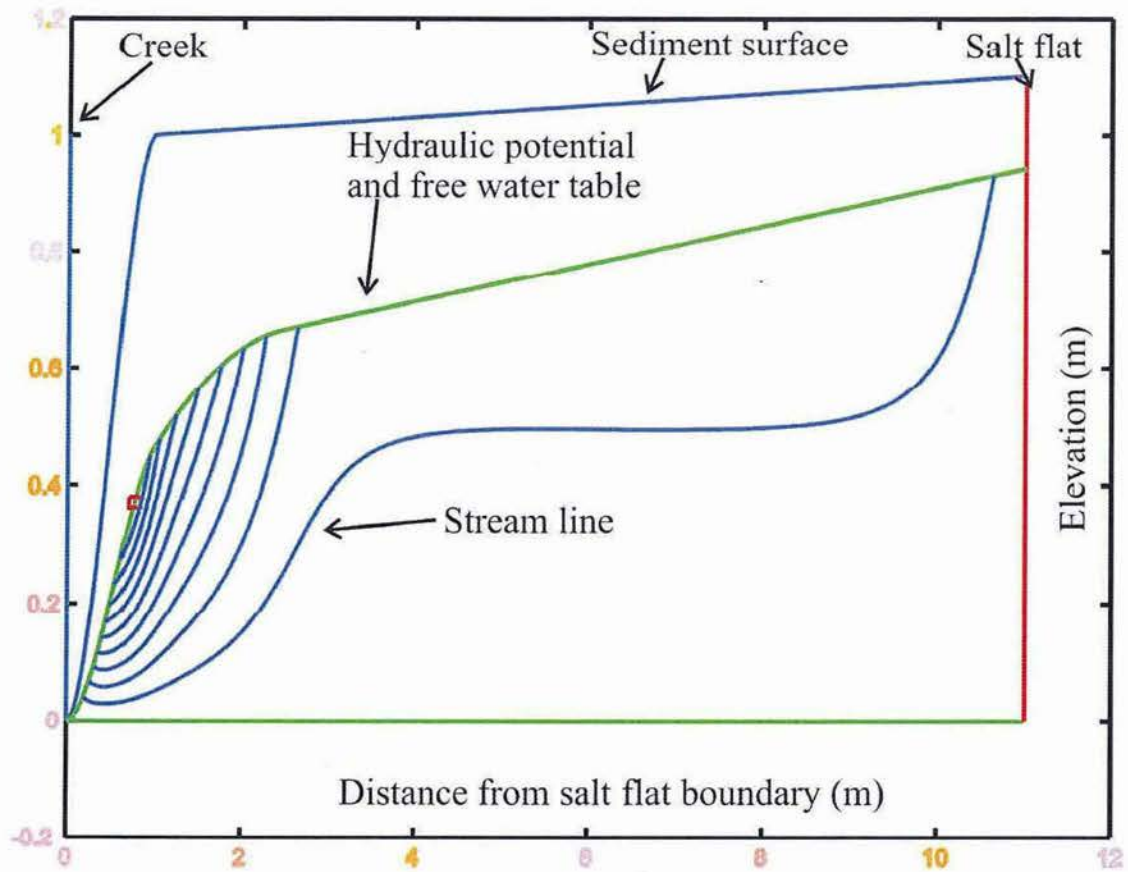


Figure 6.5: The condition of the sediment, free water table and stream line, on three days after inundation.

Figure 6.5 shows the condition of the model three days after inundation (day three), where the slope of the water table increases, from 0.02 on the day two to become 0.025 on the day three. The water table level is down by 0.16 m from the day zero at the beginning of the sediment, to 0.94 m at the salt flat.

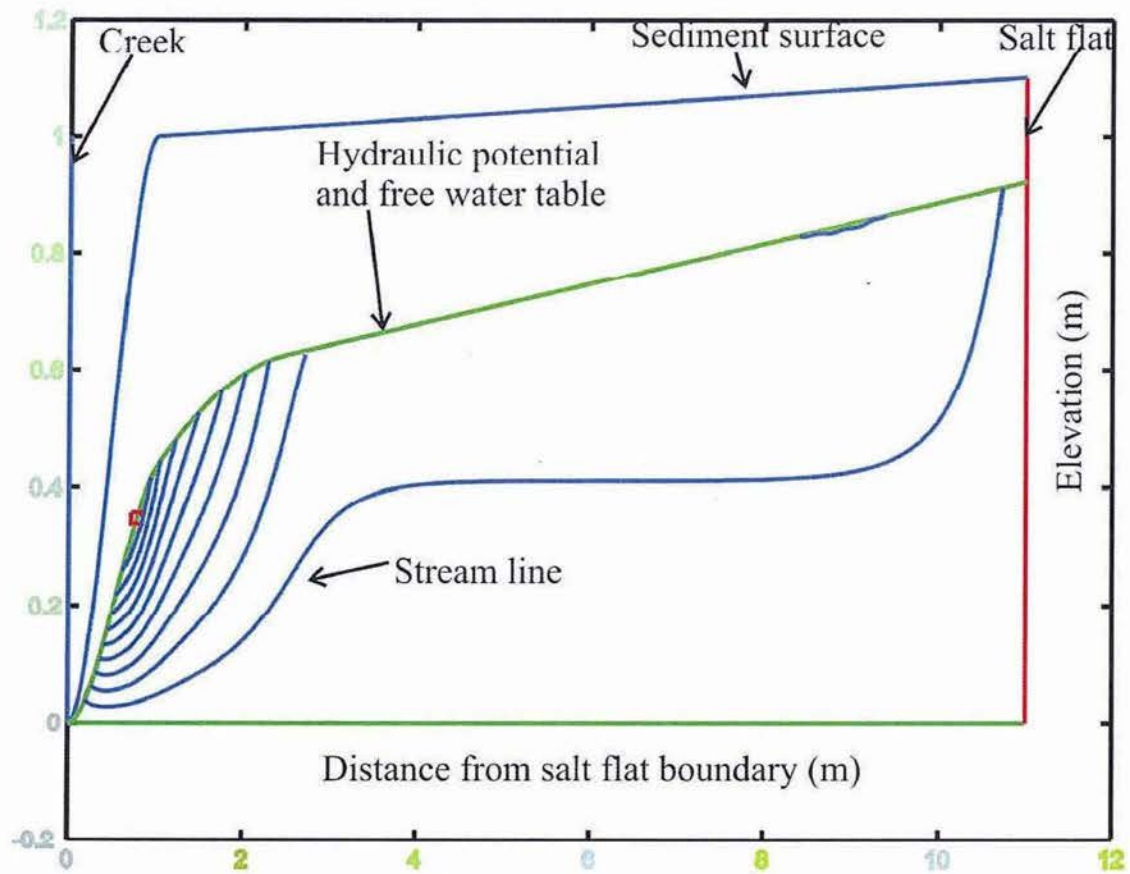


Figure 6.6: The condition of the sediment, free water table and stream line, on four days after inundation

Figure 6.6 shows the condition of the model four days after inundation (day four), where the slope of the water table increases, from 0.025 on the day three to become 0.03 on the day four. The water table level is down by 0.19 m from the day zero at the beginning of the sediment, to 0.91 m at the salt flat.

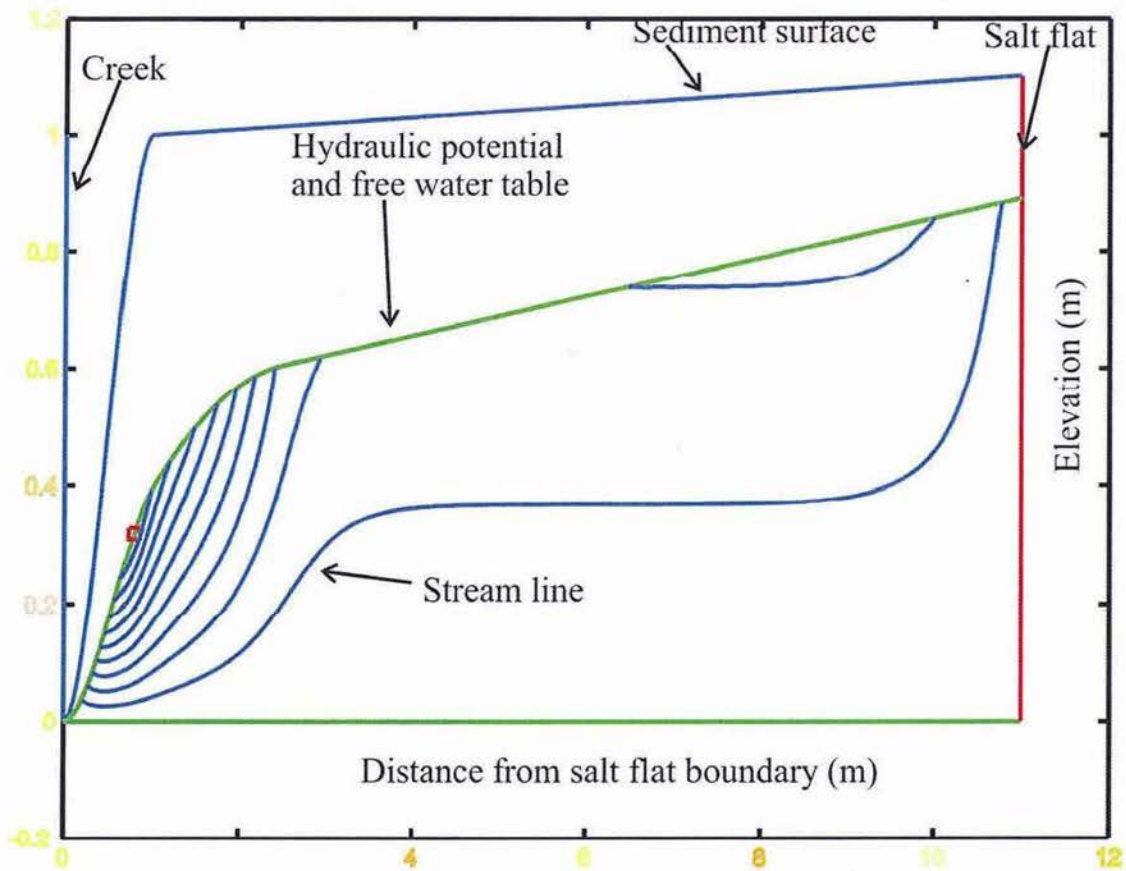


Figure 6.7: The condition of the sediment, free water table and stream line, on five days after inundation.

Figure 6.7 shows the condition of the model five days after inundation (day five), where the slope of the water table increases, from 0.03 on the day three to become 0.04 on the day five. The water table level is down by 0.26 m from the day zero at the beginning of the sediment, which is 0.84 m.

One of the results of stream calculation is shown in Figure 6.8, where the condition is water saturated. The rest are shown in Appendix 3.

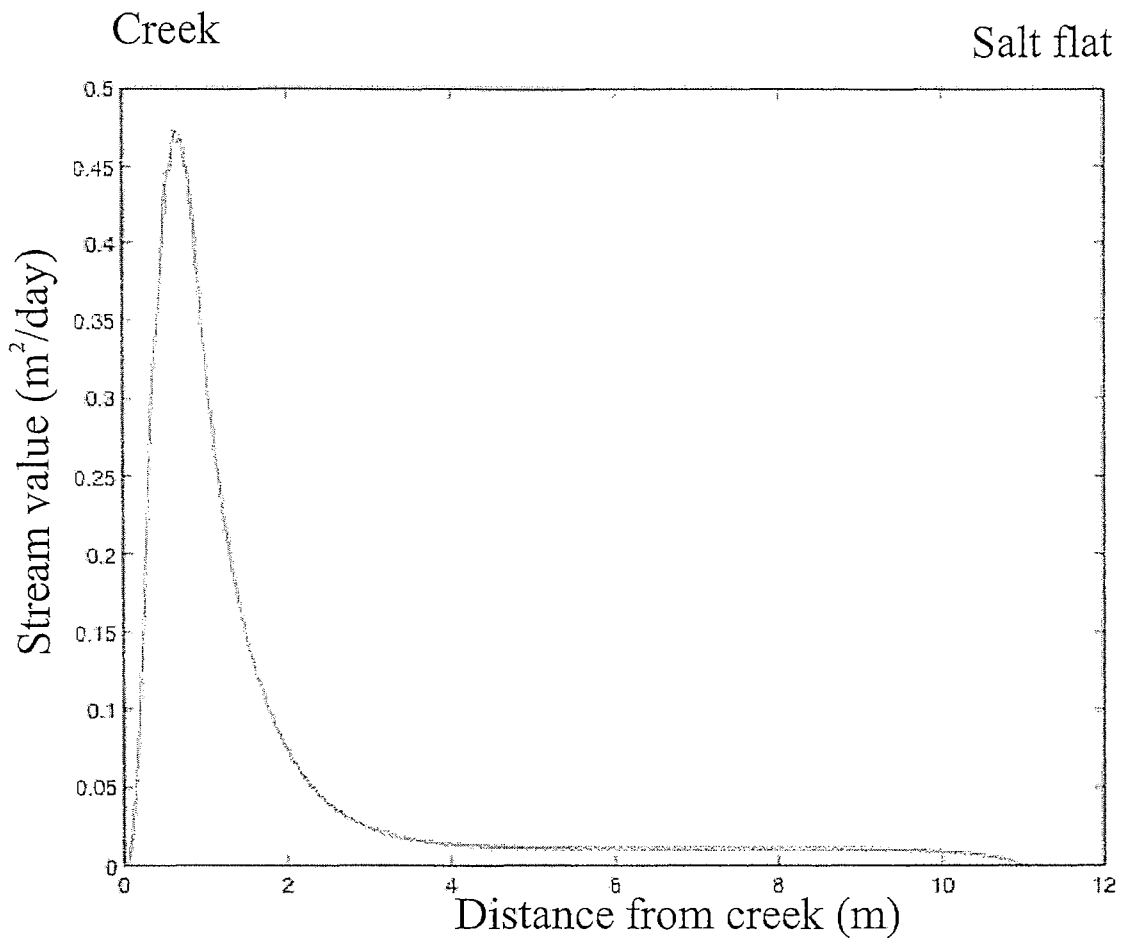


Figure 6.8: Stream value for each distance from the end of the sediment to the creek bank at the sediment is water saturated (as a condition on Figure 2)

From Chapter 4 and 5, it was found that the porosity of the sediment was *ca.* 0.45 (45 %), and the water that fills the burrows was *ca.* 0.1 (10%) from the total volume of the sediment. Therefore, the water volume is 55 % of the total volume of the sediment. The calculation of the fluxes for all conditions is multiplied by 0.55. The fluxes calculated for each of the 6 days are shown in Table 6.1 and Figure 6.9.

Day number	Flux calculated by model $\text{m}^3/(\text{m}^2 \text{ day})$	Flux inferred from piezometer data $\text{m}^3/(\text{m}^2 \text{ day})$
0	0.026 ± 0.002	0.030 ± 0.021
1	0.029 ± 0.002	0.028 ± 0.017
2	0.021 ± 0.002	0.026 ± 0.013
3	0.016 ± 0.001	0.021 ± 0.010
4	0.012 ± 0.001	0.016 ± 0.008
5	0.007 ± 0.001	0.013 ± 0.005

Table 6.1: The comparison between the result of the flux calculated from the model (stream function) and from the field measurement.

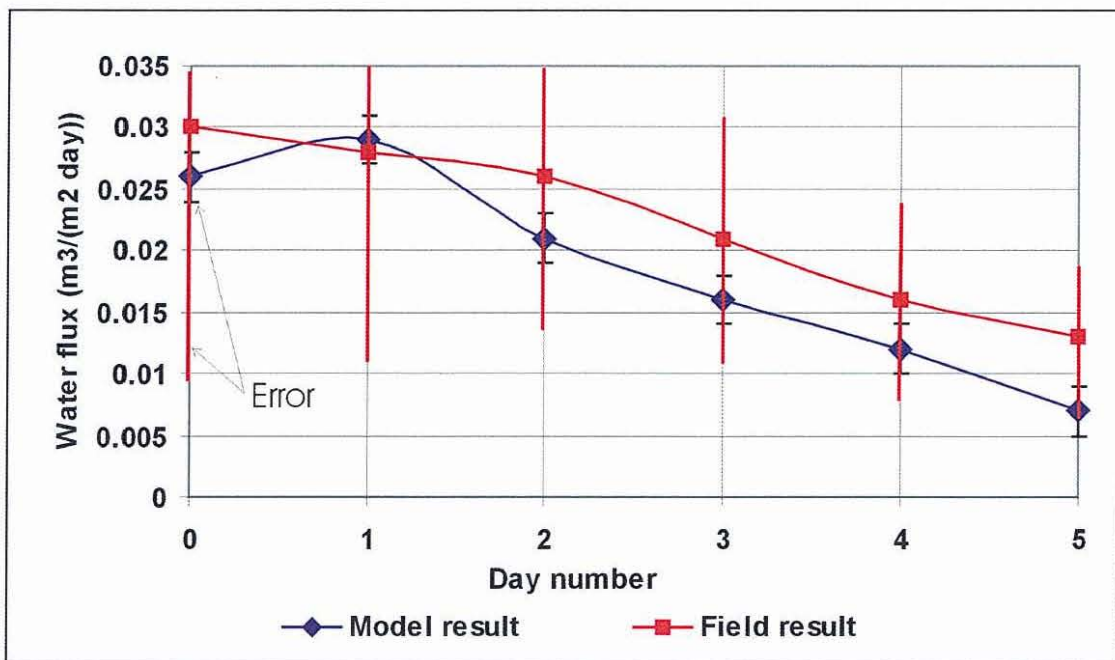


Figure 6.9: Visualisation of Table 6.1

From Table 6.1 and Figure 6.9, they can be seen that the model gives a reliable estimate of the groundwater flux.

6.4 Discussion

The success of the model is in part due to the extensive use of high quality water table data. Although in many applications such data may not be available, due to the absence of piezometers, calculations can still be performed in periods when the tides inundate the Creek, as this is when the water table is the same as the sediment surface. It is a relatively simple matter to survey the height of the sediment surface, and thus the model can be applied to many locations with a minimum of effort.

The model is applicable to spring tides as well as neap tides in many locations. In most places, because the average period of inundation during the spring tides is only a few hours per day. For this short time groundwater flow will be zero as there will be no significant pressure gradient. For the rest of the day the water table will be at the sediment surface and the results for figure 6.2 will apply.

It should be noted that this model is limited because it is not a genuine time dependent model, however useful results of groundwater fluxes can still be obtained and used in a variety of applications.

Chapter 7. Conclusions and Recommendations

7.1 Introduction

This thesis is mainly divided into three parts i.e.

- (1) the development of a new method to determine the hydraulic conductivity of mangrove sediment;
- (2) the calculation of the relative magnitude of burrow flushing or direct groundwater flow to determine which process is most important in removing groundwater and salt from mangrove soils, and ;
- (3) the development of a simple analytical model to calculate groundwater fluxes.

7.2 Practical and Academic significance of the study

(1) The new method of measurement of hydraulic conductivity of mangrove soils outlined in chapter 4 will allow for the first time the ability of researchers to quickly and cheaply determine hydraulic conductivity. Generally hydraulic conductivity is a difficult parameter to determine. Conventional methods of taking samples for analysis in the laboratory are usually unsuitable because the process of taking the sample changes the hydraulic properties of the soil. Unless extremely large samples are taken, the influence of macropores such as crab burrows can not be considered. Conventional *in-situ* methods of determining hydraulic conductivity usually involve placing piezometers in the soil. This is a usually a difficult and costly process in mangrove swamps.

The method of determining the hydraulic conductivity developed in this thesis uses the crab burrows as natural piezometers. Measurements of hydraulic conductivity can be made quickly (within a few hours) and with a minimum of equipment.

(2) There are two major pathways by which groundwater in mangrove swamps can be returned to a mangrove creek. These are (a) by direct groundwater flow, and (b) by

flushing of water in the animal burrows. The work described in chapter 5 is the first attempt to assess the relative magnitudes of these two affects. Measurements were taken in two pristine creek systems and indicated that both pathways are important. Although the results are specific to the two particular locations studied, the techniques developed can be applied by other researchers different mangrove swamps.

(3) The simple analytical model developed in Chapter 6 used to predict the groundwater flow from mangrove swamps and the results were compared with measurements. It was found that the model gave very encouraging results and indicating that the model should be able to be applied to a wide range of mangrove swamp geometries.

7.3 Recommendations for future research work.

This research has shown the importance of the burrow flushing and groundwater flow in the mangrove forest sediment. There are however many avenues for future research. Below are some suggestions.

1. The effect of burrow morphology on flushing rates and groundwater flow may be important. The bulk hydraulic conductivity of the soil depends upon the size and degree of intermingling of the burrows. It is likely that locations with burrowing species with different burrow morphologies will have different hydraulic conductivity's.
2. The role of groundwater flow in the nutrient and salt budget of the mangrove swamp/creek system is poorly understood. The method of determining hydraulic conductivity, as outlined in this thesis, with observations of groundwater salt and nutrient concentrations could be used to develop such budgets.
3. The groundwater fluxes associated with salt pans have yet to be fully investigated. These salt pans often occupy a much larger area than mangroves and the groundwater in the salt pans has very high concentrations of salt. It is improbable that the horizontal fluxes in the salt pans are significant due to low

hydraulic conductivity, however, vertical flow into lower layers of sand, where present, may be an efficient mechanism to transfer large quantities of groundwater to the creek.

7.4 Conclusions.

The conclusion of this study can be divided into 3 parts:

1. The development of a new method to determine the hydraulic conductivity of the mangrove sediment;

The measurement of hydraulic conductivity of sediments is problematic requiring piezometers which are expensive and difficult to install. In this thesis a new and innovative method is described that allows the rapid assessment of hydraulic conductivity using existing crab burrow networks. Each measurement on one burrow takes approximately 20 minutes and typically five to 10 burrows should be measured to allow averaging of a significant area of the swamp. Field results show that the new method compares well to more traditional estimates using piezometers. Thus estimation of hydraulic conductivity may be made relatively quickly and with a minimum of equipment, especially compared with the methods using piezometers. The method also does not in any way disturb the sediment matrix.

Field measurements of hydraulic conductivity of the mangrove sediment were considerable higher than would be expected with sediment with no macropores, with values ranging from 1 m/day to 10 m/day.

2. Calculation of the relative magnitude of burrow flushing or direct groundwater flow to determine which process is most important in removing groundwater

It was found that at the field sites where measurements were taken, these two processes are of similar magnitude. The groundwater flux range ($0.005 - 0.03 \text{ m}^3/(\text{m}^2 \text{ day})$), was similar to the burrow flushing flux ($0.01 - 0.04 \text{ m}^3/(\text{m}^2 \text{ day})$). Considering

the errors involved in the experiments and calculations, which are considered to introduce an error margin in the order of 50-100%, these ranges can be considered as being similar, and neither process can be considered dominant.

This result suggests that a new approach to studies of groundwater processes in mangrove swamps is required. In the past, direct groundwater flow has been considered the most important factor in transporting nutrients and flushing salt in mangrove environments (Wolanski & Gardiner, 1981; Cohen *et al.*, 1999; Kitheka *et al.*, 1999). However most researchers (Lara & Dittmar, 1999; Mazda *et al.*, 1990; Wolanski, 1992) have drawn this conclusion qualitatively rather than quantitatively. One exception is a study by Hughes *et al.* (1998) that provides calculation from piezometer measurements of groundwater flux caused by tidal water.

3. The development of a simple analytical model to calculate groundwater fluxes

Modeling of the groundwater flow in the mangrove forest area was also undertaken. This model uses a series solution to calculate the flux of the groundwater to the creek bank. It assumes that the mangrove soil is comprised of two layers, the top layer being highly permeable due to the presence of animal burrows, and a lower impermeable layer. The model was driven using water table data taken from piezometers. The flux estimates derived from the model compared favorably with experimental estimates with fluxes ranging from 0.007 to 0.026 m³/(m² day). Depending upon the time since tidal inundation of the swamp. The model is easily adaptable to a range of swamp geometry's and can thus be applied to a range of geographic locations.

References

Allen J. R. L. (1985). Principles of Physical Sedimentology. George Allen & Unwin, London page: 22

Aucan, J. & Ridd, P. V. (2000). Tidal asymmetry in Creek surrounded by saltflats and mangroves with small swamp slopes. *Wetlands Ecology and Management* 8: 223-231.

Aziz, W. (1992). Beach morphology and change in the Rowes Bay beach compartment, Townsville, North Queensland. *Unpublished BSc. Honours thesis*, James Cook University, Townsville, Australia.

Bouwer, H. (1978). Groundwater Hydrology, McGraw-Hill, Inc, USA.

Bradley, C. (1996). Transient modelling of water table variation in a floodplain wetland, Narborough Bog, Leicestershire, *Journal of Hydrology*, 185: 87-114.

Bryce, S, Larcombe, P. & Ridd, P. V. (2003). Hydrodynamic and geomorphological controls on suspended sediment transport in mangrove creek systems, a case study: Cocoa Creek, Townsville, Australia. *Estuarine, Coastal and Shelf Science*, 56: 415-431.

Bryce, S. M. (2001). Controlling Factors on Sediment Transport in Mangrove Creek Systems of North-East Queensland. *Unpublished Ph.D. Thesis*, School of Earth Sciences, James Cook University, North Queensland, Australia.

Bureau of Meteorology (2004). Annual Point Potential Evapotranspiration. http://www.bom.gov.au/cgi-bin/climate/cgi_bin_scripts/evapotrans/et_map_script.cgi

Burman, R. & Pochop, L. O. (1994). Development in Atmospheric Science 22: Evaporation, Evapotranspiration and Climatic data. Elsevier, The Netherlands 1994.

Cohen, M. C. L., Lara, R. J., Ramos, J. F. and F. & Dittmar, T. (1999). Factors influencing the variability of Mg, Ca and K in water in a mangrove Creek in Braganca, North Brazil. *Mangrove and Salt Marshes* 3: 9-15.

Commonwealth Bureau Of Meteorology (2003). Averages for TOWNSVILLE AERO. http://www.bom.gov.au/climate/averages/tables/cw_032040.shtml

Dataflow System PTY LTD. (1999). Technical handbook pressure sensors, capacitive water level probes. Post office box 93, COOROY 4563 Queensland Australia.

De Marsily, G. (1986). Quantitative hydrology. Groundwater hydrology for engineers. *Academic press, inc* (London) LTD p:75-77.

Falconer, R.A. & Goodwin, P. (1994). Wetlands Management, Proceedings of the international conference organized by the Institution of Civil Engineers and held in London on 2-3 June 1994.

Gill, A. W. & Read W. W. (1996). Efficient analytic series solutions for two-dimensional potential flow problems. *International journal for numerical methods in fluid*, 23: 415-430.

Heron, S. F. & Ridd, P. V. (2001b). The Use of Computational Fluid Dynamics in Predicting the Tidal Flushing of Animal Burrows. *Estuarine, Coastal and Shelf Science* 52, 411-421.

Heron, S. F. (2001a). Tidal Flushing of animal burrows in Mangrove Swamps, PhD dissertation, James Cook University, School of Mathematical and Physical Sciences, Townsville, Australia.

Hollins, S. E. & Ridd, P. V. (accepted). The concentration and consumption of oxygen in large animal burrows in tropical mangrove swamp. *Estuarine, Coastal and Shelf Science*

Hollins, S. E. & Ridd, P.V. (1997). Evaporation over a tropical tidal salt flat. *Mangroves and salt Marshes* 1: 95-102.

Hollins, S. E. (2001). The role of crab burrows in transport of salt and oxygen in mangrove soil. Thesis, James Cook University, School of Mathematics and Physics sciences, Townsville, Australia.

Hollins, S. E., Ridd, P. V. & Read, W. W. (2000). Measurement of the diffusion coefficient for salt in salt flat and mangrove soils. *Wetland Ecology and Management*, 8: 257-262.

Hopely, David (1978). Geographical Studies of the Townsville Area. Monograph Series Occasional Paper No. 2. Department of Geography, James Cook University of North Queensland, Australia.

Hopley, D. & Murtha, G. G. (1975). The Wuartenary Deposits of the Townsville Coastal Plain. Monograph Series No. 8, James Cook University, North Queensland, Australia.

Hopley, D. (1970). A Study of the geomorphological evolution of the North Queensland coast between Cape Upstart and Hinchinbrook Island. *Unpublished Ph.D. thesis*, James Cook University, Townsville, Australia.

Hornby, Frank (2003). The Townsville Region a Social Atlas. Community and Cultural Services Department, Townsville City Council, Australia.

Hughes, C. E., Binning, P. & Willgoose, G. R. (1998a). Characterisation of the hydrology of an estuarine wetland. *Journal of Hydrology*, 211, 34-49.

Hughes, C. E. (1998b). Hydrology of a disturbed estuarine wetland, Hunter river, Australia: Field investigation, process modelling and management implications, PhD Theses, University of New Castle, Australia.

Keller, G. V. and Frischeknecht, F. C. (1996). Electrical Methods in Geophysical Prospecting , chapter 6. Pergamon Press, Oxford.

Kitheka, J. U., Mwashote, B. M., Ohowa, B. O. & Kamu, J. (1999). Water circulation, groundwater outflow and nutrient dynamics in Mida Creek, Kenya. *Mangrove and salt marshes* 3:135-146.

Lara, R. J. & Dittmar T. (1999). Nutrient dynamics in a mangrove Creek (North Brazil) during the dry season. *Mangroves and salt Marshes* 3: 185-195.

Larcombe, P & Ridd, P.V. (1995c). Megaripple dynamics and sediment transport in a mesotidal mangrove creek – for paleoflow reconstruction. *Sedimentology*, 42, 593 –606.

Larcombe, P. & Ridd, P. V. (1996). Dry Season Hydrodynamics and Sediment Transport in a Mangrove Creek. *Mixing in Estuaries and Coastal Seas, Coastal and Estuaries Studies* vol. 50:388-404.

Larcombe, P. (1995b). The influence of sea level and sediment transport on modern and Holocene growth of the Great Barrier Reef, Australia. Research symposium proceeding, Great Barrier Reef: Terrigenous sediment flux and Human impacts. Marine geophysical laboratory, JCU and CRC Reef Research Centre, JCU, Townsville, Australia.

Larcombe, P., Carter, R. M., Dye, J., Gagan, M. K. & Johnson, D. P. (1995a): New evidence for episodic post-glacial sea-level rise, central Great Barrier Reef, Australia. *Marine Geology*, 127: 1-44.

Liggett, J. A. & Philip L. F. L. (1983). The boundary integral equation method for porous media flow, George Allen and Unwin (Publishers) Ltd., UK.

Matthews, G. V. T. (1993). The Ramsar Convention on Wetlands: Its History and Development. Ramsar Convention Bureau, Switzerland.

Mazda, Y, Yokochi H. & Sato, Y. (1990). Groundwater flow in the Bashita-Minato Mangrove Area, and its Influence on Water and Bottom Mud Properties, *Estuarine, Coastal and Shelf Science* 31:621-638.

McIntyre, C. M. (1996). The Holocene Sedimentology and Stratigraphy of the Inner Shelf of the Great Barrier Reef. *Unpublished MSc Thesis*, James Cook University, Townsville, Australia.

Mitchell, A. W. and Furnas M. J. (1996). Differences in suspended sediment flux to the GBR shelf between wet and dry catchments of north Queensland. In the Great Barrier Reef: Terrigenous Sediment Flux and Human Impacts, edited by: P. Larcombe, K. Woolfe and R. Purdon.

Mitsch, W. J. & Gosselink, J. G. (1993). Second edition Wetlands. Van Nostrand Reinhold, New York.

Muller, J. (2002). Sediment transport on the Strand, Rowes Bay, and Pallarenda Beaches, Townsville, Queensland, Australia. *Unpublished BSc. Honours thesis*, James Cook University, Townsville, Australia.

Passioura, J. B., Ball, M. C. & Knight, J. H. (1992). Mangroves may salinize the soil and in so doing limit their transpiration rate. *Functional Ecology*, 6: 476-481.

Pomery, A. Bruce (1987). A system approach to the geochemistry, mineralogy and sedimentation of a coastal catchment and tidal flats in the dry tropics near Townsville, North Queensland. *Unpublished Ph.D. thesis*, James Cook University, Townsville, Australia.

Puotinen, M. L., Done, T.J., & Skelly, W. C. (1997). An atlas of tropical cyclones in the Great Barrier Reef Region, 1969-1997. *CRC Reef Research Centre*, Technical Report No. 19, Townsville; CRC Reef Research Centre.

Queensland Department of Transport (2001). The Official Tide Tables & Boating Safety Guide 2001. Queensland Department of Transport Mineral House, Brisbane Australia.

Raghunath, H. M. (1987). Ground water, Hydrology, Ground water survey and pumping test, Rural water supply and irrigation systems. Wiley Eastern Limited, New Delhi India.

- Read, W. W. (1993). Series solution for Laplace's equation with nonhomogeneous mixed boundary conditions and irregular boundaries. *Math. Comput. Modelling*, 12: 9-19.
- Read, W. W. (1996a). Hillside seepage and the steady water table. I: Theory. *Advances in Water Resources*, vol 19, no. 2: 63-73.
- Read, W. W. (1996b). Hillside seepage and the steady water table. I: Application. *Advances in Water Resources*, vol 19, no. 2: 75-81.
- Ridd, P. V. (1996a). Flow through animal burrows in mangrove swamps. *Estuarine, Coastal and Shelf Science* 43: 617-625.
- Ridd, P.V. & Sam, R. (1996b). Profiling groundwater salt concentrations in mangrove swamps and tropical salt flats. *Estuarine, Coastal and Shelf Science* 43: 627-635.
- Ridd, P.V., Sam, R., Hollins, S. & Brunskill, G. (1997). Water, salt and nutrient fluxes of tropical tidal salt flats. *Mangroves and salt Marshes* 1: 229-238.
- Rieke III, H.H & Chilingarian, G. V. (1974). *Developments in Sedimentology* 16, Compaction of Argillaceous Sediments. Elsevier Scientific Publishing Company, Amsterdam.
- Roggeri, H. (1995). *Tropical freshwater wetlands*. Kluwer Academic Publishers, Dordrecht, The Netherlands.
- Rossfelder, André (2000). What is Vibrocoring?. www.rossfelder.com
- Rushton, K. R. & Redshaw, S. C. (1979). *Seepage and Groundwater Flow, Numerical Analysis by Analog and Digital Methods*. John Wiley & Sons, Great Britain.
- Sam, R. & Ridd, P.V. (1998). Spatial variation of groundwater salinity in a mangrove-salt flat system, Cocoa Creek, Australia. *Mangroves and salt Marshes* 2:121-132.

Sam, R. (1996). Application of Electromagnetic Induction Technology to Sensing of Sugar Cane Harvester Base-Cutter Height, Measurement of Groundwater Salt Concentration and Detection of Inactive Volcanic Lava Tubes. *Unpublished Ph.D. thesis*, James Cook University, Townsville, Australia.

Scheid, Francis (1968). Theory and Problems of Numerical Analysis. Schaum's Outline Series, McGraw-Hill Book Company, USA.

Semeniuk, V. (1983). Mangrove distribution in Northwestern Australia in relationship to regional and local freshwater seepage. *Vegetatio* 53: 11-31.

Stieglitz, T., Ridd, P. V. & Hollins, S. E. (2000b). A small sensor for detecting animal burrows and monitoring burrow water conductivity. *Wetland Ecology and Management* 8: 1-7.

Stieglitz, T., Ridd, P. V. & Muller, P. (2000a). Passive irrigation and functional morphology of crustacean burrows in a tropical mangrove swamp. *Hydrobiologia* 421: 69-76.

Strack, O. D. L. (1989). Groundwater Mechanics. Prentice Hall, Englewood Cliffs, New Jersey.

Susilo, A. & Ridd, P. V. (in press). The bulk hydraulic conductivity of mangrove soil perforated with animal burrows. *Wetland Ecology and Management*.

Taal, M. D. (1994). Communications on hydraulic and geotechnical engineering, flow and salt transport in mangrove swamps. TUDELFT, Faculty of Civil Engineering, Delft University of Technology, the Netherlands.

Thompson J. R. & Hollis G. E. (1995). Hydrological modelling and the sustainable development of the hadejia-nguru wetlands, Nigeria. *Hydrological science journal*, 40 (1): 997-1016.

Tomlinson, P. B. (1986). *The Botany of Mangrove*. Cambridge University Press, Cambridge, 413 pp.

Treize, D. L. & Stephenson, P. J. (1990). Rocks and landscapes of the Townsville district. Department of Resource Industries, Queensland, Australia.

Ward, A. D. & Elliot, W. J. (1995). Environmental hydrology. CRC Lewis Publishers, the USA.

Williams, W. D. & Kokkinn, M. J. (1988). Wetlands and aquatic saline environment. AWRC Research Project 84/160, Department of Resources and Energy, Australia.

Wilson, E. M. (1994). Engineering Hydrology. The MacMillan Press LTD., UK.

Wolanski, E. & Ridd, P. V. (1986). Tidal mixing and trapping in mangrove swamps. *Estuarine, Coastal and Shelf Science* 23: 759-771

Wolanski, E & Gardiner R. (1981). Flushing salt from Mangrove Swamps. *Australian Journal of Marine and Freshwater Research* 32: 681-683.

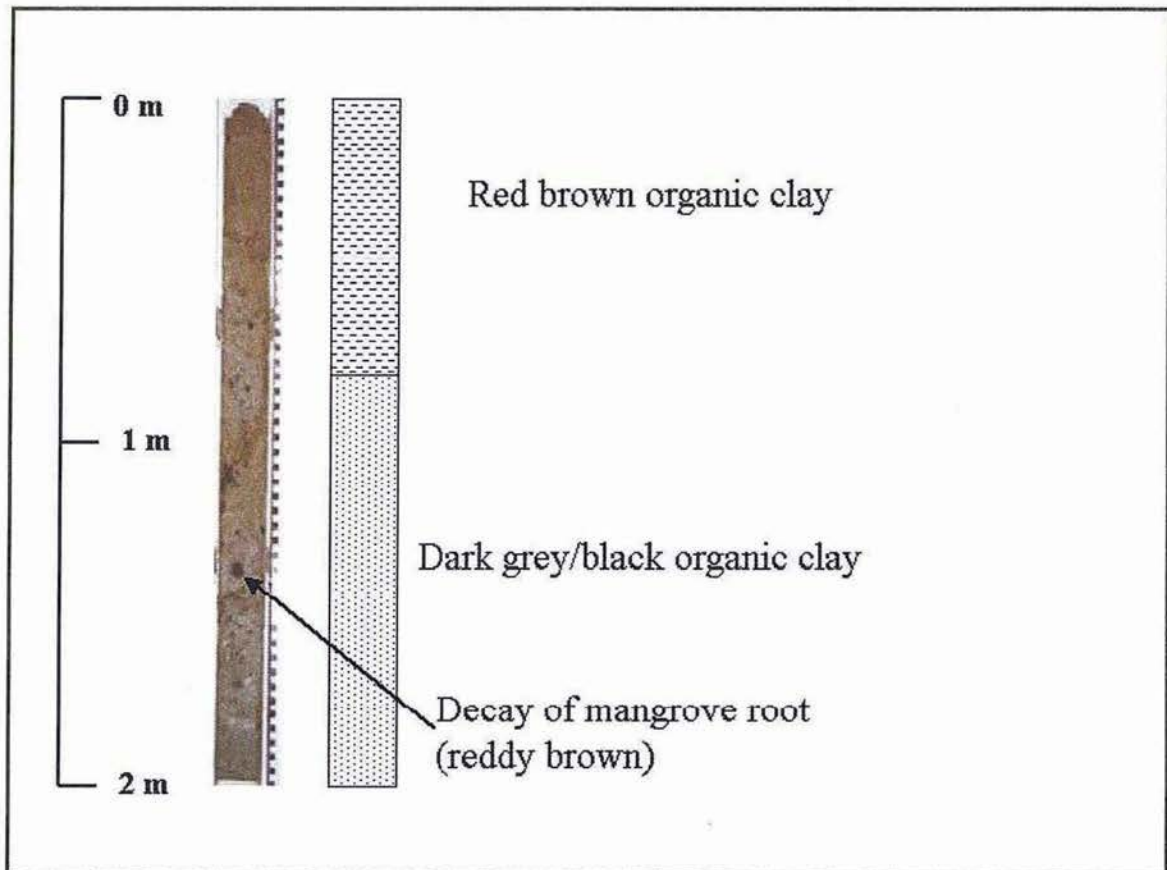
Wolanski, E. (1992). Hydrodynamics of mangrove swamps and their coastal waters. *Hydrobiologia* 247: 141-161.

Appendix 1

Visual analysis and colour photographing of the core

Core for the site A2

Site description : Mangrove forest at upper reaches of Cocoa Creek
Core length : 0.85 m
Sediment depth : 2.00 m
Compaction : 2.4



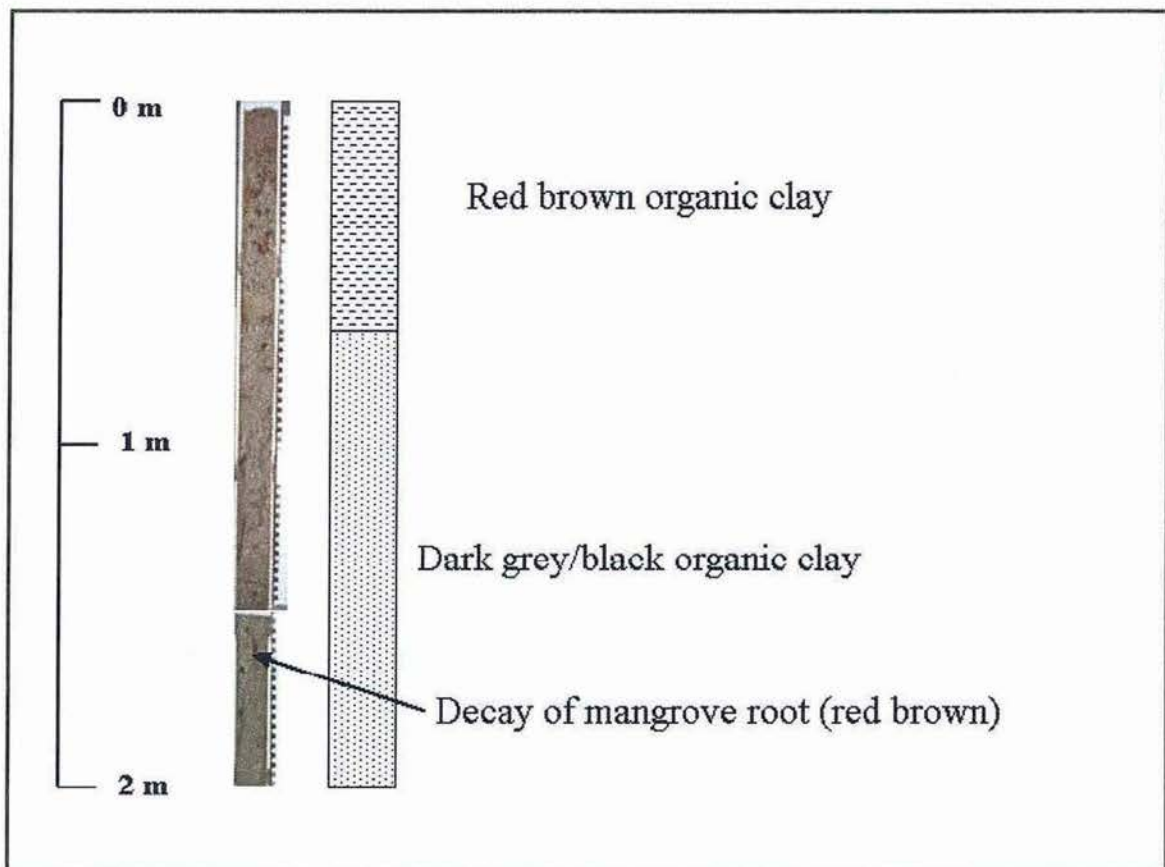
Core for the site B2

Site description : Mangrove forest at upper reaches of Cocoa Creek

Core length : 1.31 m

Sediment depth : 2.00 m

Compaction : 1.5



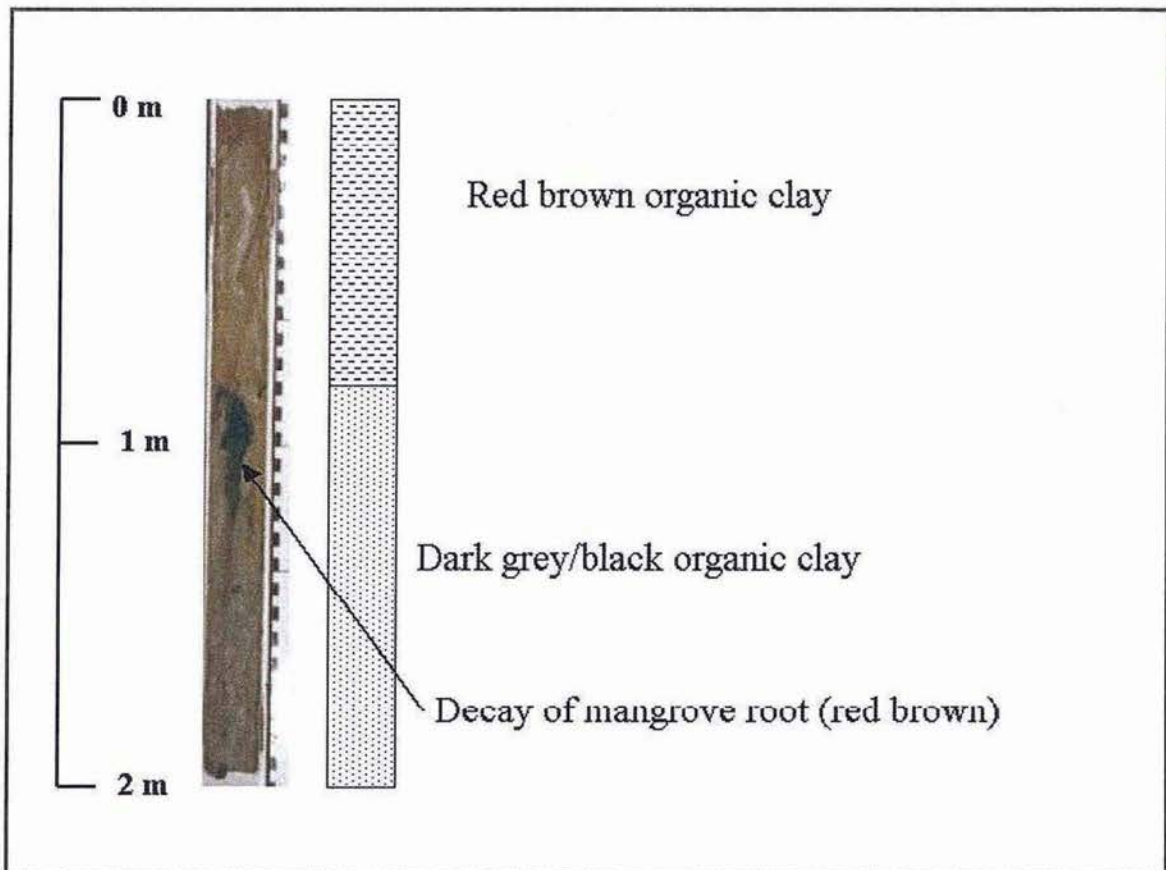
Core for the site C2

Site description : Mangrove forest at upper reaches of Cocoa Creek

Core length : 1.50 m

Sediment depth : 2.00 m

Compaction : 1.3



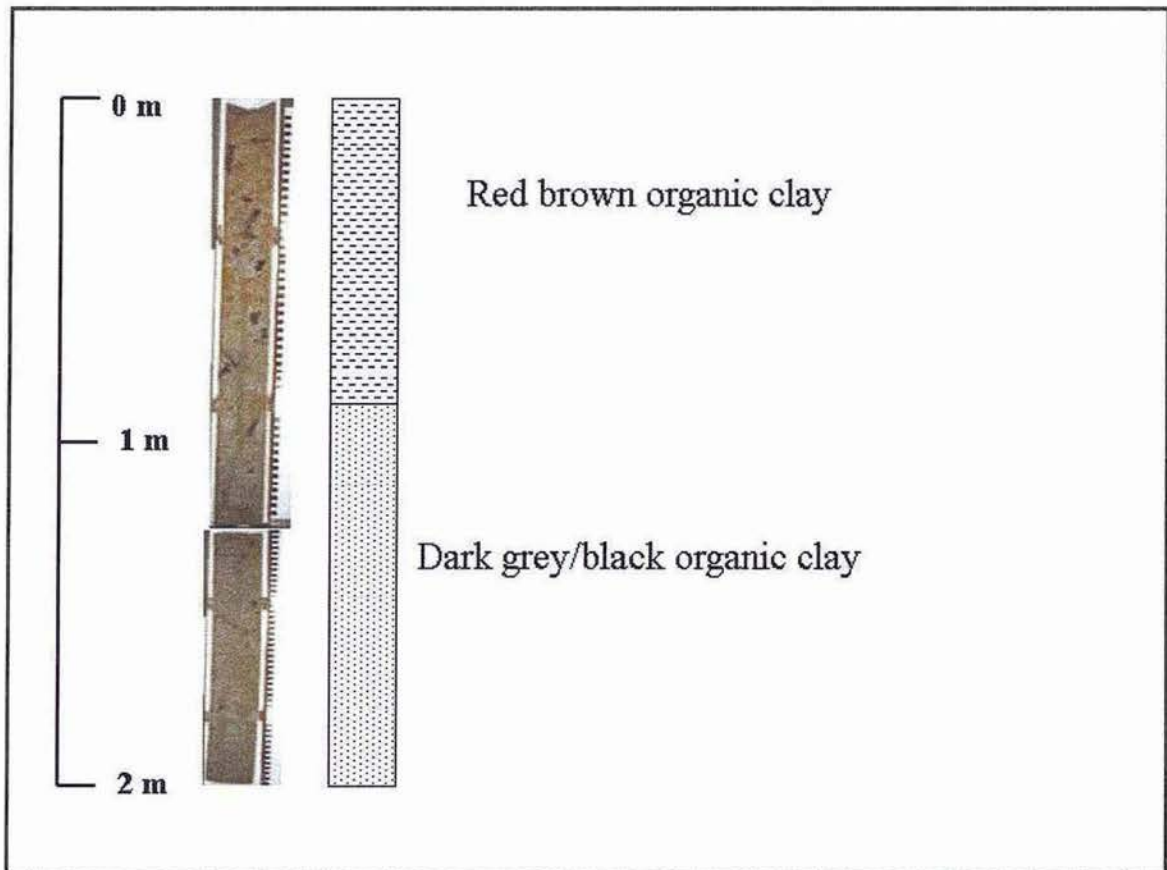
Core for the site D2

Site description : Mix, Mangrove and dead mangrove at upper reaches of Cocoa
Creek

Core length : 1.87 m

Sediment depth : 2.00 m

Compaction : 1.1



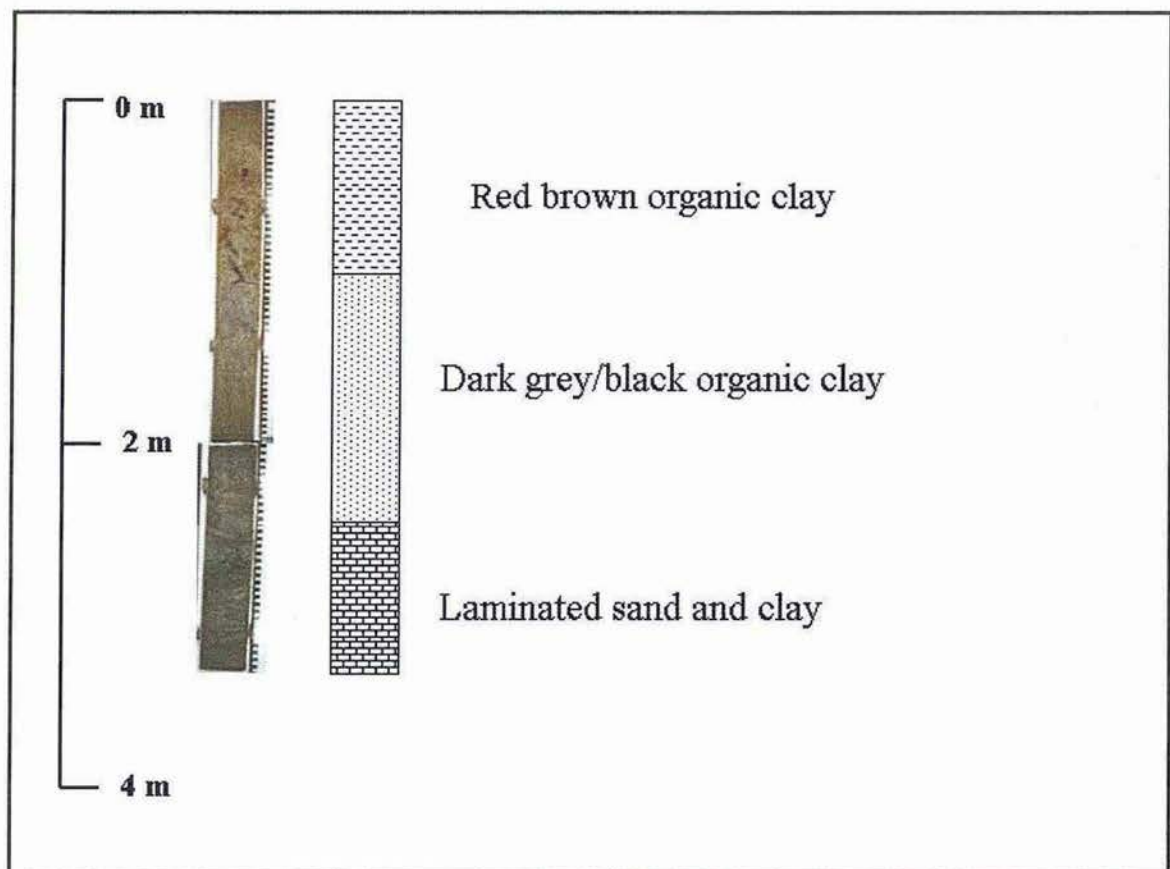
Core for the site D4

Site description : Mix, Mangrove and dead mangrove at upper reaches of Cocoa
Creek

Core length : 1.60 m

Sediment depth : 3.35 m

Compaction : 2.1



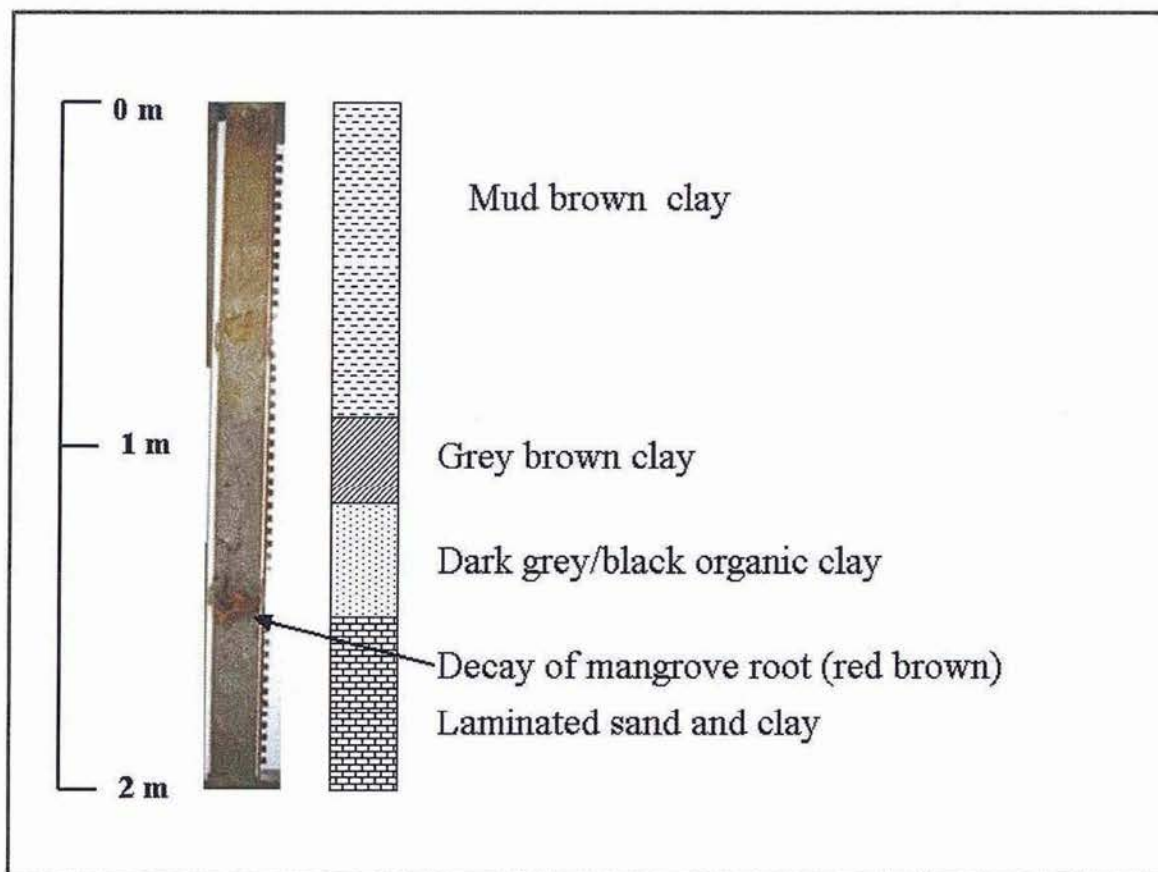
Core for the site E2

Site description : Salt flat at upper reaches of Cocoa Creek

Core length : 0.46 m

Sediment depth : 2.00 m

Compaction : 4.3



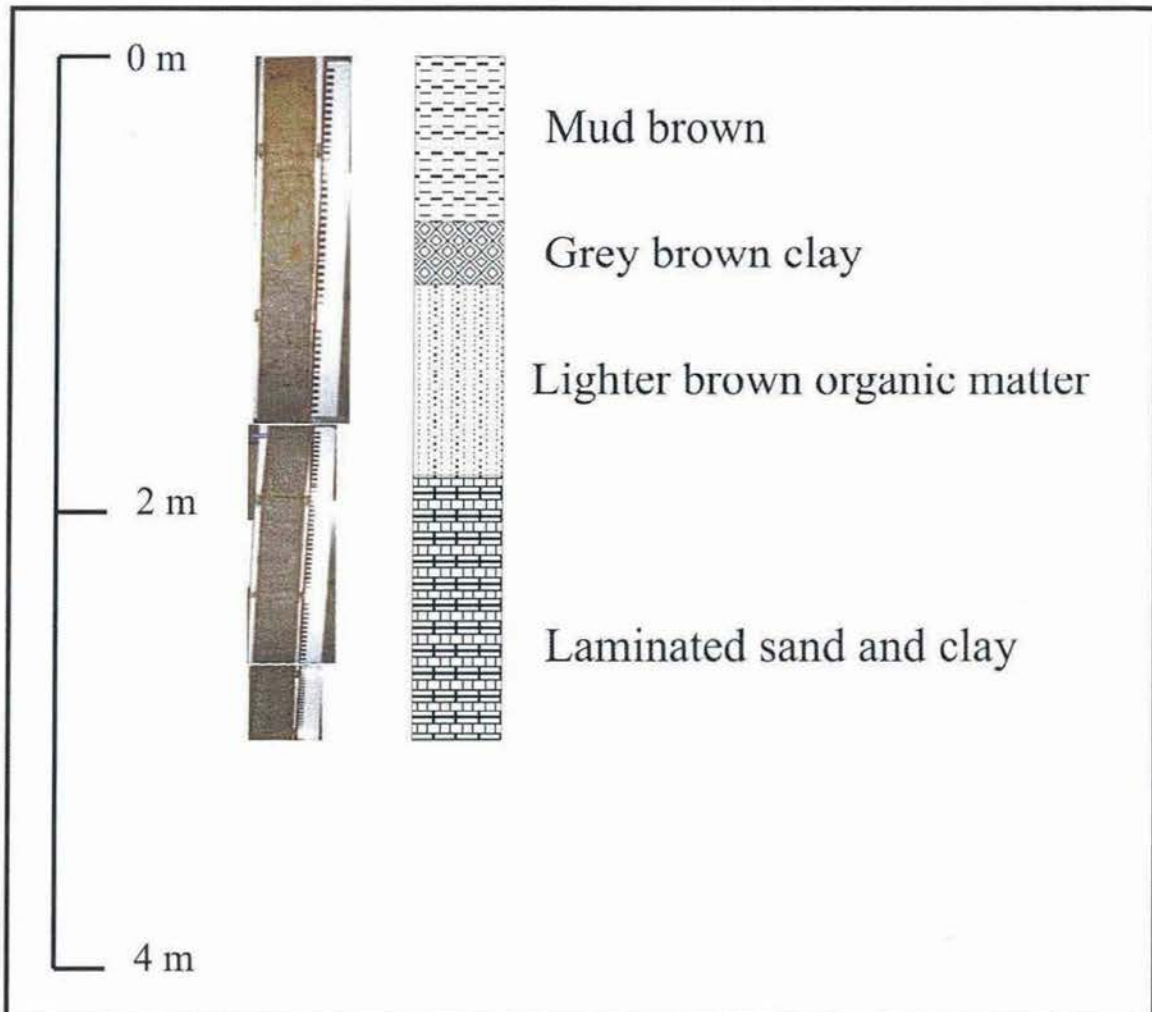
Core for the site E4

Site description : Salt flat at upper reaches of Cocoa Creek

Core length : 1.76 m

Sediment depth : 2.91 m

Compaction : 1.7



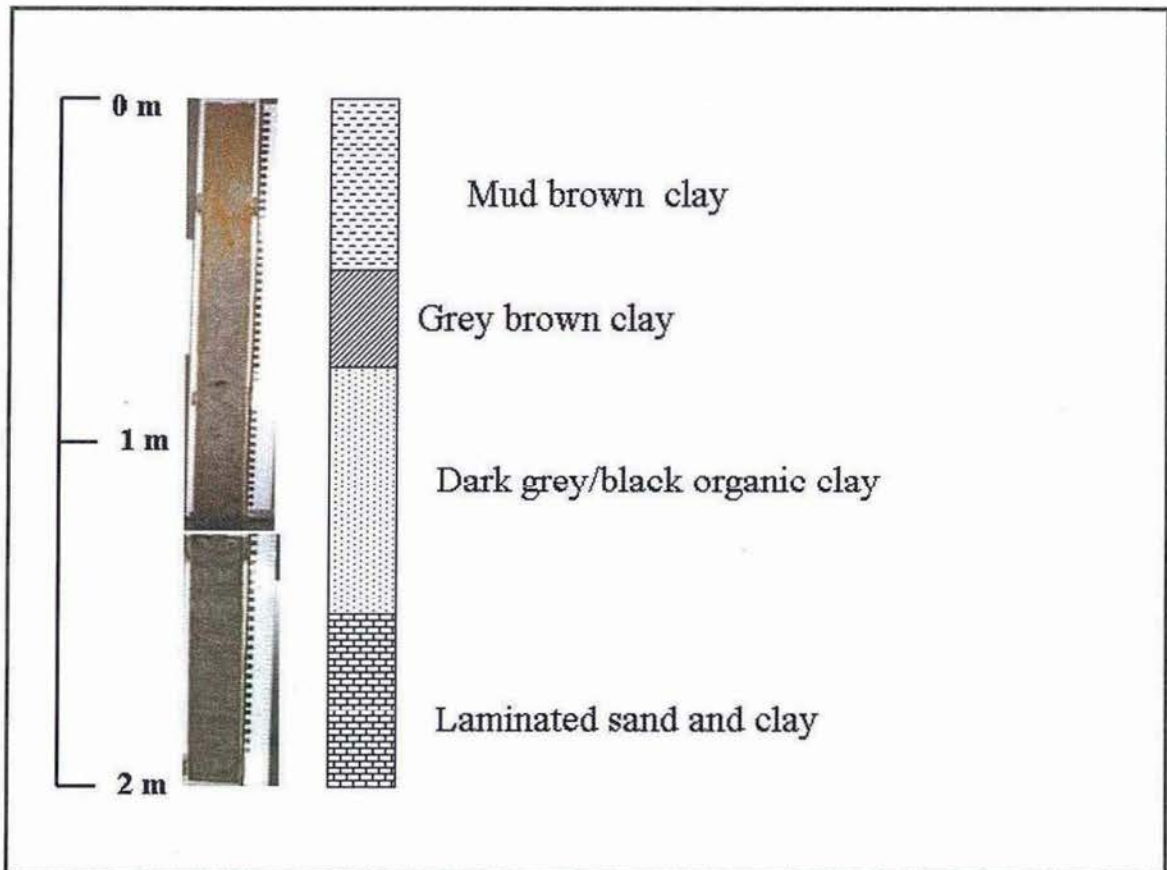
Core for the site F2

Site description : Salt flat at upper reaches of Cocoa Creek

Core length : 1.51 m

Sediment depth : 2.00 m

Compaction : 1.7



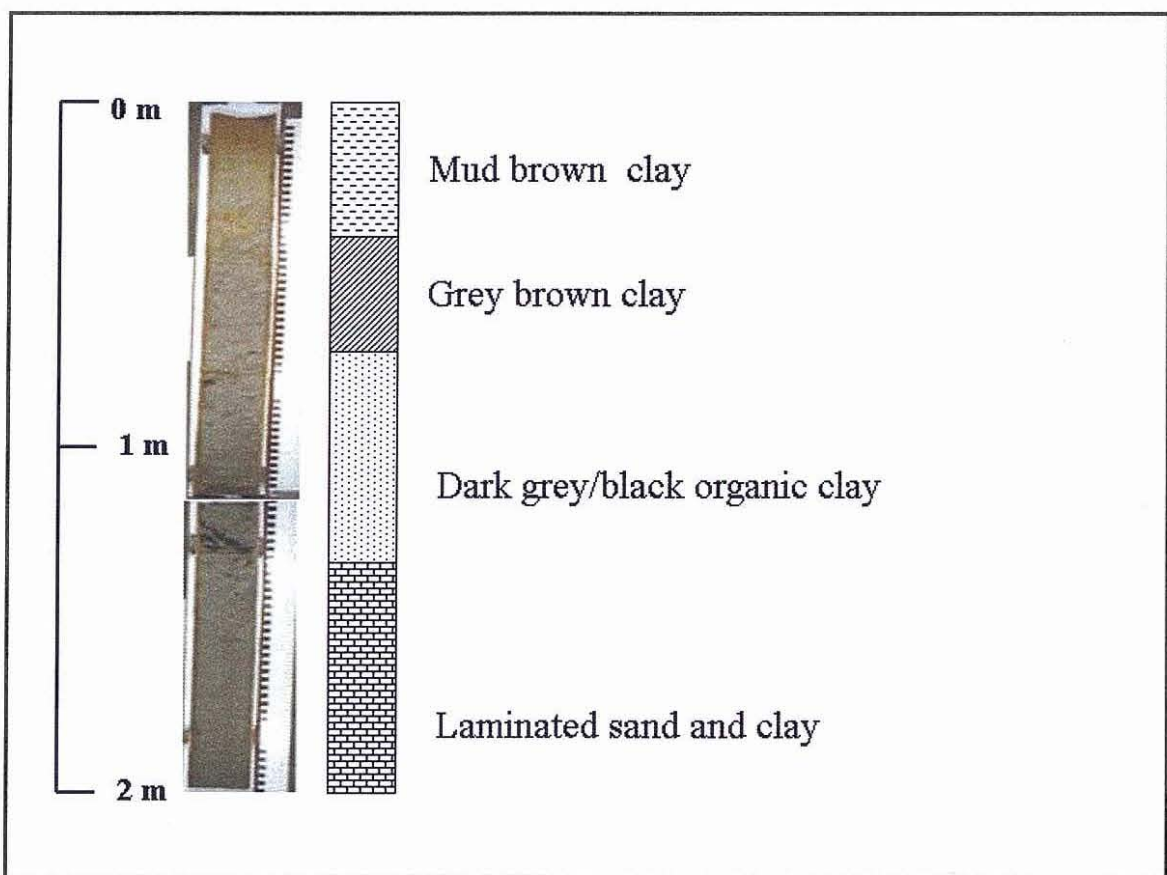
Core for the site G2

Site description : Salt flat at upper reaches of Cocoa Creek

Core length : 1.70 m

Sediment depth : 2.00 m

Compaction : 1.2



Reconstruction of the sediment from mangrove forest to salt flat areas, left to right



Appendix 2

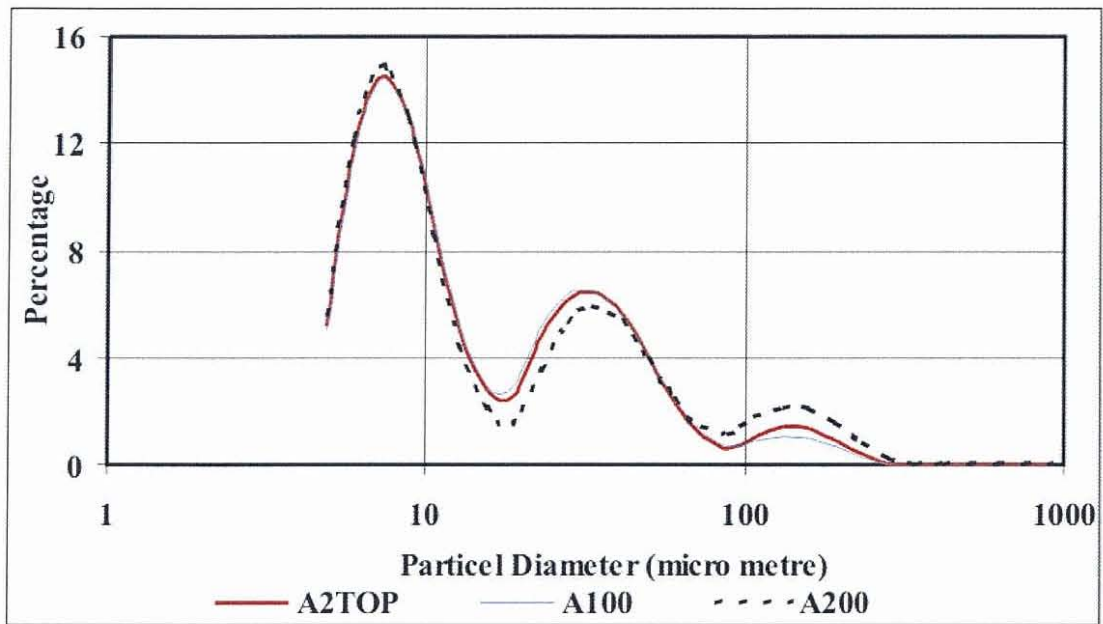
Grain Size Analysis of the Cores

Core A2

Site description : Mangrove forest at upper reaches of Cocoa Creek

Sediment depth : 2.00 m

Analysis at depth : 0, 1.00, 2.00 meters

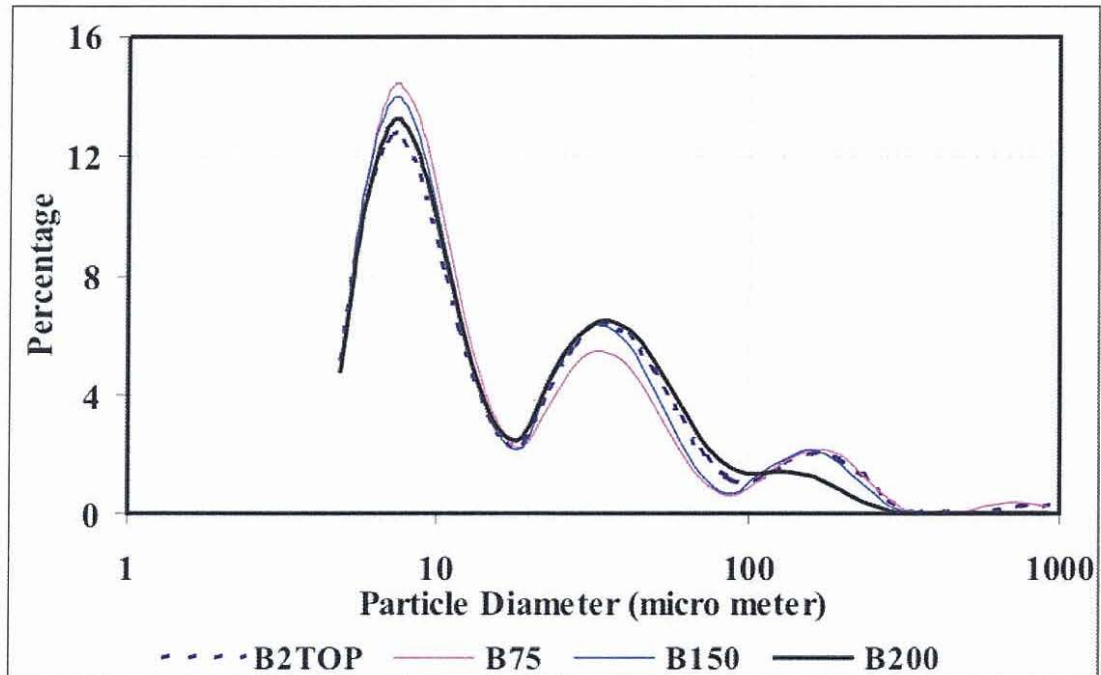


Core B2

Site description : Mangrove forest at upper reaches of Cocoa Creek

Sediment depth : 2.00 m

Analysis at depth : 0, 0.75, 1.50, 2.00 meters

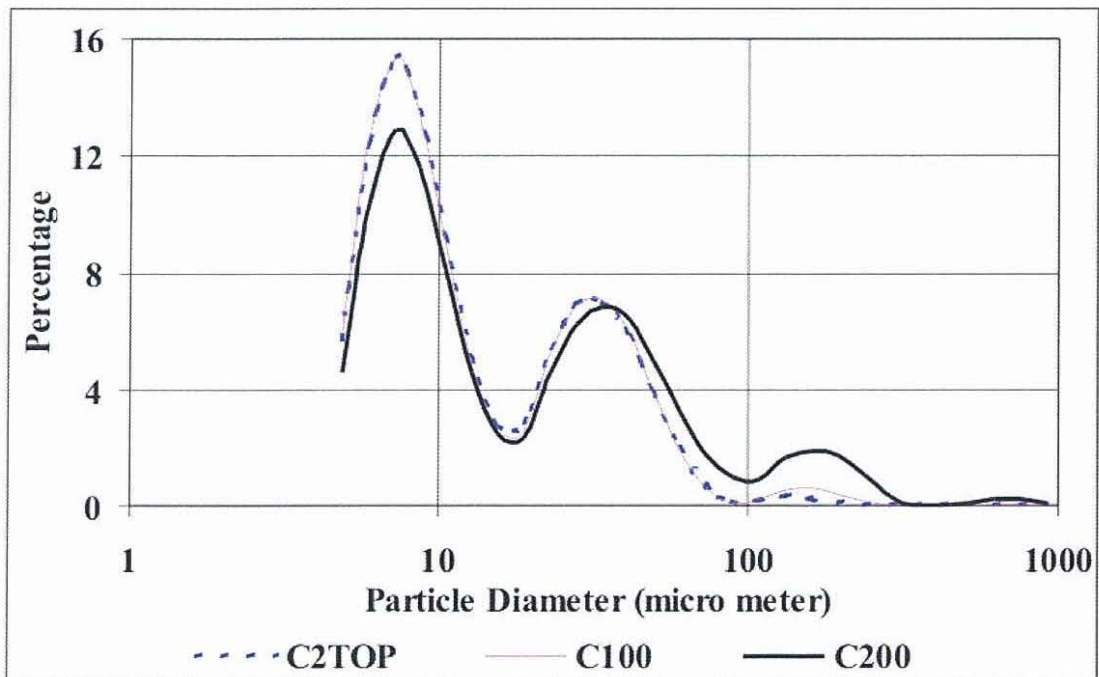


Core C2

Site description : Mangrove forest at upper reaches of Cocoa Creek

Sediment depth : 2.00 m

Analysis at depth : 0, 1.00, 2.00 meters

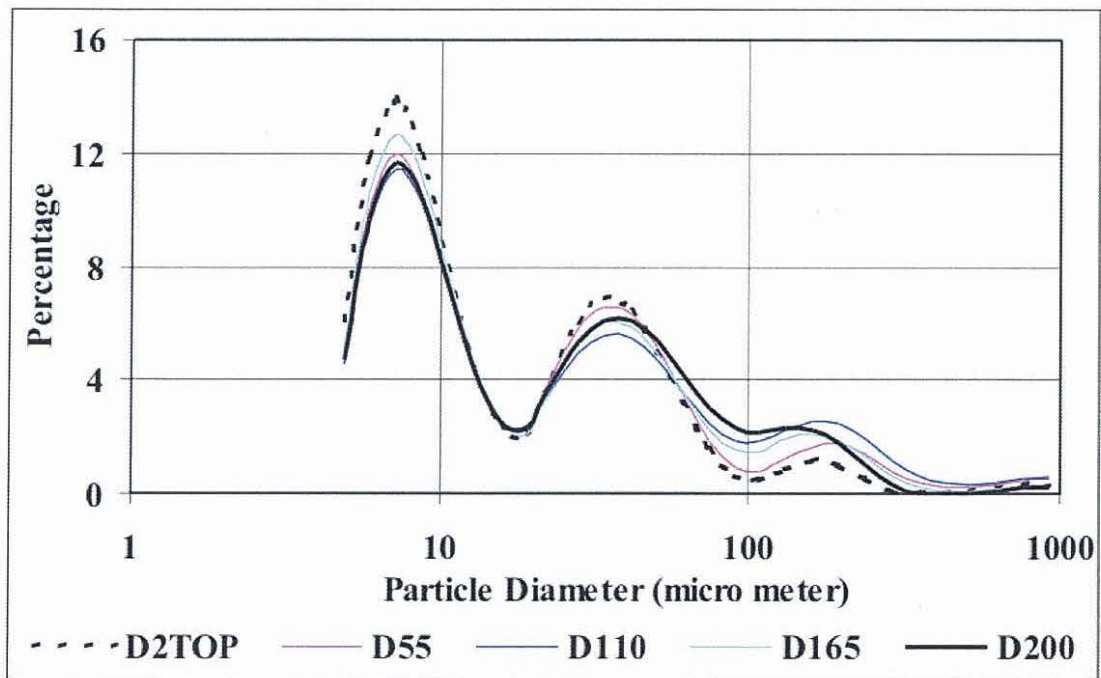


Core D2

Site description : Mix, mangrove and dead mangrove at upper reaches of Cocoa
Creek

Sediment depth : 2.00 m

Analysis at depth : 0, 0.55, 1.10, 1.65, 2.00 meters

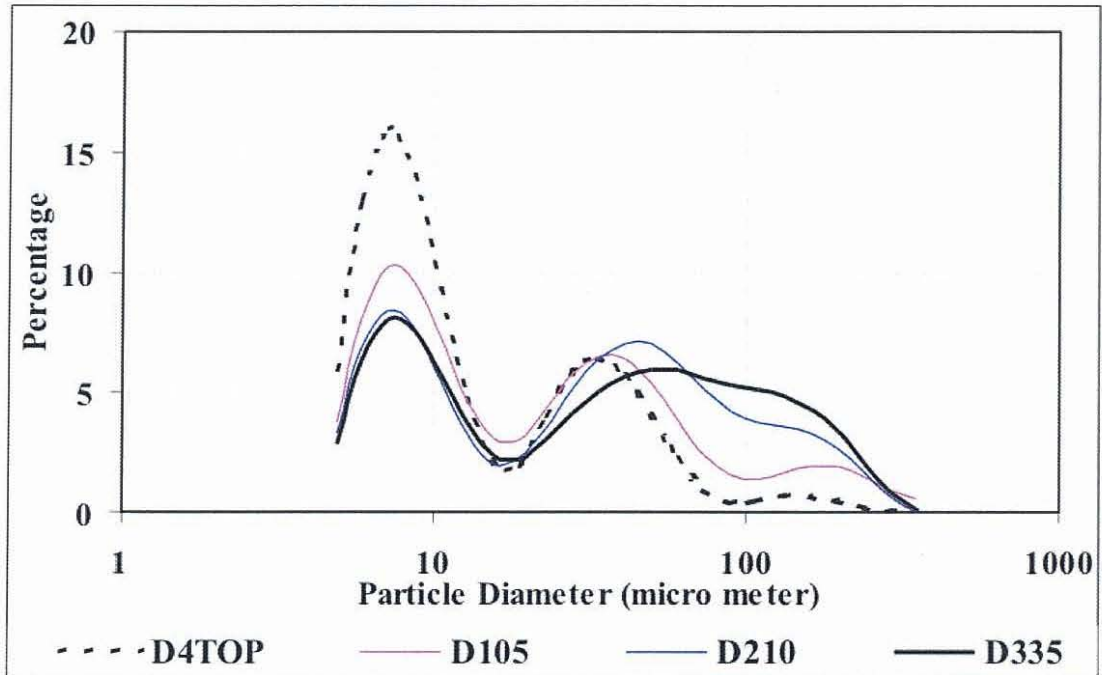


Core D4

Site description : Mix, mangrove and dead mangrove at upper reaches of Cocoa
Creek

Sediment depth : 3.35 m

Analysis at the depth : 0, 1.05, 2.10, 3.35 meters

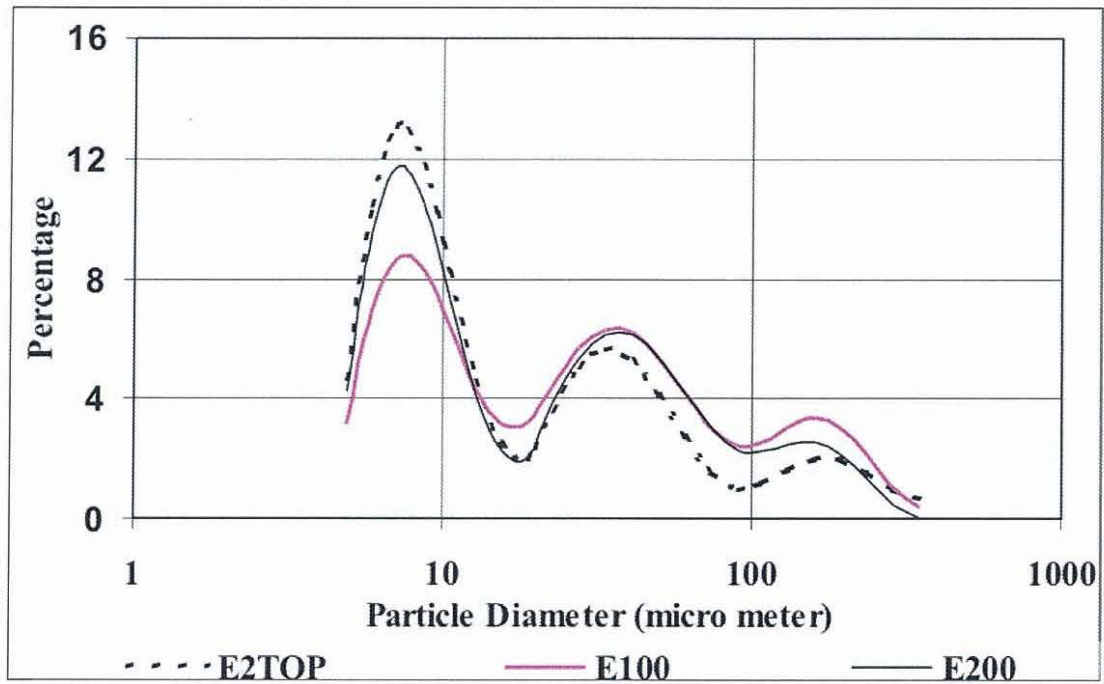


Core E2

Site description : Salt Flat

Sediment depth : 2.00 m

Analysis at depth : 0, 1.00, 2.00 meters

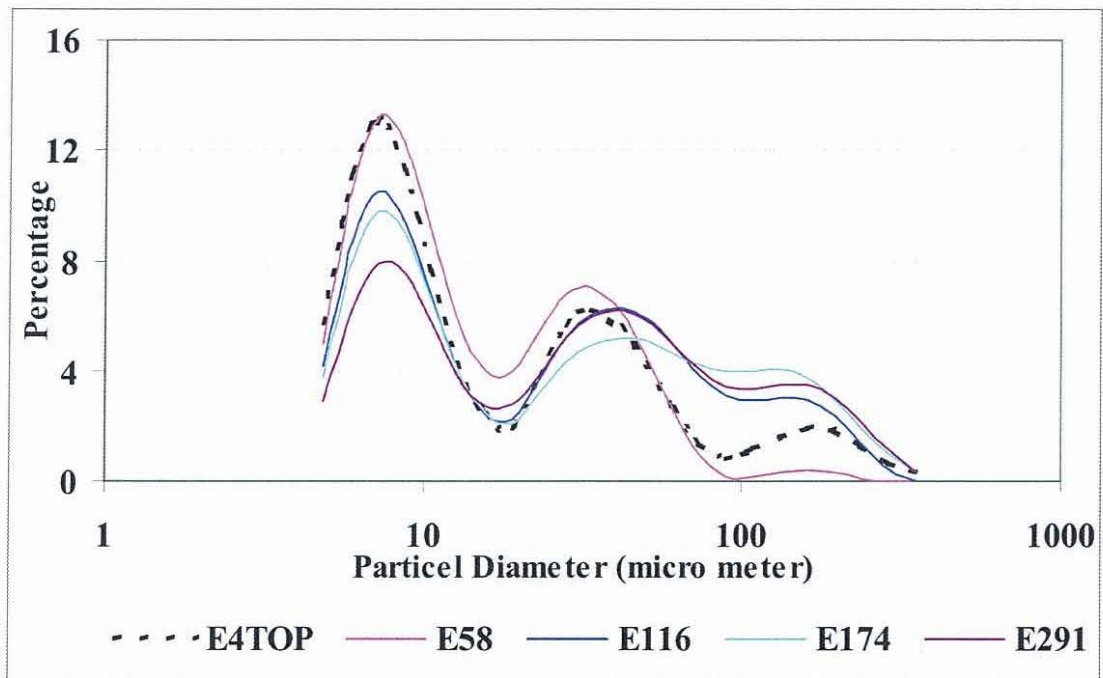


Core E4

Site description : Salt Flat

Sediment depth : 2.91 m

Analysis at depth : 0, 0.58, 1.16, 1.74, 2.91 meters

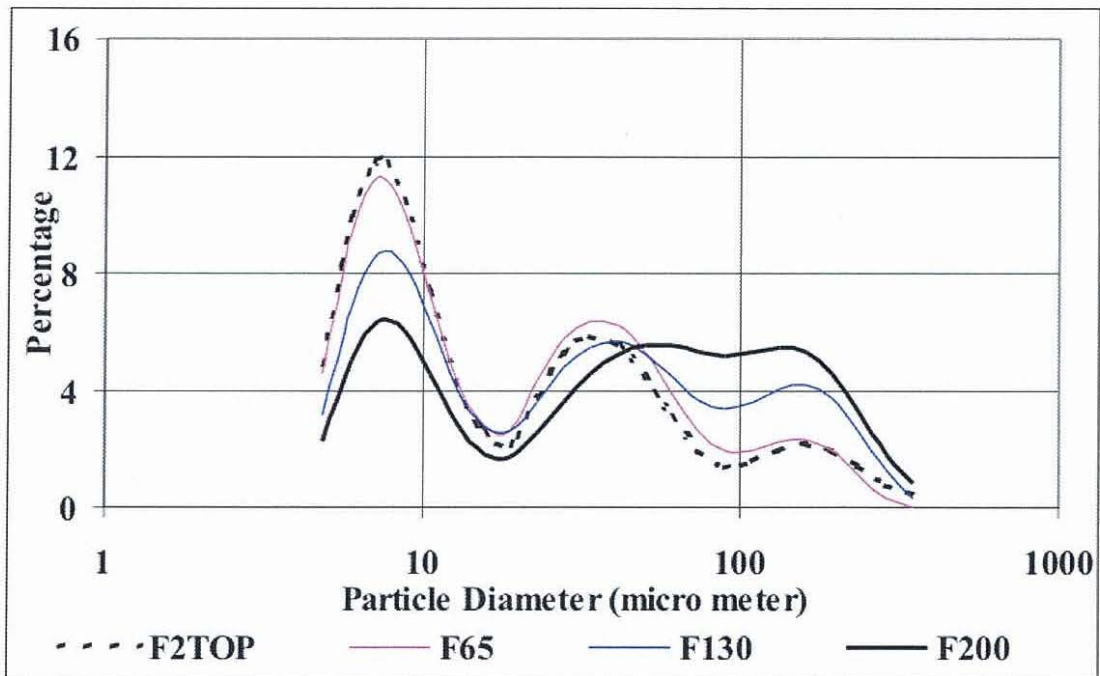


Core F2

Site description : Salt Flat

Sediment depth : 2.00 m

Analysis at depth : 0, 0.65, 1.30, 2.00 meters

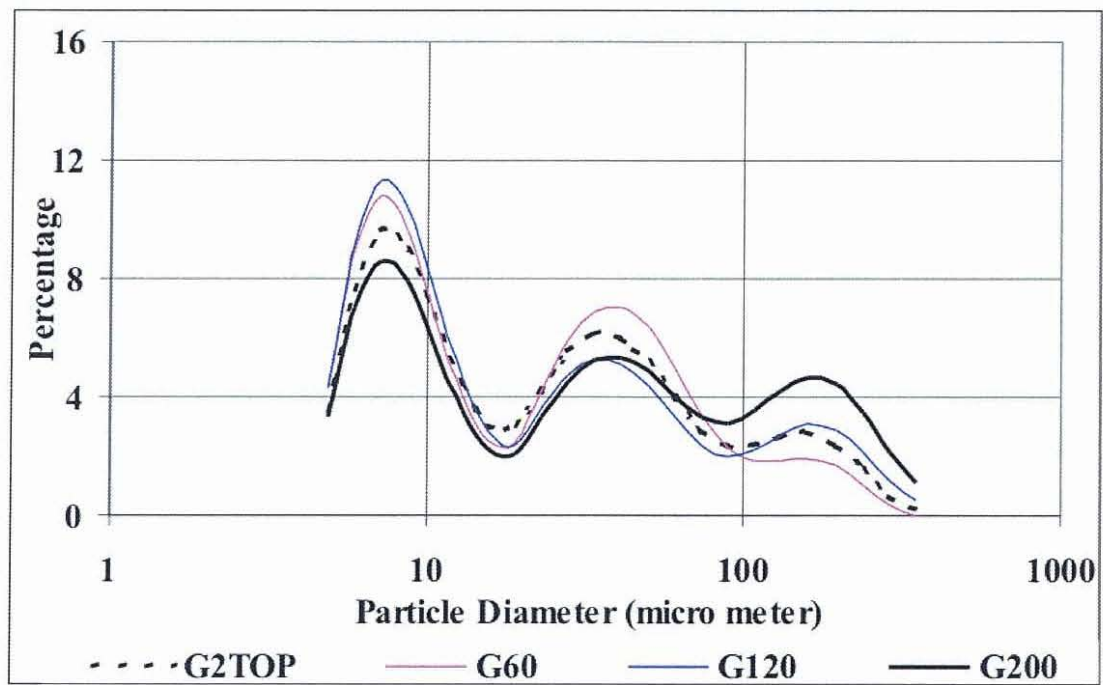


Core G2

Site description : Salt Flat

Sediment depth : 2.00 m

Analysis at depth : 0, 0.60, 1.20, 2.00 meters

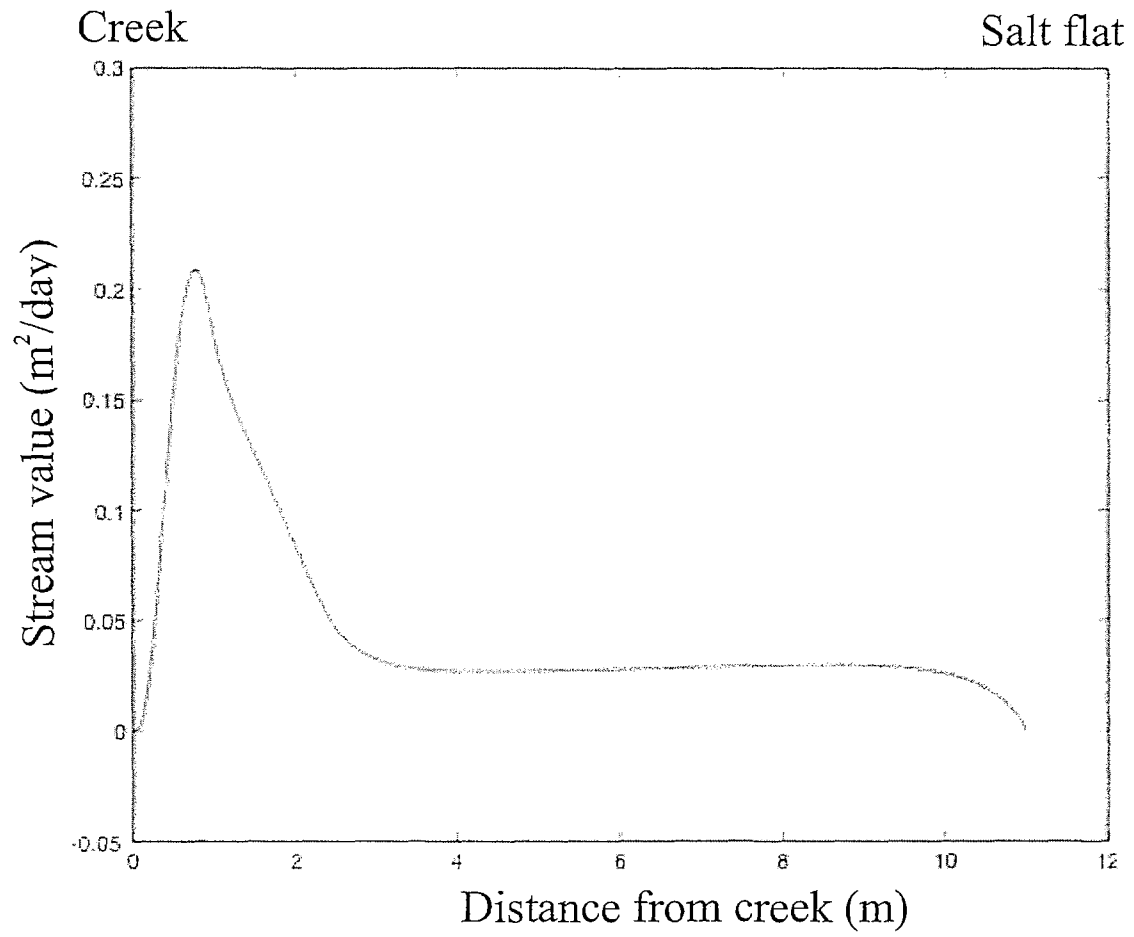


Appendix 3

Calculation of stream values of the groundwater flow modelling

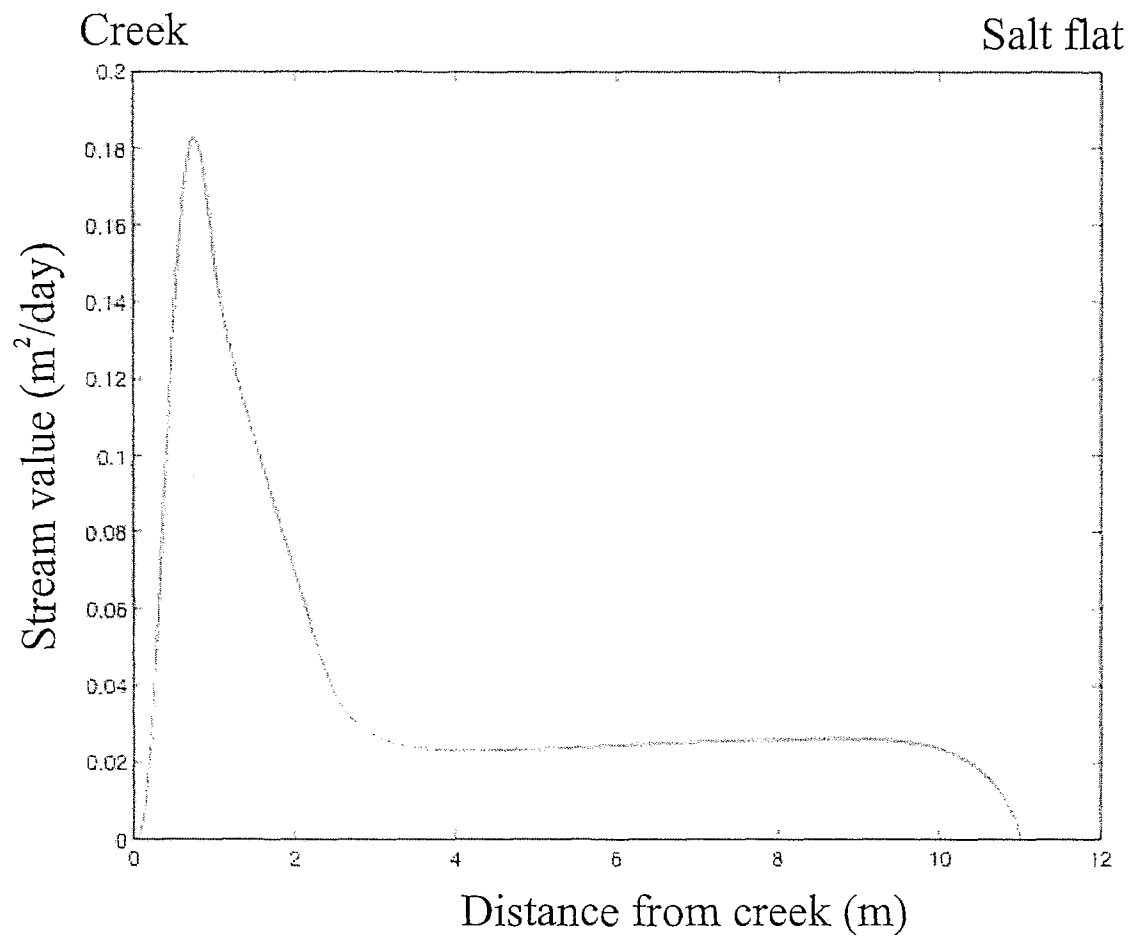
Model for Day 1

Model description : Mangrove forest sediment



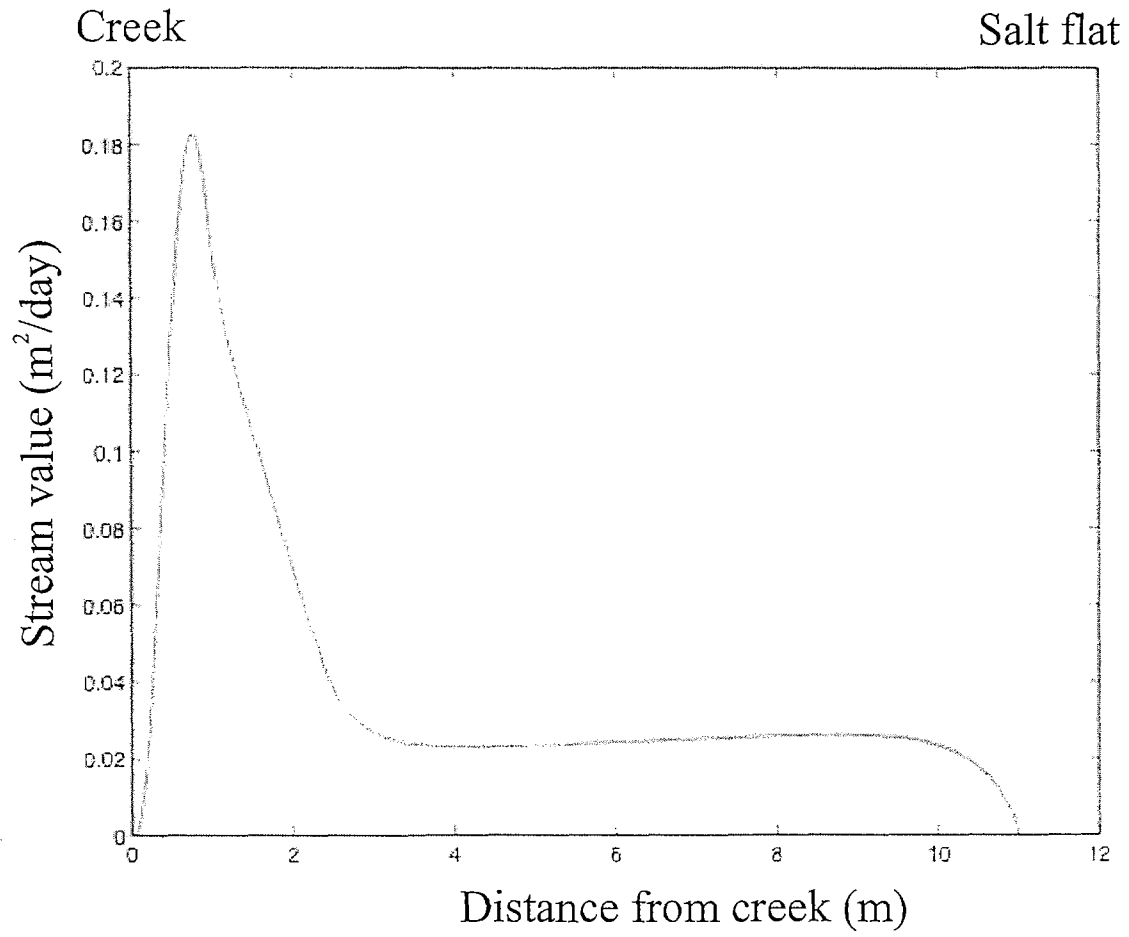
Model for Day 2

Model description : Mangrove forest sediment



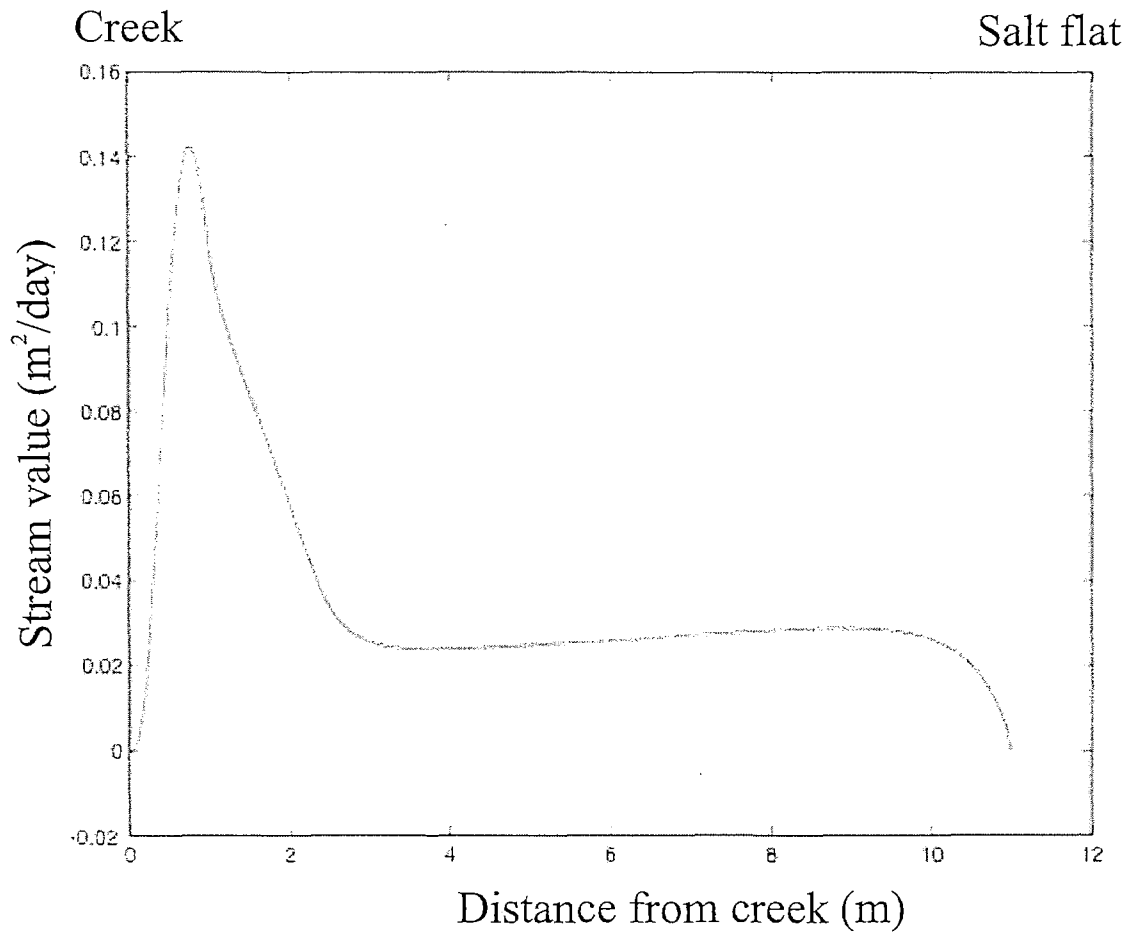
Model for Day 3

Model description : Mangrove forest sediment



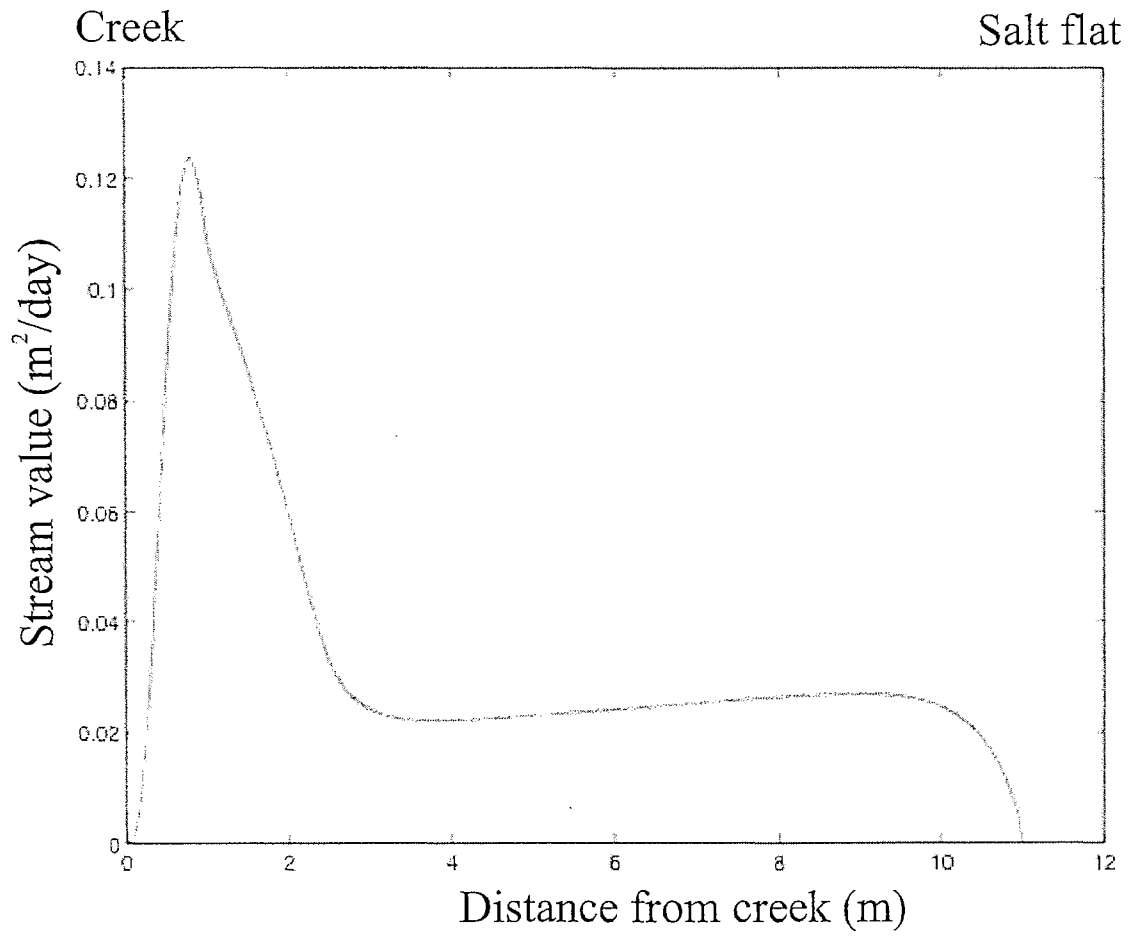
Model for Day 4

Model description : Mangrove forest sediment



Model for Day 5

Model description : Mangrove forest sediment



Appendix 4

Calculation of the porosity, equation 4.10 on Chapter 4

**Saturated bulk density of the sediment in the different days
after inundation and different depth from the surface**

Density (gr/cm ³) one day after inundation		
Depth (10 cm)	Depth (20 cm)	Depth (30 cm)
1.62	1.59	1.59
1.63	1.59	1.59
1.63	1.60	1.60
1.57	1.59	1.69
1.59		

Density (gr/cm ³) three days after inundation		
Depth (10 cm)	Depth (20 cm)	Depth (30 cm)
1.61	1.60	1.59
1.63	1.60	1.59
1.60	1.63	1.59
1.63	1.63	1.60

Density (gr/cm ³) five days after inundation		
Depth (10 cm)	Depth (20 cm)	Depth (30 cm)
1.62	1.63	1.60
1.63	1.63	1.63
1.63	1.60	1.53
1.62	1.63	1.63

Density (gr/cm ³) ten days after inundation		
Depth (10 cm)	Depth (20 cm)	Depth (30 cm)
1.61	1.61	1.59
1.63	1.61	1.61
1.61	1.59	1.60
1.63	1.59	1.60

From these above results, the porosity of the sediment can be calculated using

equation $p = \frac{\rho_g - \rho_{bw}}{\rho_g - \rho_f}$ and the result ranges from 0.41 to 0.51.